Characterization and Prevention of Chemotherapy Induced Cardiac Dysfunction

By

Matthew Zeglinski

A thesis submitted to the Faculty of Graduate Studies of

The University of Manitoba

In partial fulfillment of the requirements

Of the degree of

Master of Science

Department of Physiology

Faculty of Medicine

University of Manitoba

Winnipeg, Manitoba, Canada

Abstract

Background: Anthracyclines, in particular Doxorubicin (DOX), are highly effective chemotherapeutic agents in the breast cancer setting, which are limited by their cardiotoxic side effects. Recently, the introduction of Trastuzumab (TRZ), a novel monoclonal antibody against the HER2 receptor, in the breast cancer setting compounds the issue of DOX mediated cardiac dysfunction. Amongst the potential mechanisms for the deleterious effects of this drug-induced cardiomyopathy, the relationship between nitric oxide synthase 3 (NOS3) and oxidative stress has gained recent attention.

Objective: To determine the role of NOS3 in a clinically relevant female murine model of DOX+TRZ induced heart failure.

Methods: A total of 120 C57Bl/6 female mice [60 wild type (WT) and 60 NOS3 knockout ($NOS3^{-/-}$)] were treated with either 0.9% saline, DOX (20 mg/kg), TRZ (10 mg/kg), or DOX+TRZ. Serial echocardiography was performed daily for a total of 10 days, after which the mice were euthanized for histological and biochemical analyses.

Results: As compared to WT, $NOS3^{-/-}$ mice demonstrated increased cardiotoxicity following treatment with DOX. This effect was potentiated with DOX+TRZ combination therapy. In WT female mice receiving DOX+TRZ, left ventricular ejection fraction (LVEF) decreased from 75±3% at baseline to 46±2% at day 10 ($p<0.05$). In the $NOS3^{-/-}$ group, LVEF decreased from 72±3% at baseline to 35±2% at day 10 ($p<0.05$). LVEF was significantly lower in $NOS3^{-/-}$ mice than WT at day 10 in those receiving DOX+TRZ

($p<0.05$). As compared to WT, $NOS3^{-/-}$ mice also demonstrated increased mortality following treatment with DOX+TRZ, corroborating the echocardiographic findings. Histological analysis using light and electron microscopy demonstrated increased loss of cell integrity including myofibrillar degradation, cytoplasmic vacuolization, and enlargement of the smooth endoplasmic reticulum in both the WT and $NOS3^{-/-}$ mice treated with DOX+TRZ. There was no significant difference, however, in the degree of cardiac remodeling between the WT and $NOS3^{-/-}$ groups. There was an increasing trend in the degree of cardiac apoptosis in both WT and $NOS3^{-/-}$ mice treated with DOX+TRZ therapy.

Conclusion: Congenital absence of NOS3 potentiates the cardiotoxic effects of DOX+TRZ in an acute female murine model of chemotherapy-induced cardiomyopathy.

Acknowledgments

First and foremost, I offer my sincerest gratitude to my supervisors, Dr. Davinder S. Jassal and Dr. Pawan K. Singal, for their patience, knowledge, and guidance throughout my thesis. Without their efforts, I could not have accomplished all that I have over the past 2 years. I would also like to acknowledge the members of my committee Dr. Ian Dixon, Dr. Jeffrey Wigle, and Dr. Todd Duhamel for their encouragement and belief in me as a student and as a researcher. Finally, I owe a big thank-you to Dr. James Thliveris for his histological expertise and guidance in light and electron microscopy.

To the members of the Cardiovascular Imaging Laboratory, I would like to thank you for your support over the past 2 years. Specifically, I owe my deepest gratitude to Ms. Sheena Bohonis, not only for her help with cardiac imaging, but also for the countless hours of paper work and prep that were required to allow me to complete this project so smoothly. To the members of the Cell Pathophysiology Laboratory, I would like to thank all of you for the in-depth discussions, support, and rich learning environment you provided. It was truly and honor to work with all of you. Specifically, I would like to show my gratitude and thanks to Ms. Anita Sharma for her time and patience with teaching me western blotting.

Naturally, this thesis would not have been possible without the support of my family. I am forever in debt to my mother, Cindy, Father, Bob, and sister Amanda; for their love and support not only in my move from Maple Ridge, British Columbia, to Winnipeg but for believing in me to be the best researcher I can be. I also would like to

thank my grandparents Lou and Pat Spado, and Paul and Helen Zeglinski, for helping me in any way possible to make my life easier so I could focus on the science. Finally, I would like to thank my girlfriend Jessica Beaton for her love and patience with the long hours and weekend work that accompanies scientific research.

Table of Contents

Table Synopsis

Figure Synopsis

Figure 10. Tissue Velocity imaging of a normal healthy mouse. A V_{Endo} for mice between 2.5 and 3.5 cm/s is considered to be within normal range. A V_{Endo} less than one is indicative of cardiac systolic dysfunction. V_{Endo}, Endocardial Velocity. (pg. 45)

Figure 11. A) Comparison of LVEF between WT and $NOS3^{-/-}$ female mice treated with DOX alone. Although the LVEF significantly decreased in both groups (*$p<0.05$), the LVEF in the $NOS3^{-/-}$ group was significantly reduced as compared to WT group at day 10 (#$p<0.05$). **B)** Comparison of LVEF between WT and $NOS3^{-/-}$ female mice treated with DOX+TRZ. Similar to the DOX alone treated group, there was a significant decrease in LVEF at day 10 in both groups (*$p<0.05$). The LVEF in the $NOS3^{-/-}$ group, however, was significantly reduced as compared to the WT group at day 10 (#$p<0.05$). Finally, the LVEF was significantly reduced in $NOS3^{-/-}$ female mice receiving DOX+TRZ, as compared to DOX alone. WT Saline n=5; WT DOX n=15; WT TRZ n=15; WT DOX+TRZ n=25; $NOS3^{-/-}$ Saline n=5; $NOS3^{-/-}$ DOX n=15; $NOS3^{-/-}$ TRZ n=15; $NOS3^{-/-}$ DOX+TRZ n=25. LVEF, left ventricular ejection fraction; WT, Wild type; $NOS3^{-/-}$, Nitric Oxide Synthase 3 Knockout; DOX, Doxorubicin; DOX+TRZ, Doxorubicin and Trastuzumab. (pg. 54-55)

Figure 12. Percent survival of C57Bl/6 and $NOS3^{-/-}$ female mice. Mice treated with DOX demonstrated increased mortality than mice treated with either saline or TRZ. Furthermore, the combination of DOX+TRZ therapy demonstrated increased mortality in both the WT and $NOS3^{-/-}$ groups as compared to DOX alone. $NOS3^{-/-}$ mice treated with DOX+TRZ had a significantly higher mortality rate than WT at day 10. WT Saline n=5;

List of Abbreviations

AC	Adriamycin, Cyclophosphamide
ACEi	Angiotensin-Converting Enzyme Inhibitor
ANG II	Angiotensin II
ATP	Adenosine Triphosphate
AT1R	Angiotensin 1 Receptor
βB	Beta-Blocker
Bcl-X_L	B-Cell Lymphoma-Extra Large
Bcl-X_S	B-Cell Lymphoma-Extra Small
BNP	Brain Natriuretic Peptide
CHF	Congestive Heart Failure
CMR	Cardiac Magnetic Resonance Imaging
CRP	C-Reactive Protein
DEX	Dexrazoxane
DNA	Deoxyribonucleic Acid
DNR	Daunorubicin
DOX	Doxorubicin
EF	Ejection Fraction
EGF	Epidermal Growth Factor
EGFR	Epidermal Growth Factor Receptor
EPI	Epirubicin
ErbB (HER) 1/2/3/4	Human Epidermal Growth Factor Receptors 1/2/3/4
ERK 1/2	Extracellular Signal Related Kinase 1/2
FAK	Focal Adhesion Kinase
FEC	5’ Fluorouracil, Epirubicin, Cyclophosphamide
FPS	Frames Per Second
HDL	High Density Lipoproteins
HLD	High Lipid Diet
IVS	Interventricular Septum
Grb2	Growth Factor Receptor Bound Protein 2
GSH	Glutathione
LDL	Low Density Lipoproteins
LLD	Low Lipid Diet
LV	Left Ventricle
LVH	Left Ventricular Hypertrophy
LVEF	Left Ventricular Ejection Fraction
LVEDD	Left Ventricular End Diastolic Diameter
LVEDP	Left Ventricular End Diastolic Pressure
LVESD	Left Ventricular End Systolic Diameter
MAPK	Mitogen Activated Protein Kinases
MEK	MAPK/ERK 1/2 Kinase
MUGA	Multi-Gated Acquisition Scan
NAD(P)H	Nicotinamide Adenine Dinucleotide Phosphate
NDF	*neu*-Differentiating Factor
NOS3	Nitric Oxide Synthase 3

$NOS3^{-/-}$	Nitric Oxide Synthase 3 Knock out
$NOS3^{TG}$	Nitric Oxide Synthase 3 Transgenic
NOX	NAD(P)H Oxidase
NRG	Neuregulin
NYHA	New York Heart Association
PARP	Poly (ADP-ribose) polymerase
PI3K	Phosphatidylinositol 3-kinases
PIP_2	Phosphatidylinositol 4,5-bisphosphate
PIP_3	Phosphatidylinositol (3,4,5)-triphosphate
PLAX	Parasternal Long Axis
PW	Posterior Wall
RAS	Renin Angiotensin System
ROS	Reactive Oxidative Species
RTK	Receptor Tyrosine Kinase
RT3D TTE	Real Time 3D Transthoracic Echocardiography
SAX	Short Axis
SR	Strain Rate
TBS-T	Tris-Buffered Saline, Tween 20
TGFα	Transforming Growth Factor α
TnI	Troponin I
TnT	Troponin T
topo II	Topoisomerase II
TTE	Transthoracic Echocardiography
TUNEL	Terminal deoxynucleotidyl transferase dUTP nick end labeling
V_{Endo}	Endocardial Velocity
VLDL	Very-Low Density Lipoprotein

Chapter 1: Literature Review

Breast Cancer: Prevalence, Diagnosis, and Treatment

Cancer is a major public health issue in Canada and is the second leading cause of death next to cardiovascular disease. In 2010, approximately 174,000 new cases and 76,000 deaths from cancer were reported. [1] This represents a 1.6% increase in the number of reported cases and a 1.2% increase in the number of reported deaths as compared to 2009.[2] In 2011, the number of new cases of cancer is expected to increase to greater than 177,000. In contrast, the number of reported deaths will remain approximately constant at 75,000.[1] The risk of developing cancer increases with age. In the past year, 43% of new cases and 61% of deaths occurred in individuals over the age of 70.[2] Canada is one of the few nations that has developed a national cancer registry, the Canadian Cancer Registry, that allows for tracking and comparison of all cancers.

Breast cancer is a major health concern for Canadian women as it is the leading cause of cancer related illness and the second leading cause of cancer related deaths.[1] It is expected that more than 23,000 new cases and 5,000 deaths from breast cancer will be reported this year.[1] Women have a 1 in 9 (11%) lifetime risk of developing breast cancer and a mortality rate of approximately 1 in 27 (4%).[2-4] In the United States, breast cancer affects more than 200,000 women and results in 40,000 deaths annually.[3, 5]

Treatment of breast cancer relies primarily on early detection. Early detection and diagnosis can only be accomplished if the population is well educated and screening resources are readily available. Recent decreases in the rates of morbidity and mortality in breast cancer patients are attributed to advancements in clinical imaging that allow for the early detection of tumors.[6-9] Some of these advances in early detection include full-

field digital mammography, ultrasound, magnetic resonance imaging, and positron-emission tomography.[6, 7-10]

Breast cancer treatment is multifaceted including surgery, radiation therapy, chemotherapy including anthracyclines, and the recent addition of novel monoclonal antibodies. Surgical approaches vary from node specific lymphadenectomies to complete radial mastectomy, in which all of the breast tissue is removed.[11] Radiation therapy used in conjunction with surgical and chemotherapy treatments has been demonstrated to have tremendous benefits in early breast cancer treatment.[12, 13] When used as part of a multifaceted treatment regimen, radiation therapy has been demonstrated to significantly reduce the rate of localized (74% combination vs. 90% chemotherapy alone, $p = 0.002$) and systemic (31% combination vs. 48% chemotherapy alone, $p = 0.004$) breast cancer recurrence as compared to chemotherapy alone.[12] The mainstay of chemotherapy for breast cancer patients includes the combination of 5-fluorouracil-epirubicin-cyclophosphamide (FEC) or adriamycin-cyclophosphamide (AC).[14]

Anthracycline History

Since the early 1930's, anthracyclines have been used in the clinical setting.[15] Anthracycline antibiotics have been recognized for over 75 years for their antibacterial properties. However, it was not until the early 1960's, that their efficacy in treating cancer came to the forefront of scientific research. Two anthracycline compounds, Daunorubicin (DNR) and Doxorubicin (DOX), were isolated from the pigment producing soil bacterium *Streptomyces peucetius*.[16] This discovery marked a major advancement in the treatment against cancer as it has been demonstrated that these compounds contain significant antitumor activity.[15-17] Numerous studies have demonstrated that DOX has a

greater efficacy and activity level than DNR, despite their structural similarities (Figure 1). This contributed to DOX's rapid transition into clinical trials, a mere 6 years after the discovery of its anticancer properties.

Doxorubicin's unique structure is highly lipophilic, which allows it to have a long half-life within the body.[17] Doxorubicin and DNR contain several structural similarities including gylconic and sugar moieties as seen in Figure 1.[18] In fact, the only structural difference between DOX and DNR is that the side chain on DOX terminates with a primary alcohol, whereas the side chain on DNR terminates with a methyl group (Figure 1).[16, 18-20] While DNR is highly effective in acute lymphoblastic and myeloblastic lymphomas, DOX has become a key component of breast cancer treatment. Furthermore, DOX therapy has been extended for the use within other cancers including childhood solid tumors, soft tissue sarcomas, and aggressive Hodgkin's and non-Hodgkin's lymphomas.[18, 19, 21]

A) Doxorubicin [16, 20]

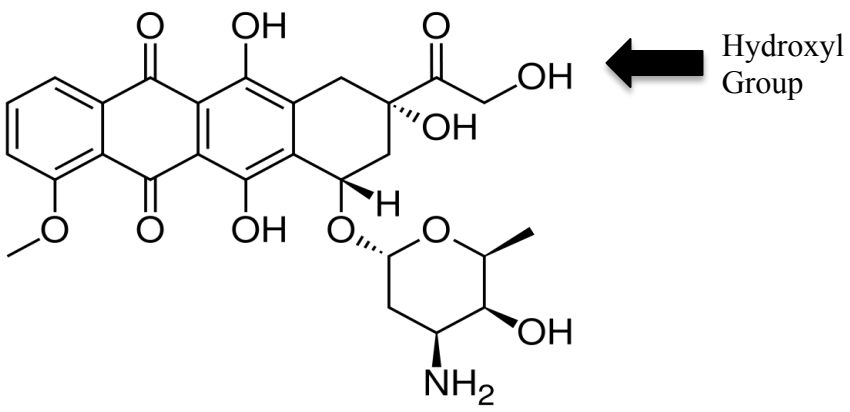

B) Daunorubicin [16, 20]

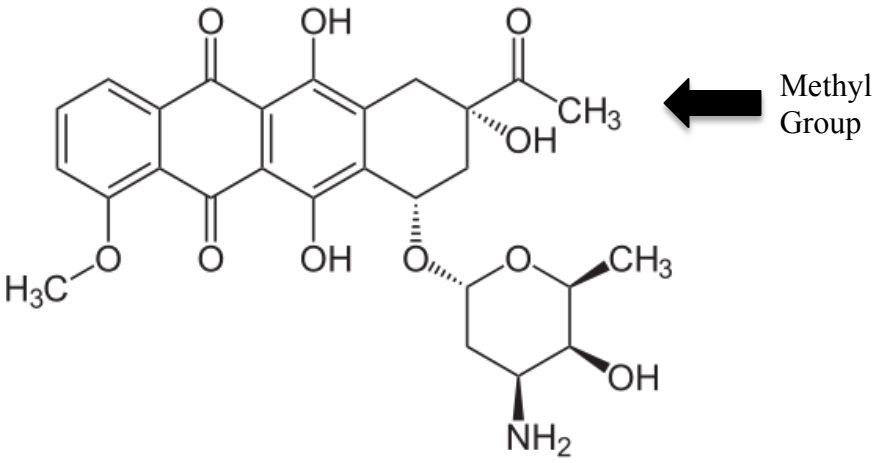

Figure 1. The chemical structures of A) Doxorubicin (8S,10S)-10-{[(2R,4S,5S,6S)-4-amino-5-hydroxy-6-methyloxan-2-yl]oxy}-6,8,11-trihydroxy-8-(2-hydroxyacetyl)-1-methoxy-5,7,8,9,10,12-hexahydrotetracene-5,12-dione, and B) Daunorubicin (8S,10S)-8-acetyl-10-{[(2R,4S,5S,6S)-4-amino-5-hydroxy-6-methyloxan-2-yl]oxy}-6,8,11-trihydroxy-1-methoxy-5,7,8,9,10,12-hexahydrotetracene-5,12-dione.[16, 20, 22]

Anthracycline Anticancer Mechanisms

Multiple theories have been proposed regarding the mechanisms by which DOX is able to reduce solid tumor size. These mechanisms include: 1) intercalation in DNA; 2) generation of free radicals; 3) DNA binding and alkylation; 4) DNA cross-linking; 5) interference with DNA unwinding; 6) direct membrane damage; 7) inhibition of topoisomerase II (topo II); and 8) induction of apoptosis.[18, 19, 21, 23-25] It is likely that several of these mechanisms are required for DOX to demonstrate such a high efficacy in the cancer setting. To date, inhibition of topo II and free radical generation have been identified as the major contributors to the activity of DOX.[18, 21, 26, 27]

Anthracyclines, in particular DOX, is a type II DNA topoisomerase inhibitor that acts by intercalating their B and C rings into adjacent DNA base pairs. The sugar moiety plays an integral role in the formation and stabilization of the transient complex. The major determinant of DOX's ability to be a topo II toxin is within the sugar moiety, which lies in the minor groove of the double helix. Under normal physiologic conditions, topo II is able to cleave the DNA double helix, thereby, allowing DNA fragments to pass through the break before rejoining the two strands. In a sense, topo II acts as a molecular gatekeeper for DNA regulation.[28, 29] Furthermore, topo II is an essential nuclear enzyme that is required for processes including replication, transcription, and recombination.[29, 30] The addition of DOX to the breast cancer setting creates a transient DNA-topo II complex that causes damage to the topo II protein. The creation of this transient complex modifies the enzyme, allowing it to become a DNA damaging agent. Doxorubicin and other anthracycline treatments for human cancers regulate the creation of the transient complex.[27]

Anthracyclines, in particular DOX, are highly vulnerable to redox-cycling. The reduction of oxygen on the C ring gives DOX its ability to cleave and degrade DNA.[21] This quinone structure of DOX allows it to act as an electron acceptor in reactions mediated by oxidative enzymes including cytochrome P450 and nicotinamide adenine dinucleotide phosphate (NAD(P)H) dehydrogenase. The addition of one electron to DOX produces a semiquinone free radical that is capable of inducing DNA damage under aerobic conditions by donating its unpaired electron to molecular oxygen generating a superoxide radical.[18, 19, 21] It is important to note that under anaerobic conditions, DOX is stable and does not undergo redox-cycling. Redox-cycling is harmful to cells as only a small quantity of drug is required to induce the production of numerous superoxide radicals. When DOX is complexed with iron, it forms an intermediate that is capable of binding DNA and producing partially reduced forms of oxygen. In the vicinity of DNA, superoxide is capable of inducing significant DNA damage including single and/or double stranded breaks. Furthermore, DOX is capable of reducing the protein levels of glutathione (GSH) peroxidase, a critical mediator required for scavenging free radicals.[31] Therefore, DOX's cytotoxic properties stem from its ability to increase free radical production, while simultaneously decreasing the availability of antioxidant enzymes within tumor cells.[31]

Doxorubicin-induced Cardiotoxicity

Doxorubicin is a broad-spectrum antibiotic that has been in use for cancer treatment since the mid 1960's.[31, 32] Although DOX is a highly effective anticancer agent, it is associated with significant side effects including myelosupression, nausea, vomiting, arrhythmia, and more importantly cardiac dysfunction.[32] While many of the side effects are reversible and/or clinically manageable, cardiomyopathy leading to congestive heart failure (CHF) is not. Doxorubicin demonstrates a dose-dependent cardiac dysfunction property that may limit its use within the clinical setting.[33] Numerous studies have demonstrated that women who receive a lifetime cumulative dose of DOX exceeding 500mg/m^2 of body surface area are at a high risk of developing DOX-induced cardiac dysfunction.[26, 32-34] A retrospective study of 399 patients demonstrated that CHF developed in 4% of women who received 500-550mg/m^2 of DOX, and rose to 18% in those women who received between 550-600mg/m^2.[32, 35] The prevalence of CHF due to DOX therapy continued to rise to over 36% in women that received greater than 600mg/m^2.[32, 35] Other risk factors for developing DOX-induced cardiac dysfunction include age >70, left chest radiotherapy, combination therapy (cyclophosphatide, actinomycin D, or mitomycin C), or a history of pre-existing cardiac disease.[32] Initial clinical trials of DOX revealed modifications in electrocardiogram (EKG) recordings that included sinus tachycardia, ST segment depression, and T wave abnormalities.[31, 36-38] Furthermore, clinical use of DOX has also demonstrated that DOX-induced cardiac dysfunction can present in either the acute or chronic setting (Table 1). Acute cardiac dysfunction due to DOX is rare, but does occur and is identified primarily through abnormal EKG tracings (Table 1). Chronic cardiac dysfunction due to DOX is common

and often life threatening. Onset of symptoms usually occurs within a year and is directly related to the dose dependency action of DOX. Chronic cardiac dysfunction is characterized by tachycardia, LV cavity dilation, pulmonary/venous congestion, exercise intolerance, and progressive cardiac injury (Table 1). Cardiac dysfunction that presents after one-year of completing DOX treatment is classified as late onset. Key features of late onset cardiac dysfunction include arrhythmias, LV systolic dysfunction, myocyte damage and CHF (Table 1).

Type	Onset	Features
Acute	Immediate	Uncommon (<1%), Abnormal ECG, CHF symptoms rarely observed
Chronic	≤ 1 Year	Common (7-26%) Life threatening, Dose related, tachycardia, LV dilation, pulmonary/venous congestion, exercise intolerance, progressive cardiac injury
Late Onset	≥ 1 Year	Common (5%) LV systolic dysfunction, arrhythmias, CHF, myocyte damage

Table 1. Outline of the onset and clinical symptoms of Doxorubicin (DOX) mediated cardiomyopathy.[32, 39, 40]

Doxorubicin mediated cardiotoxicity has a negative influence on the long-term survival rate of breast cancer survivors. Many women do not present with cardiac dysfunction until weeks or years after they have discontinued the use of DOX. The Society of Clinical Oncology has recommended women receiving DOX should not exceed a cumulative dose of 500mg/m^2 of body surface area to reduce the risk of developing CHF.[31, 32, 41] While limiting cumulative exposure to DOX is a useful tool,

identifying risk factors remains the front line defense in the prevention of DOX-mediated cardiotoxicity.

Doxorubicin is not tumor cell specific. Its cytotoxic properties also affect healthy cells and tissues including cardiomyocytes. Within the heart, DOX induces myocardial and cellular damage leading to apoptosis and CHF. The degree of cardiomyopathy is directly correlated with the cumulative dose of DOX administered. A number of DOX analogs have been produced in hopes of creating a compound that is less cardiotoxic, without compromising the anticancer properties. While most of the analogs developed have been less cardiotoxic, they are also less active in tumor suppression.[18, 20] There have also been numerous studies that have investigated the use of prophylactic therapy to mitigate the cardiotoxic effects of DOX, while leaving the antitumor properties unaltered.[18, 20, 31, 39, 42] These studies used compounds such as vitamins (A, C, E), thiol-containing reducing agents (N-acetylcysteine, GSH) and iron chelating agents (Dexrazoxane).[18, 20, 31, 39, 42-44] Other studies have attempted to use current CHF treatments, including β-blockers (βB), angiotensin converting enzyme inhibitors (ACEi), and angiotensin receptor blockers (ARBs), in combination with DOX in hopes of mitigating the development of cardiac dysfunction.[45, 46] However, these studies were largely unsuccessful. The use of antioxidants, however, has demonstrated promising results and is discussed later in further detail. Therefore, it is essential that research continues to investigate the underlying mechanisms that characterize DOX-induced cardiotoxicity in order to develop novel cardioprotective therapies for women undergoing DOX treatment for breast cancer.

Human Epidermal Growth Factor Receptors: Cell Survival Pathways

The human epidermal growth factor receptors (ErbB) are a group of receptor tyrosine kinases (RTK).[47-49] To date, there have been four ErbB receptors identified in mammals. They include ErbB1 (HER1, EGFR), ErbB2 (HER2/*neu*), ErbB3 (HER3), and ErbB4 (HER4). The HER signaling network has been the focus of extensive research as it has been demonstrated to play a central role in various developmental and physiological processes.[47, 49, 50] Each RTK is a cell surface receptor that consists of three parts; (i) a single membrane-spanning domain; (ii) a ligand activated tyrosine kinase domain; and (iii) a carboxyl-terminal regulatory domain that contains multiple tyrosine residues capable of being a SH2 docking site when phosphorylated.[51-53] Careful analysis of the molecular structure reveals that the tyrosine kinase domain is highly conserved (44% identical, 63% similar) among the ErbB receptors. Conversely, a closer look into the C-terminal domain reveals a highly divergent structure (3% identical, 15% similar) amongst the 4-receptor isoforms.[51]

Initiation of HER signaling is the result of a ligand binding to its specific receptor located on the extracellular domain of the HER protein. There are numerous ligands that bind to the receptors of the HER family. The ligands that bind only to HER1 include the epidermal growth factor (EGF), transforming growth factor α (TGF-α), and amphiregulin (Table 2). Ligands that bind to both the HER3 and HER4 isoforms include *neu*-differentiating factors (NDF), neuregulins (NRG) and heregulins (Table 2). Finally, the ligands that bind to and activate both HER1 and HER4 include betacellum, epiregulin, and heparin-binding EGF-like growth factors (Table 2).[48, 53] To date, no ligand has been identified that binds to and activates the HER2 receptor.[52, 54, 55] HER2 is, however, the

receptor of choice for heterodimerization for all other HER receptors, and results in a variety of cellular processes including cell proliferation, differentiation, and apoptosis.[47, 52]

Receptor	Ligand	Reference
HER1	EGF, TGF-α, amphiregulin, betacellum, epiregulin, heparin-binding EGF-like growth factor	Moghal and Sternberg 1999; Cho et al. 2003
HER2	None	Landgraf 2007
HER3	NDF, NRG, heregulins	Moghal and Sternberg 1999; Cho et al. 2003
HER4	NDF, NRG, heregulins, betacellum, epiregulin, heparin-binding EGF-like growth factor	Moghal and Sternberg 1999; Cho et al. 2003

Table 2. List of the 4 HER receptors found within the heart and the ligands that bind them.

Neuregulins (NRG), specifically neuregulin-1 (NRG-1), are intimately involved in the survival of cardiomyocytes through signaling of the HER2/4 heterodimer.[50] Genetic studies of NRG-1 have demonstrated that NRG-1/HER signaling is a key mediator of cell-to-cell interactions that are not only capable of regulating tissue organization during development, but are also critical in maintaining cardiac function throughout adulthood.[56, 57] Binding of NRG-1 to HER4 allows HER4 to interact with HER2 and form a heterodimer. The dimerization process is the primary initiating event of

several cell-signaling pathways that include cell growth, myofilament structure and organization, survival, myocyte-matrix coupling, glucose uptake, and angiogenesis.

Dimerization of HER2 to HER4 leads to the trans-phosphorylation of several tyrosine (Y) residues (Y1248, Y1023, Y1139, Y1196, Y1121/1122), thus initiating multiple cell survival signaling cascades within cardiomyocytes (Figure 2).[58] In adult cardiomyocytes, NRG-1 is an activator of the mitogen activated protein kinases (MAPK), through HER2 signaling. Activation of the 185kDa HER2 receptor leads to the recruitment of several adaptor proteins including Shc and Grb2.[56] Together, these adaptor proteins activate MAPK signaling through phosphorylation of Ras (Figure 2). Activated Ras directly interacts with Raf, leading to the activation of MAPK/ERK kinase (MEK). MEK is then capable of phosphorylating ERK 1/2 threonine (T)/ tyrosine (Y) residues (T202/Y204) to initiate ERK 1/2 mediated nuclear signaling (Figure 2). ERK 1/2 activates several transcription factors (Elk-1, STAT3, c-myc, n-myc) that ultimately lead to cell survival, growth, and hypertrophy. Furthermore, ERK 1/2 signaling is intimately involved in sarcomere synthesis and organization.[56]

A second pathway by which NRG-1 is able to initiate cardioprotective signals is through the phospholinostide-3 kinase (PI3K)/Akt pathway (Figure 2). This pathway has been extensively described in the protection of cardiomyocytes against cell death, as well as regulation of metabolism and growth.[56] Phospholinostide-3 kinase catalyzes the conversion of phosphatidylinositol-3,4-diphosphate (PIP_2) to phosphatidylinositol-3,4,5-triphosphate (PIP_3). Dimerization of HER2 with another HER receptor activates PI3K which subsequently phosphorylates PIP_2 to PIP_3. PIP_3, a potent second messenger, is then able to activate the critical cell survival mediator Akt/protein kinase B. Akt is able to

phosphorylate a number of proteins to maintain the balance between anti- and pro-apoptotic processes through changes in mitochondrial respiration and decreases in ROS (Figure 2).

Finally, a third mechanism by which HER2 signaling is able to initiate cell survival is through the formation of focal adhesion kinase (FAK) complexes (Figure 2).[56, 59] Focal adhesion kinases are important to normal cardiomyocyte homeostasis, as they are intricately involved in sarcomere maintenance. FAK is a known substrate of Src. Therefore, upon HER2 activation by NRG-1 and subsequent recruitment of Src, FAK and $p130^{CAS}$ form the base of a focal adhesion complex that is able to maintain sarcomere structure, thereby increasing cell survival (Figure 2).

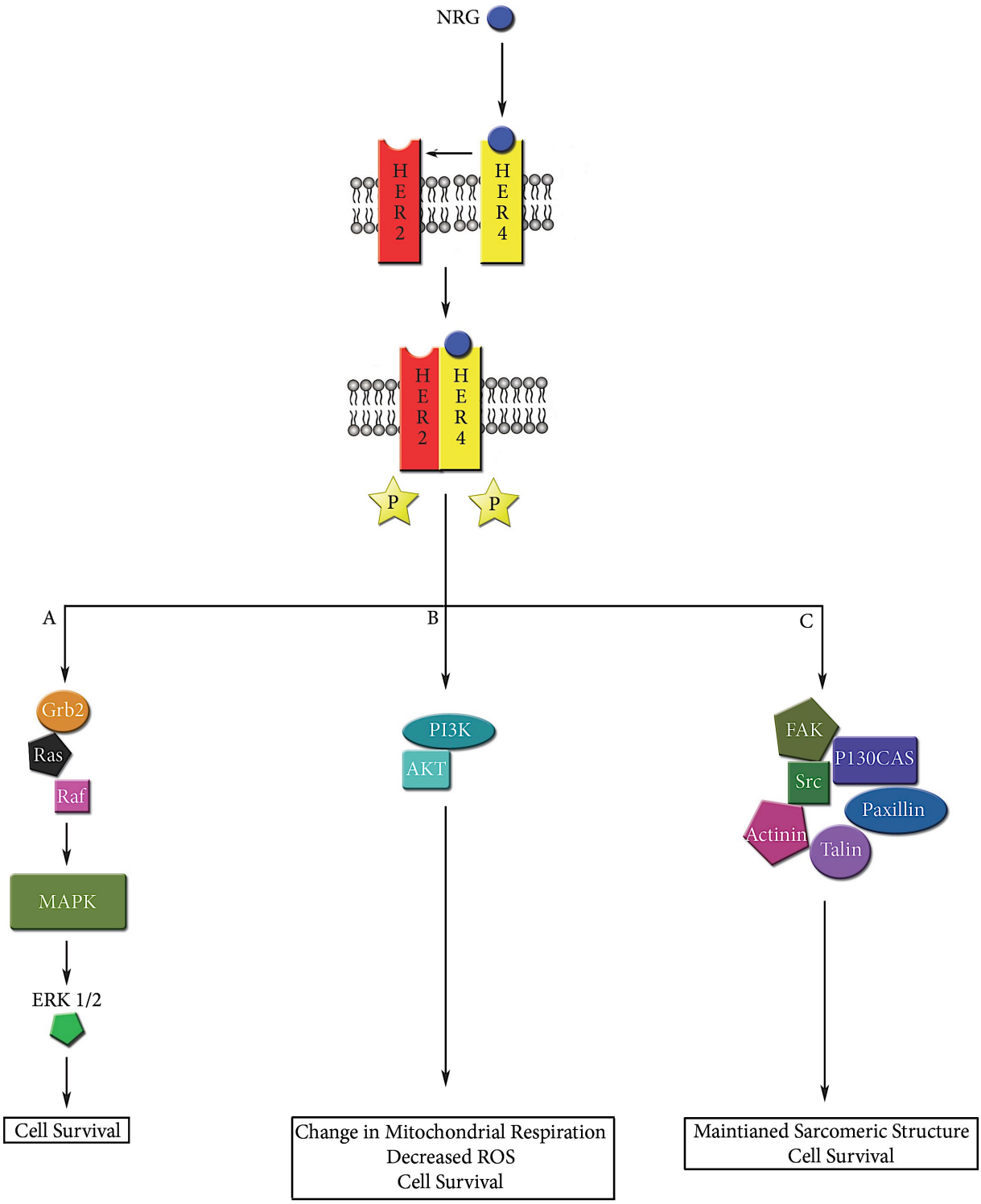
NRG
HER2
HER4
HER2
HER4
P
P
A
B
C
Grb2
Ras
Raf
MAPK
ERK 1/2
Cell Survival
PI3K
AKT
Change in Mitochondrial Respiration
Decreased ROS
Cell Survival
FAK
P130CAS
Src
Paxillin
Actinin
Talin
Maintianed Sarcomeric Structure
Cell Survival

Figure 2. Under normal physiological conditions, heterodimerization between HER2 and HER4 in cardiomyocytes initiates several cell survival signaling pathways including: A) MEK; B) PI3K/AKT; and C) FAK. MEK, MAPK/ERK kinase; PI3K, Phospholinostide-3 Kinase; Akt, Protein Kinase B; FAK, Focal Adhesion Kinase.[56, 58, 59]

Breast Cancer and Overexpression of HER2

Breast cancer is the second leading cause of cancer related deaths among Canadian women. Approximately 25% of women who present with breast cancer overexpress the HER2 receptor.[60-63] Overexpression of the HER2 receptor has been associated with more aggressive tumors and high mortality rate. Breast cancer overexpressing the HER2 receptor have anywhere between 25-to-50 copies of the HER2 gene, which corresponds with a 40-100 times increase in HER2 protein. This accounts for roughly 2 million HER2 receptors expressed within tumor cells. Therefore, due to an increase in receptors, there is a significant up-regulation of cell survival pathways within the cell allowing the tumor to evade apoptosis and enter the cell cycle.

Fortunately, HER2 overexpression is a fairly early event in the progression of human breast cancers. Therefore, early diagnosis is key, as receptor amplification is consistent with invasiveness, and nodal and distant metastasis throughout the progression of the disease. Only 20% of metastases are HER2 positive suggesting that many *in situ* tumors never develop into an invasive state. Methods for early diagnosis of HER2 overexpression include: immunohistochemistry (IHC), fluorescence in situ hybridization (FISH), chromogenic *in situ* hybridization (CISH) and silver-enhanced *in situ* hybridization (SISH).[64, 65] Immunohistochemistry and FISH are the most commonly used

methods for detecting HER2 overexpression in Canadian centers. Immunohistochemistry uses monoclonal or polyclonal antibodies that recognize and bind to the HER2 protein in a tissue section taken during a biopsy. The relative amount of staining is then scored: a score of 0-1 is considered negative; a score of 2 is uncertain; and a score of 3 is positive.[66-69]

Trastuzumab and Inhibition of HER2

Trastuzumab (Herceptin, Genetech Inc) is a humanized monoclonal antibody directed against the extracellular domain of the HER2 receptor.[70-73] It acts by binding to the extracellular domain of HER2, thereby preventing its ability to dimerize with other HER receptors, specifically HER4 in the heart. The inhibition of HER2 has a significant affect on several downstream cell survival signaling pathways including MAPK/ERK 1/2, PI3K/AKT, and FAK.[56, 59, 74, 75] A study by Sliwkowski *et al*. 1999 demonstrated that Trastuzumab (TRZ) is able to reduce the number of SK-BR-3 cells undergoing S-phase and increase the number of cells that arrest in G_0/G_1.[76] This reduction of S-phase and subsequent increase of cells in G_0/G_1 is attributed to the increased production of $p27^{kip1}$ and p130, a retinoblastoma related protein, by TRZ.[61, 76]

Trastuzumab and the Clinical Setting

In Canada, TRZ is only used for women who have an IHC score of 3 or a positive FISH test.[67] Fluorescence *in situ* hybridization uses fluorescence probes that bind to the HER2 gene within the nuclei. This allows for quantification of the number of HER2 gene copies being expressed and determines whether excessive copies of the HER2 gene are present, as observed in women with HER2 positive breast cancer.

As TRZ targets the extracellular domain of the HER2 receptor, it is highly effective in treating breast cancers in which HER2 is overexpressed. Clinical trials have demonstrated that TRZ is highly efficacious in both the adjuvant and metastatic breast cancer settings. When used in conjunction with chemotherapy, TRZ reduces the risk of cancer related death by 33%.[63, 77-83] In the adjuvant setting, TRZ is generally administered weekly for one year following a complete course of anthracycline-based chemotherapy. Conversely, in the metastatic setting, TRZ is administered with a primary loading dose, followed by tri-weekly maintenance doses.[84] Further studies have evaluated the use of TRZ as a front-line treatment option when used in addition to chemotherapeutic agents such as paclitaxel or anthracycline/cyclophosphamide therapies.[78, 85] Additionally, TRZ has been administered as a monotherapy with varying success in the metastatic setting.[77, 81, 86]

The beneficial use of TRZ in the adjuvant setting has been evaluated in four large multi-center randomized controlled studies. These studies included the Herceptin Adjuvant trial (HERA), National Surgical Adjuvant Breast and Bowel Project trial B-31 (NSABP), North Central Cancer Treatment Group Trial N9831 (NCCTG-N9831), and the Breast Cancer International Research Group 006 data trial (BCIRG 006).[63, 70, 79, 87] These studies evaluated the use of TRZ following anthracycline treatment.[63, 70, 79, 87] There was an overall reduction in both mortality and recurrence of malignancies in women who received TRZ therapy by 33% and 50% respectively. Given the overall positive results from these landmark trials, TRZ is now a key component in the anthracycline/taxane based chemotherapy treatments for breast cancer.

While TRZ is not approved for monotherapy treatment in metastatic breast cancer, its efficacy has been evaluated when used in conjunction with standard chemotherapy treatment in clinical trials. Of the approximately 10% of women who present with metastatic breast cancer, 35-45% present with overexpression of HER2.[78] Palliative care is often the best course of treatment for these patients. In 2001, Slamon *et al*. evaluated the efficacy and safety profile of TRZ in the metastatic setting. A total of 469 patients with metastatic breast cancer were randomized to receive either standard chemotherapy (DOX/EPI and cyclophosphamide) alone (n=234) or chemotherapy plus TRZ (n=235).[78] Women who had previously received anthracycline (DOX/EPI) therapy were randomized to receive paclitaxel (n=96) or paclitaxel plus TRZ (n=92). Women who had not previously received anthracycline (DOX/EPI) therapy were randomized to a treatment regimen of anthracycline (DOX/EPI) plus cyclophosphamide (n=143), or the combination of anthracycline (DOX/EPI), cyclophosphamide and TRZ (n=138).[78] DOX ($60mg/m^2$) or EPI ($75mg/m^2$) were administered in combination with cyclophosphamide ($600mg/m^2$) once a week for 6 weeks. Women receiving TRZ were administered a standard loading dose of 4mg/kg followed by weekly maintenance doses of 2mg/kg and was continued until evidence of disease progression. Median overall survival of the group receiving DOX, cyclophosphamide and TRZ was 25.1 months, in contrast to 20.3 months with anthracycline and cyclophosphamide treatment alone ($p=0.046$).[78] Women receiving chemotherapy plus TRZ also demonstrated a longer time to disease progression (7.4 months vs. 4.6 months; $p<0.001$) as well as a greater rate of objective response (50% vs. 32%; $p<0.001$). Overall, women receiving chemotherapy plus TRZ experienced a 20% mortality risk reduction. The most prevalent side effect due to treatment was the

development of adverse cardiac dysfunction and was highest in women who underwent therapy with an anthracycline, cyclophosphamide, and TRZ (39 of 143; 27%). In women receiving anthracycline and cyclophosphamide alone, 11 of 135 (8%) experienced CHF symptoms. Twelve of 91 (13%) women who underwent therapy with paclitaxel plus TRZ and 1 of 95 (1%) whom underwent therapy with paclitaxel alone developed cardiac dysfunction and CHF. Of this population, the prevalence of New York Heart Association (NYHA) class III or IV CHF was highest (16%) in the group that received DOX/EPI, cyclophosphamide plus TRZ compared to women who were administered anthracycline and cyclophosphamide alone (3%), paclitaxel plus TRZ (2%) and paclitaxel alone (1%). Taken together, these results suggest that combination therapy of TRZ with anthracycline (DOX/EPI)/cyclophosphamide treatment in women who overexpress HER2 is beneficial and leads to an overall improved survival rate, albeit at an increased risk of developing LV systolic dysfunction.

Trastuzumab-induced Cardiac Dysfunction

Despite the therapeutic benefits of TRZ in the breast cancer setting, cardiotoxicity remains a major issue. This drug-induced cardiotoxicity is potentiated when TRZ is used following anthracycline-based treatments. The most adverse side effect of adjuvant TRZ treatment is the development of NYHA class III and IV CHF (Table 3). Out of the four major clinical trails, approximately 5-10% of women who receive adjuvant TRZ therapy developed LV systolic dysfunction.

Class	Patient Symptoms
Class I (Mild)	No limitation of physical activity. Ordinary physical activity does not cause undue fatigue, palpitation, or dyspnea (shortness of breath).
Class II (Mild)	Slight limitation of physical activity. Comfortable at rest, but ordinary physical activity results in fatigue, palpitation, or dyspnea.
Class III (Moderate)	Marked limitation of physical activity. Comfortable at rest, but less than ordinary activity causes fatigue, palpitation, or dyspnea.
Class IV (Severe)	Unable to carry out any physical activity without discomfort. Symptoms of cardiac insufficiency at rest. If any physical activity is undertaken, discomfort is increased.

Table 3. Classification of New York Heart Association heart failure[88]

The prevalence of symptomatic CHF in these clinical studies was lower than the prevalence of asymptomatic CHF. The BCIRG 006 compared the use of AC treatment with and without subsequent docetaxel plus TRZ therapy. They demonstrated that women who received docetaxel following AC therapy were less likely to relapse than those who received doxetaxel alone. Furthermore, women who received a combination of docetaxel and TRZ demonstrated a 39% risk reduction of breast cancer recurrence. In the HERA trial, the incidence of severe symptomatic heart failure in women receiving TRZ was less then 1%, whereas in Trial B-31, the incidence of CHF was 4.1%.[78] Furthermore, Trial N9831 demonstrated that 2.9% of patients who underwent TRZ therapy developed symptomatic NYHA class III/IV heart failure. Although it is difficult to compare these trials, there appears to be some agreement that the incidence of symptomatic heart failure

lies between 0-4% in women treated with TRZ. As a guideline for physicians, the Cardiac Review and Evaluation Committee has developed four general criteria that signify TRZ-mediated cardiac dysfunction. These include: (i) symptoms of heart failure; (ii) symptoms associated with CHF including S3 gallop or tachycardia; and (iii) a greater than 5% decline in LVEF associated with CHF symptoms, or a greater than 10% decline in LVEF without symptoms of CHF.[89]

While clinical trials have demonstrated that 5-10% of all patients treated with TRZ in the adjuvant setting develop asymptomatic cardiac dysfunction and 0-4% of patients develop symptomatic CHF, little is known regarding the prevalence of TRZ-mediated cardiac dysfunction in the real world. Wadhwa *et al*. 2009 conducted a retrospective study and evaluated 152 HER2 positive breast cancer patients who received adjuvant TRZ therapy.[90] Of the 152 women, 36 (24%) developed TRZ-mediated cardiac dysfunction, of which 31 (86%) were asymptomatic and 5 (14%) were symptomatic. It is interesting to note that the development of TRZ-mediated cardiac dysfunction could be predicted in this population if the woman had a pre-existing history of hypertension, smoking, family history of coronary artery disease and/or have used diuretics. Although LVEF was reduced in all patients who underwent TRZ therapy, at three-month follow-up, LVEF was significantly lower in the 36 patients that developed CHF as compared to those who did not display evidence of cardiotoxicity (61±5 % vs. 51±8% respectively). At 6-month follow-up, cardiac magnetic resonance imaging (CMR) demonstrated sub-epicardial linear delayed enhancement of the lateral wall of the LV in 34/36 (94%) women, confirming TRZ mediated cardiac dysfunction. Upon discontinuation of TRZ, 20 of 36 (55%) regained LV systolic function and demonstrated an increase in LVEF >50%

at 6 months. TRZ was restarted in 4 of the 20 (20%) women in combination with ACEi and βB with no further evidence of cardiac dysfunction. However, of the 16 of 20 women in which TRZ was not re-administered, 10 (63%) demonstrated no improvement in LVEF (39±5%) and 6 (38%) demonstrated further impairment of cardiac function with an average LVEF of 25±5%. A selection bias may account for the conflicting reports between the real world study by Wadhwa *et al.* 2009 and the large-scale clinical trials. The large clinical trials excluded women if they had a pre-existing history of CHF, coronary artery disease, valvular disease, poorly controlled hypertension, and LVEF less than 55% following chemotherapy. Conversely, Wadhwa *et al.* 2009 included those women with cardiovascular risk factors including hypertension, diabetes, hyperlipidemia, and a history of smoking and coronary artery disease. Additionally, these risk factors were directly correlated with and increased susceptibility to the development of heart failure following TRZ. While large-scale clinical trials have indicated that the incidence of TRZ mediated cardiac dysfunction (asymptomatic and symptomatic) is less than 10%, this was the first trial to report that in a real world setting, the incidence of cardiac systolic dysfunction due to TRZ therapy is higher than previously indicated.

In the metastatic setting, 27% of women who received AC and TRZ treatment developed NYHA class III or IV heart failure. In contrast, only 8% who received AC treatment alone or 13% who were treated with TRZ and paclitaxel developed NYHA class III or IV heart failure. This finding led to the recommendation that anthracycline plus TRZ therapy should not be used concurrently to avoid the development of severe cardiac dysfunction. While there is a high risk of developing adverse cardiac dysfunction

with TRZ, the risk is warranted due to a limited number of treatment options for metastatic breast cancer.

Mechanisms of Trastuzumab-induced Cardiac Dysfunction

While the underlying mechanisms for DOX-induced cardiac dysfunction have been extensively explored,[18-20, 25, 26, 33, 34] little is known regarding the mechanisms of TRZ-induced cardiac dysfunction. Several theories have been proposed including: (i) an alteration in the anti- to pro-apoptotic protein ratio; (ii) decreased cell survival through inhibition of NRG-1/HER2 signaling; and (iii) activation of the renin-angiotensin system (RAS).[56, 59, 75, 86, 91-94]

First, the binding of TRZ to HER2 has been correlated with a significant change in the ratio between anti- and pro-apoptotic proteins. Upon binding to HER2, there is an immediate down-regulation of the anti-apoptotic protein Bcl-$X_{L,}$ and up-regulation of the pro-apoptotic protein Bcl-X_S.[93] The ratio of anti- to pro-apoptotic proteins from the Bcl protein family is significant, as they are key mediators in mitochondrial function and apoptosis. Therefore, while an increase in pro-apoptotic proteins is beneficial in cancer treatment, it is also correlated with mitochondrial dysfunction, leading to cardiomyocyte death.[93, 95]

Second, TRZ binds to HER2 with high affinity, thereby eliminating its ability to dimerize with other HER receptors. By inhibiting HER2's ability to dimerize and signal cell survival through MAPK/ERK 1/2, PI3K/AKT, and FAK dependent pathways, cardiomyocytes are unable to deal with added stress.[56, 59, 75] As cardiomyocytes are constitutively active cells, there is a large demand for adenosine triphosphate (ATP) production in the mitochondria, which are prone to the generation of ROS. Fortunately,

endogenous antioxidants are able to scavenge the majority of ROS from the mitochondria. However, there is a limited antioxidant reserve. By blocking HER2 signaling, cardiomyocytes are unable to activate cell survival pathways that are able to cope with the excess ROS. Therefore, blockage of HER2 causes the accumulation of ROS within the cardiomyocytes, leading to the development of cardiac dysfunction by stimulating cardiomyocyte apoptosis.[74, 95]

The third mechanism that has been proposed for HER2 mediated cardiotoxicity includes the over activation of the RAS. When TRZ binds HER2 and inhibits cell survival signaling pathways, there is an added stress placed on the myocardium. This added stress leads to an increase in circulating levels of angiotensin II (ANG II), which has three major effects on the heart. First, ANG II is a potent inhibitor of NRG-1 signaling. By decreasing the amount of NRG-1 protein that is produced, ANG II can directly inhibit cell survival signaling pathways. Second, ANG II acts by preventing NRG-1 protein from binding to the HER4 receptor (Figure 3). This further decreases the activation of cell survival pathways by preventing other members of the HER family from forming dimers and initiating cell survival pathways. Third, ANG II leads to the activation of NAD(P)H oxidase (Figure 3).[86, 94] Angiotensin II binds to the angiotensin 1 (AT1) receptor, a well-known G-protein coupled receptor, which activates NOX through a protein kinase C dependent action.[86] NOX produces the potent ROS superoxide and begins a vicious cycle of superoxide production leading to enhanced accumulation of ROS. Accumulation of ROS within the heart further potentiates cardiac damage.

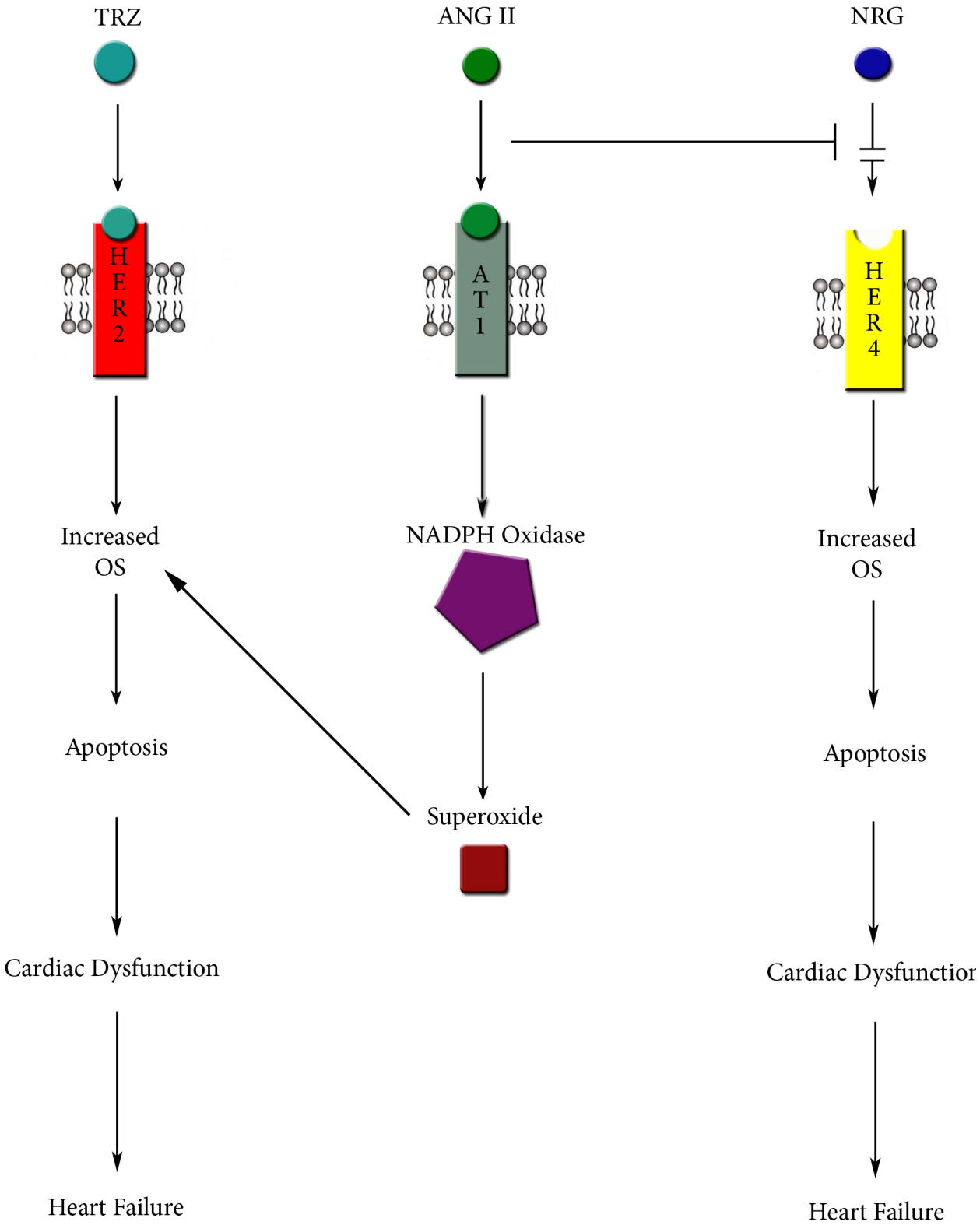
TRZ
ANG II
NRG
HER2
AT1
HER4
Increased OS
NADPH Oxidase
Increased OS
Apoptosis
Superoxide
Apoptosis
Cardiac Dysfunction
Cardiac Dysfunctior
Heart Failure
Heart Failure

Figure 3. TRZ inhibits HER2 signaling which leads to the production of ROS. First, activation of the angiotensin 1 receptor leads to activation of NOX and the production of free radicals. Second, angiotensin II is a potent inhibitor of NRG-1 signaling which further inhibits cell survival and increases ROS. TRZ, Trastuzumab; ROS, Reactive Oxygen Species; OS, Oxidative Stress; NOX, NAD(P)H oxidase; NRG-1, Neuregulin-1.[86, 94]

Reversibility of Trastuzumab-induced Cardiac Dysfunction

Unlike anthracycline-induced cardiotoxicity, TRZ-mediated cardiac dysfunction is not dose dependent.[96-99] Furthermore, unlike DOX-induced cardiotoxicity, TRZ-induced cardiac dysfunction may be partially reversible.[90, 96-99] In 2005, Ewer *et al*. evaluated the reversibility of TRZ-induced cardiac dysfunction.[96] The average LVEF at baseline was 61±13% and decreased to 43±13% following TRZ treatment. In this study, immediate discontinuation of TRZ therapy was the result of a significant drop in LVEF or the identification of symptomatic CHF.[100] Ewer *et al*. 2005 found that 1.5 months after discontinuing TRZ therapy, LVEF returned to baseline values. Of the 38 women enrolled in the study, 20 experienced symptoms of CHF while 16 were asymptomatic. Thirty-one patients underwent standard medical therapy for CHF including ACEi and βB. These patients either recovered cardiac function or entered a period of stability. To further examine the reversibility of TRZ-mediated cardiac dysfunction, 25 women were re-challenged with TRZ. Interestingly, 22 of the 25 patients (88%) did not display any further reductions in LVEF.[96] Unfortunately, 3 of the 25 women (12%) experienced a further decline in LVEF and were permanently removed from TRZ therapy.

Despite these promising results, the extent to which TRZ-induced cardiac dysfunction is reversible remains unknown. A retrospective study by Wadhwa *et al*. 2009 demonstrated that 34 of 36 women demonstrated sub-epicardial linear delayed enhancement of the lateral portion of the left ventricle on CMR that persisted for up to 6 months.[90] Only 20 of the 36 patients (56%) completely recovered LVEF from TRZ-mediated cardiac dysfunction within a 6-month period. Despite aggressive high-dose treatment with ACEi and βB, 16 patients had no change or worsening of LVEF values. Although the therapeutic benefits of TRZ therapy are extensive, approximately 25% of women may experience adverse cardiac side effects including LV systolic dysfunction. Although cardiac function may recover following discontinuation of TRZ[89, 96, 97, 99, 101] the presence of delayed enhancement of the mid myocardium on CMR brings into question the true reversibility of TRZ mediated cardiac dysfunction.[90] Caution should still be taken when weighing the benefits and risks of TRZ therapy.[102]

Early Detection of TRZ-induced Cardiac Dysfunction: Non-invasive Imaging

Basic Science

Early detection and monitoring of breast cancer patients receiving TRZ is useful in the prevention of TRZ-induced cardiac dysfunction. Non-invasive monitoring of LV systolic function is useful to identify chemotherapy-induced cardiac dysfunction. Multi-gated acquisition scans (MUGA), echocardiography, and CMR are useful non-invasive tools to serially monitor cardiac function in this patient population.[92, 103-105] Although MUGA and two-dimensional (2D) transthoracic echocardiography (TTE) are routinely used and reproducible methods for the assessment of LVEF, once EF decreases below 40%, irreversible cardiac injury may have already occurred.

In the emerging field of Cardio-Oncology, early indices of left ventricular (LV) systolic dysfunction would be useful for addressing the cardiac safety profile of cancer drugs, potentially avoiding the detrimental effects of end stage heart failure. Tissue velocity imaging (TVI) and strain imaging, are sensitive, non-invasive echocardiographic techniques that allow for the early detection of LV systolic dysfunction, prior to a decrease in conventional LVEF.[106-108] Neilen *et al*. 2006 described the use of tissue velocity imaging (TVI) in a murine model of DOX-induced cardiac dysfunction.[109] They found that there was a significant reduction in TVI parameters including endocardial velocity (V_{Endo}) and strain rate (SR) prior to any changes in traditional LVEF. Recently, Jassal *et al*. 2009 validated the use of TVI in a murine model of DOX+TRZ mediated cardiotoxicity.[3] They found that in an acute murine model of DOX+TRZ induced cardiac dysfunction, a significant reduction in V_{Endo} was detected as early as 24 hours post-treatment, whereas LVEF did not change until day 3. This early decrease in V_{Endo} was found to be a reliable, reproducible marker in predicting future LV systolic dysfunction. This basic science study was the first to validate the use of TVI in the detection of DOX+TRZ induced cardiac dysfunction.[3] In the clinical setting, the use of TVI to detect early subtle changes in the myocardium requires further evaluation.

Clinical Setting

Although MUGA and TTE are common modalities for monitoring cardiac function in the clinical setting, each has its limitations.[92, 103-105] MUGA scans are highly reproducible and demonstrate low intra- and inter-observer variability. However, the use of ionizing radiation limits its clinical use.[103, 104] Transthoracic echocardiography studies are easy to acquire and do not have an issue with radiation. Transthoracic

echocardiography, however, has a greater intra- and inter-observer variability as compared to other non-invasive imaging modalities.[105] Cardiac MRI (CMR) is considered the gold standard for non-invasively monitoring LVEF. However due to its high cost and low availability, its use for monitoring LV systolic dysfunction in breast cancer patients who experience cardiotoxicity is limited.[110, 111]

A recent study by Walker *et al*. 2010 evaluated the use of real time three-dimensional transthoracic echocardiography (RT3D-TTE) for the evaluation of cardiac function in the breast cancer setting.[92] A cohort of 50 women underwent MUGA, 2D TTE, RT3D-TTE and CMR at baseline, 6 month and 12-month follow-up. Serial analysis revealed a low correlation between 2D-TTE and CMR (r = 0.31, 0.53, and 0.42 at baseline, 6 months and 12 months respectively). On the contrary, serial LVEF values assessed by RT3D-TTE and CMR had a significant correlation at all three time points (r = 0.91, 0.97, and 0.90 at baseline, 6 months and 12 months respectively). These results were similar to the comparison made between MUGA and CMR (r = 0.88, 0.97 at baseline, 6 months and 12 months respectively).[92] Despite an inherent underestimation of LVEF by RT3D-TTE, this study suggests that RT3D-TTE is a feasible and reproducible method for assessing LVEF in the breast cancer setting.

To expand our basic science work to the clinical arena, we sought to determine whether non-invasive cardiac imaging would be useful in the early detection of TRZ-induced cardiac dysfunction. We recently evaluated the utility of cardiac biomarkers, TVI and strain imaging, and CMR for predicting early LV systolic dysfunction in HER-2 positive breast cancer patients treated with TRZ in the adjuvant setting. Ten of 42 (24%) patients developed TRZ mediated cardiac dysfunction within 3 months of treatment. As

compared to TVI and strain, traditional measures of LV systolic dysfunction, specifically LVEF, did not change until 6 months in this patient population. This study was able to confirm that both TVI and strain imaging were able to detect early, subtle changes in LV systolic function prior to conventional changes in LVEF, in women receiving TRZ in the adjuvant setting. Four independent studies have recently confirmed this novel finding.[112-115]

Early Detection of TRZ-induced Cardiac Dysfunction: Cardiac Biomarkers

The use of cardiac biomarkers including troponin T (TnT), C-reactive protein (CRP) and brain natriuretic peptide (BNP) have previously been reported to be highly sensitive markers of anthracycline-mediated CHF. Our group has recently evaluated the use of cardiac biomarkers, TVI, and CMR in detecting early subtle changes in LV function in HER2 positive breast cancer patients receiving TRZ therapy.[116] A cohort of 42 women were prospectively enrolled in the study between 2007 and 2009 at a single tertiary care centre. All biomarkers were within normal limits at baseline. Although 25% of patients developed TRZ-mediated cardiac dysfunction, there were no significant changes in cardiac biomarkers amongst the women who developed TRZ-mediated cardiac dysfunction.

Unlike cardiac TnT (cTnT), cardiac TnI (cTnI) has been identified to be a sensitive marker for the early detection of TRZ-induced cardiac dysfunction.[115, 117-119] Studies, conducted by Cardinale *et al*. 2000, 2004, 2010 and Sawaya *et al*. 2011, have demonstrated that high dose chemotherapy treatment correlated well with an increase in cTnI levels and is a useful marker for detecting early reductions in LVEF and CHF.[115, 117-119] Additionally, Cardinale *et al*. 2000, 2004, 2010 found that cTnI was an important

early screening method for women who may be less likely to recover from TRZ mediated cardiac dysfunction, despite high-dose CHF therapy.[117-119] Elevated circulating cardiac biomarkers may be one of the best early indicators for diagnosing TRZ-mediated cardiotoxicity prior to the development of irreversible cardiac damage.

Prevention of Trastuzumab-induced Cardiac Dysfunction

Dexarozoxane

Doxorubicin exerts its cardiotoxic effects through anthracycline-iron complexes that are capable of catalyzing electron transfer, thereby forming free radicals.[39] The formation of free radicals through redox-cycling has been well documented. It is now well established that oxidative stress is a major component of DOX-mediated cardiac dysfunction.[39]

Dexrazoxane (DEX, Cardioxane®, Zinecard®) is a cyclic derivative of edetic acid and a cardioprotective agent in anthracycline-mediated cardiac dysfunction (Figure 4).[39] Unlike other cardioprotective agents, DEX acts by preventing free-radical formation, whereas most other pharmacological agents act by scavenging free radicals once they have formed.[39, 40, 120] Dexarozxane acts by preventing iron-based oxidative damage to cardiac mitochondria. Metal chelation of free or anthracycline-bound ferric ions in the myocardium is thought to be the mechanism by which DEX provides cardioprotection.[39, 40, 120] Numerous animal studies have demonstrated that there is a significant reduction in the number of cardiac lesions, and increased survival in those animals treated with DEX. Several clinical trials have evaluated the use of DEX as a cardioprotective agent.[121-123] Patients who received DEX demonstrated a significantly lower rate of cardiac events (>15%) compared to control (16-50%) and the incidence of CHF ranged from 0-3% in

the DEX-treated group. Despite the potential cardioprotective effects of DEX, its interaction with DOX limits its use within the clinical setting. This is due to the fact that DEX significantly reduces the cytotoxic abilities of DOX, thereby mitigating its efficacy within the breast cancer setting.[39]

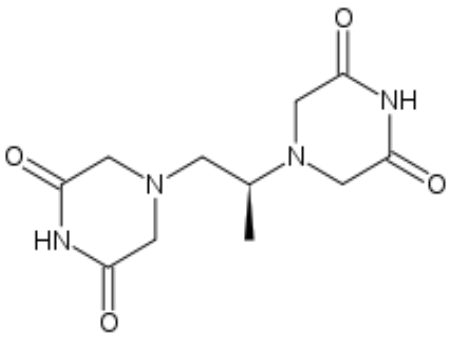

Figure 4. The chemical structure of Dexrazoxane 4-[(2S)-1-(3,5-dioxopiperazin-1-yl)propan-2-yl]piperazine-2,6-dione.[22]

Probucol

Probucol, IUPAC name 2,6-di-tert-butyl-4-({2-[(3,5-di-tert-butyl-4-hydroxyphenyl)sulfanyl]propan-2-yl}sulfanyl)phenol, is a lipid lowering agent, as well as a potent antioxidant (Figure 5).[22] Chemically, Probucol is composed of two butylated hydroxytoulene moieties that are connected by a sulfur-carbon-sulfur bridge. The active antioxidant feature of Probucol is its pair of biphenyl rings (Figure 5).

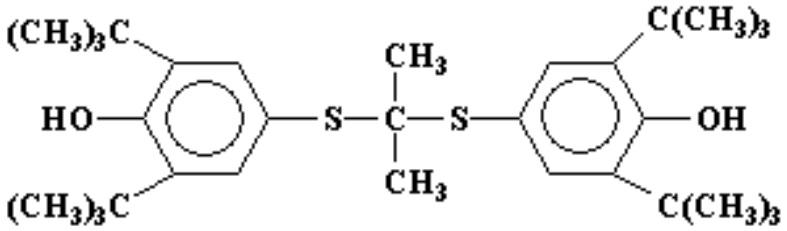

Figure 5. The chemical structure of Probucol 2,6-di-tert-butyl-4-({2-[(3,5-di-tert-butyl-4-hydroxyphenyl)sulfanyl]propan-2-yl}sulfanyl)phenol.[22]

Probucol was first identified in the mid 1970's as an efficacious lipid-lowering agent that acts by lowering LDL levels within the blood.[124, 125] It was later demonstrated that Probucol was more effective at reducing HDL than LDL.

Probucol is a potent antioxidant.[124, 126-128] It has been implicated to have significant cardioprotective effects in mice that receive anthracyclines, in particular, DOX.[126, 129, 130] It is well established that DOX therapy leads to the increased formation of ROS and the development of OS in the heart. Singal *et al*. 1995 and Siveski-Iliskovic *et al*. 1994 were the first to demonstrate that simultaneous treatment of rats that received

DOX with Probucol significantly reduced DOX-mediated cardiac dysfunction and subsequent CHF.[42, 124, 126, 128, 130] In a similar study, Siveski-Iliskovic *et al*. 1994, 1995 demonstrated that the addition of Probucol to DOX was able to completely rescue (100% survival) the mortality rate that is usually seen with DOX therapy.[42, 127] Furthermore, prophylactic treatment with Probucol was able to significantly decrease the cardiotoxic effects of DOX, rescue myocardial ATP/ADP nucleotide levels, attenuate progression of LV systolic dysfunction, and improve survival after myocardial infarction.

While there is significant evidence that Probucol can prevent DOX-induced cardiac dysfunction[26, 42, 124, 126-131], little is known on whether Probucol has cardioprotective effects when TRZ is added to DOX. Recent work by Walker *et al*. 2011 evaluated the cardioprotective effects of Probucol in an acute murine model of DOX+TRZ-induced cardiac dysfunction.[129] They demonstrated that co-administration of DOX+TRZ corresponded to an 80% mortality rate at day 5 and a 90% mortality by day 10. Conversely, mice prophylactically treated with Probucol demonstrated a mortality rate of only 10% at day 5 and 40% at day 10. Furthermore, they were the first to demonstrate that prophylactic treatment with Probucol may attenuate myofibril and LV systolic changes in the setting of DOX+TRZ therapy. Antioxidants, such as Probucol, are biologically important molecules as they are responsible for the neutralization of oxidative free radicals that are detrimental to the integrity and survival of the cell. However, at low physiological levels, ROS are biologically important cell signaling molecules that are critical regulators of numerous cellular processes such as cell proliferation, activation, and migration.[132-135]

Nitric Oxide

Nitric oxide (NO) is a free radical gas that is involved in a variety of physiological processes including vasodilation, angiogenesis, wound healing, and neuronal signaling.[136, 137] Nitric oxide and L-citrulline are produced following the oxidation of L-arginine (Figure 6).[136, 138-144] This reaction is catalyzed by three separate nitric oxide synthase (NOS) isoforms that include NOS1 (neuronal NOS, nNOS), NOS2 (inducible NOS, iNOS), and NOS3 (endothelial NOS, eNOS). NOS1 and NOS3 are constitutively expressed and are calcium (Ca^{2+})/calmodulin (CaM) dependent.[143, 145, 146] Therefore, NO production is directly correlated with intracellular Ca^{2+} levels.

Nitric Oxide Synthase 3

Nitric oxide synthase 3 (NOS3) is constitutively active in the vascular endothelium and cardiomyocytes.[143, 145, 146] It is the key mediator in the synthesis of NO through the 5 electron oxidation of a guanidine nitrogen of L-arginine to form L-citrulline in the presence of oxygen and NAD(P)H (Figure 6).[147] The NOS3 protein consists of two important domains including a N-terminal oxygenase domain and a reductase domain. The N-terminal domain consists of amino acids 1-491 and contains the binding site for heme, L-arginine (at Glu361), and tetrahydrobiopterin (H_4B).[147,148] The reductase domain occupies amino acids 492-1205 and contains the binding sites for FFMN, FAD, NAD(P)H and CaM.[147,149]

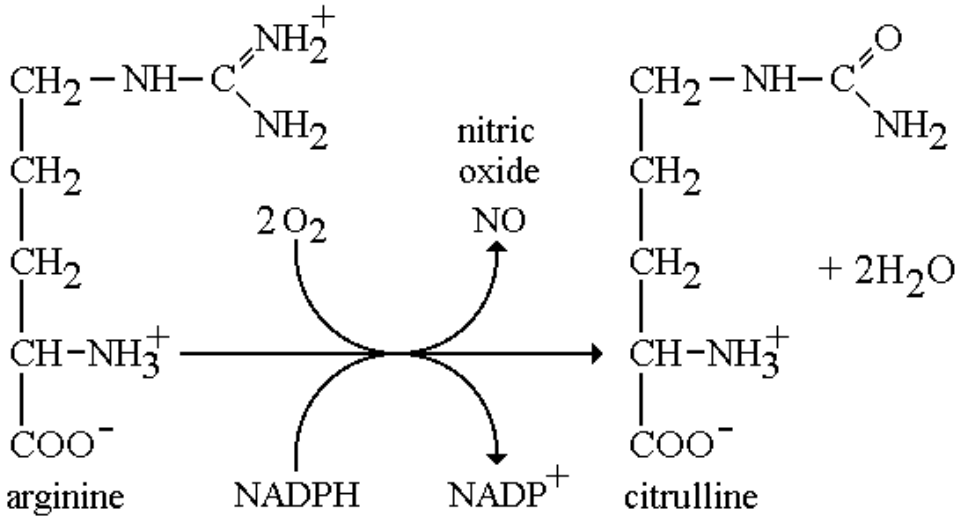

Figure 6. Schematic of the conversion of L-arginine to L-citruline by nitric oxide synthase 3(NOS3) and co-production of nitric oxide (NO).

All NOS isoforms consist of two identical subunits of 134 kDa that form an active dimer.[147,150] Tetrahydrobiopterin appears to be important in the homodimerization of the two NOS3 subunits. As individual monomers, these proteins are inactive and incapable of binding to L-arginine or H_4B.[147] Electrons are transferred from NAD(P)H to the reductase domain flavins before they can be transferred to the heme molecule located in the oxygenase domain. This is an important step as it catalyzes the formation of NO from L-arginine and is mediated by CaM binding to its binding domain between amino acids 493 and 512.[151, 152]

Nitric oxide synthase 3 has been implicated in several cardiac pathologies including chronic pressure overload, ischemia, myocardial infarction, and septic shock.[153-157] In each model, mice genetically lacking NOS3 ($NOS3^{-/-}$) demonstrated a significant increase in LV systolic dysfunction, hypertrophy and mortality. Ahmadie *et al*.

2010, recently described the effects of NOS3$^{-/-}$ on cardiac remodeling in a murine model of chronic pressure overload due to transverse aortic constriction (TAC).[157] Transthoracic echocardiography demonstrated an increase in posterior wall thickness (PWT) in all 4 groups (WT + low lipid diet (LLD), WT + high lipid diet (HLD), NOS3$^{-/-}$ + LLD, NOS3$^{-/-}$ + HLD) at week 12 compared to baseline. Furthermore, TTE also demonstrated increased LV end-diastolic diameter (LVEDD) at week 12 in all groups. This increase in LVEDD was significantly potentiated in the NOS3$^{-/-}$ + HLD group ($p<0.05$). Further TTE analysis demonstrated significant reductions in LVEF ($p<0.05$), TVI ($p<0.05$), and SR ($p<0.05$) at week 12 in all 4 groups. NOS3$^{-/-}$ + HLD also demonstrated significant ($p<0.05$) reductions in LVEF, TVI, and SR at week 12 compared to the other groups. Histological evidence further corroborated TTE analysis, as the NOS3$^{-/-}$ + LLD and NOS3$^{-/-}$ + HLD demonstrated LV hypertrophy (LVH) compared to WT mice fed the same diet. Molecular evidence of increased hi-FGF-2 was greater in the NOS3$^{-/-}$ + HLD group compared to their WT controls at week 12 post-TAC, as well as compared to NOS3$^{-/-}$ + LLD mice at week 12 post-TAC. This study demonstrated that NOS3$^{-/-}$ mice, which underwent TAC and fed a HLD, displayed increased LV systolic dysfunction, LV hypertrophy, fibrosis, and coronary intimal thickening when compared to all other groups.[157] This result lends evidence that mice fed a HLD potentiates cardiac remodeling in NOS3$^{-/-}$ mice in a model of chronic pressure overload. These results were in agreement with those previously reported by Ichinose *et al*. 2004, and Ruetten *et al*. 2005.[155] Furthermore, histological evidence supports the TTE data as it displayed a significant increase in LVH in the NOS3$^{-/-}$ group.[157] Therefore, it is evident from these studies that various models of cardiovascular injury (chronic pressure overload, ischemia, myocardial

infarction, and septic shock) lead to significant LV systolic dysfunction in NOS3$^{-/-}$ mice as compared to WT.

NOS3, Doxorubicin, and Cardiac Dysfunction

Doxorubicin binds to all three isoforms of NOS (NOS1, NOS2, NOS3) preferentially to the reductase domain.[158, 159] This leads to immediate inhibition of the NOS enzyme and subsequent reduction of DOX.[158, 159] NOS3 demonstrates the highest affinity for DOX among the NOS isoforms.[159] The reduction of DOX on the reductase domain significantly alters the NO:superoxide ratio. This is important to note as this has the potential to generate peroxynitrite and hydrogen peroxide, two potent oxidants that are capable of potentiating cardiac dysfunction.[160]

Vasquez-Vovar *et al*. 1997 and Griffith and Stuehr 1995 found that DOX binding to the reductase domain diverts electron flow away from the oxygenase domain decreasing the amount of available NO and increasing the levels of superoxide.[158, 161] They further demonstrated this by administering L-NAME, a known inhibitor of the oxygenase domain. The reaction was not inhibited and therefore not dependent on Ca^{2+} and CaM. Therefore, they concluded that NOS3 can shift from a NOS to a NAD(P)H oxidase and mediate the formation of superoxide rather than NO.[158, 161] This causes a shift in the NO:superoxide ratio in favor of superoxide. Additionally, this alteration has been implicated in the production of peroxynitrite and subsequent development of cardiac dysfunction.[158, 161]

Previously, Neilan *et al*. 2007 demonstrated that NOS3 and oxidative stress might contribute to the pathogenesis of DOX mediated cardiac dysfunction, in a predominantly male murine model (>95%) of DOX-induced cardiac dysfunction.[162] This study was not

powered to detect any potential gender differences amongst the transgenic mice. Following the administration of DOX, $NOS3^{-/-}$ male mice demonstrated preserved LV systolic function and reduced production of ROS and apoptosis as compared to WT.[162] As administration of DOX leads to superoxide production in cardiac tissues of WT male mice, but not $NOS3^{-/-}$ mice, this suggests that DOX induces cardiac ROS production via a NOS3 dependent mechanism.[162] Genetic disruption of NOS3 ($NOS3^{-/-}$ mice) thus protected against DOX-induced cardiac dysfunction, injury and mortality in a male model of chemotherapy induced cardiac dysfunction. On the other hand, transgenic male mice with systemic overexpression of NOS3 ($NOS3^{TG}$) demonstrated increased degree of LV systolic dysfunction in this male model of anthracycline-induced cardiomyopathy.[162]

Although the previous study[162] confirms an important role for NOS3 as a key mediator in ROS production in a predominantly male model of DOX induced cardiotoxicity, little is known about the role of NOS3 and ROS in a clinically relevant female murine model. As breast cancer predominantly affects women, the role of NOS3 and oxidative stress in a female model of DOX+TRZ mediated heart failure needs to be further evaluated.

Study Rationale

Working Hypothesis

Congenital absence of NOS3 ($NOS3^{-/-}$) is cardioprotective against the effects of DOX+TRZ treatment in a clinically relevant female murine model of chemotherapy-induced heart failure.

Aim 1: To determine the effects that congenital absence of NOS3 ($NOS3^{-/-}$) has *in vivo*, in a clinically relevant female murine model of acute DOX+TRZ mediated cardiac dysfunction.

Hypothesis: Congenital absence of NOS3 ($NOS3^{-/-}$) will attenuate DOX+TRZ mediated cardiac dysfunction and injury, and reduce mortality. Furthermore, we hypothesize that as compared to WT controls, female $NOS3^{-/-}$ mice will be characterized by preserved LV systolic function, and decreased mortality. Specifically, we will focus on the degree of LV systolic dysfunction, and histological damage including vacuolization and cytoplasmic clearing in WT C57Bl/6 and $NOS3^{-/-}$ female mice treated with DOX, TRZ or the combination of DOX+TRZ.

Aim 2: To determine the effect congenital absence of NOS3 ($NOS3^{-/-}$) has on the apoptotic process in a clinically relevant female murine model of acute DOX+TRZ mediated cardiac dysfunction.

Hypothesis: A congenital absence of NOS3 ($NOS3^{-/-}$) will attenuate DOX+TRZ mediated apoptosis. We hypothesize that as compared to WT controls, female $NOS3^{-/-}$ mice will demonstrate elevated levels of the anti-apoptotic protein Bcl-X_L and decreased levels of the pro-apoptotic proteins Bax, Caspase 3, and PARP.

Chapter 2: Methodology

All animal procedures were conducted in accordance with the guidelines published by the Canadian Council on Animal Care. All procedures, including drug administration and longitudinal echocardiographic studies, were approved by the Animal Protocol Review Committee at the University of Manitoba.

Animal Model

A total of 120, 7 to 8 week old C57Bl/6 female mice (60 WT, and 60 $NOS3^{-/-}$; Jackson Laboratories, MA) were randomized into 4 treatment categories including: (1) 0.9% saline; (2) TRZ; (3) DOX; or (4) DOX+TRZ (Figure 7).

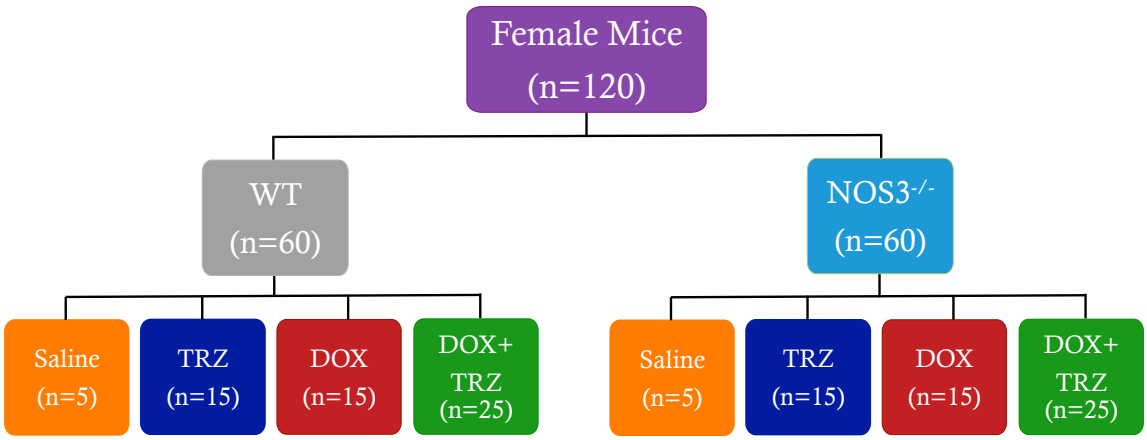

Figure 7. A flow diagram representing the treatment regimens algorithm and the number of animals randomized to each treatment arm. WT, Wild type; $NOS3^{-/-}$, Nitric Oxide Synthase 3 Knock-out; TRZ, Trastuzumab; DOX, Doxorubicin.

All female mice were quarantined for 1 week, prior to being randomized to each treatment arm. Prior to chemotherapy administration, all mice underwent baseline TTE and weight analysis. Single intraperitoneal (IP) injections of 0.9% saline, DOX (20mg/kg), TRZ (10mg/kg), or DOX (20mg/kg) + TRZ (10mg/kg) were administered following baseline data acquisition (Figure 8). Serial echocardiography and weight measurements were performed daily for 10 days at which point surviving female mice were euthanized and their hearts preserved for histological and biochemical analyses (Figure 8).

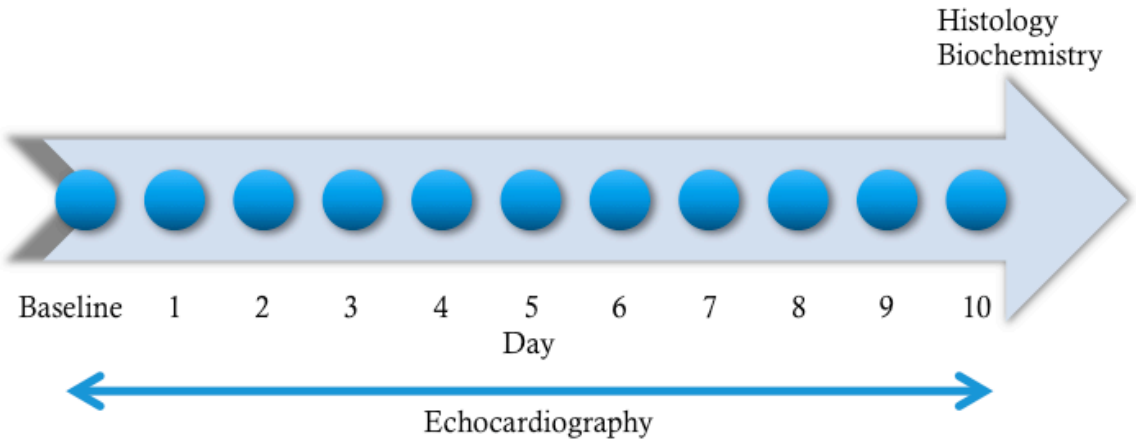

Figure 8. Methodology timeline. Prior to receiving acute treatment (0.9% saline, DOX, TRZ, or DOX+TRZ), all mice underwent baseline echocardiography to determine cardiac function. Following acute therapy, mice were followed daily to assess cardiac dimensions and function. At day 10, all surviving mice were euthanized and the hearts removed for histological and biochemical analyses. DOX, Doxorubicin; TRZ, Trastuzumab.

Echocardiography

Non-invasive assessment of cardiac function was performed via murine echocardiography in awake mice.[3, 129, 157, 163] All echocardiographic data was collected using a 13-MHz probe (Vivid 7, GE Medical Systems, Milwaukee, WI, US) capable of TVI. Each mouse was imaged in the parasternal long (PLAX) and short (SAX) axis windows, as previously described.[3, 129, 157 162, 163] All post processing of images was conducted offline using the EchoPAC PC software (Vivid 7, GE Medical Systems, Milwaukee, WI, US). In the PLAX window, LVEF was determined by manually tracing the LV end-diastolic and end-systolic volumes (Figure 9). LV cavity dimensions including LVEDD, LVESD, PWT, and interventricular septal thickness (IVS), were calculated using M-mode echocardiography.[3, 129, 157 162 163] Furthermore, TVI was acquired in the parasternal SAX window at the level of the papillary muscles at a rate of at least 483 FPS, from a 0.2 mm x 0.2 mm region of interest in the posterior wall of the LV (Figure 10).[3, 157 163, 164]

$$\text{Ejection Fraction (EF)} = \left(\frac{\text{LVEDv (cc)} - \text{LVESv (cc)}}{\text{LVEDv (cc)}}\right) * 100$$

Figure 9. Determination of left ventricular ejection fraction (LVEF). LVEDv, left ventricular end-diastolic volume; LVESv, left ventricular end-systolic volume; cc, cubic centimeter.

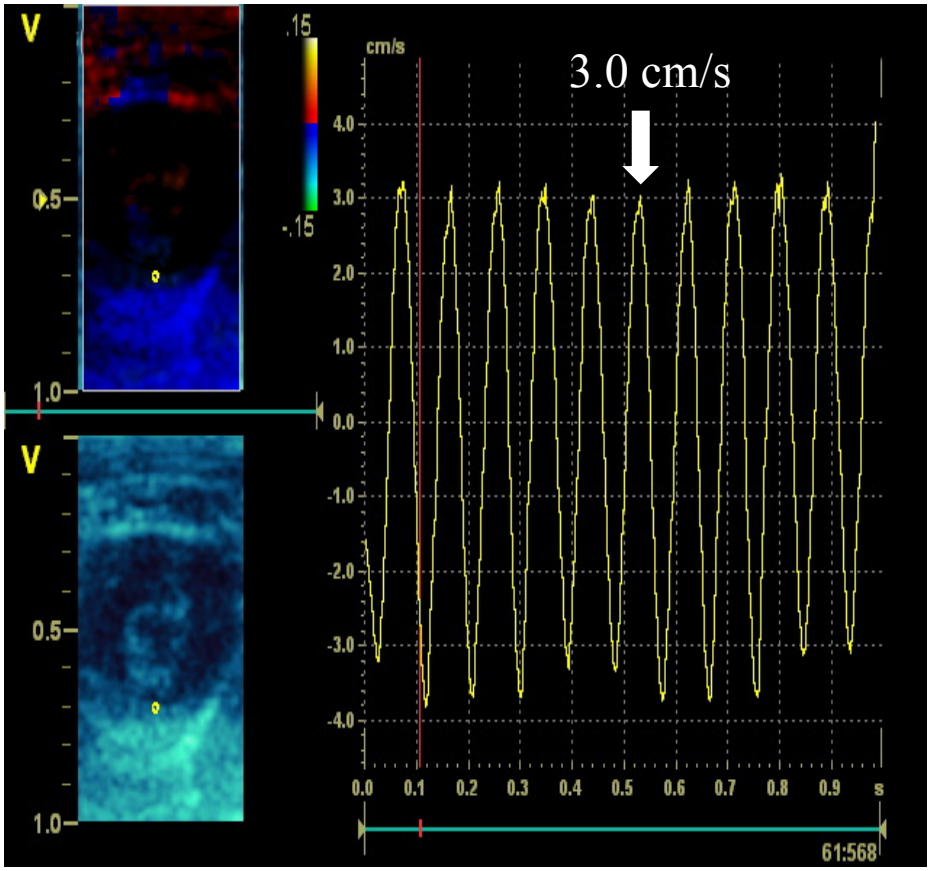

Figure 10. Tissue Velocity imaging of a normal healthy mouse. A V_{Endo} for mice between 2.5 and 3.5 cm/s is considered to be within normal range. A V_{Endo} less than one is indicative of cardiac systolic dysfunction. V_{Endo}, Endocardial Velocity.

Histology

At day 10, all surviving mice were euthanized. Upon removal, each heart was rinsed and cleaned in 0.9% saline and halved. Half of the heart was collected for histological analysis via light and electron microscopy. The other half of the heart was flash frozen in liquid nitrogen for biochemical assays.

For light microscopy, half hearts were stored in a fresh 10% buffered formalin solution. Serial dehydration with ethanol was performed to remove all unbound water from the tissue. Xylene was then used to clear the tissue of all ethanol prior to embedding. Tissues were then embedded in paraffin and serially sectioned. Mason's Trichrome was applied to 6-micron thick sections in order to assess cell damage, vacuolization, and myofibril degeneration. All tissues were processed at our core facility at the University of Manitoba.

For electron microscopy, half hearts were fixed in 0.1M phosphate buffer with 3% glutaraldehyde at room temperature for 2-4 hours. Tissue was rinsed 3 times for 10 minutes each, in 0.1M phosphate buffer pH=7.2. Post fixation was done in 0.1M phosphate buffer with 1% osmium tetroxide at room temperature sealed from the light. Following another course of washing in 0.1M phosphate buffer pH=7.2, all samples underwent serial dehydration in ethanol and were embedded in Epon 812 following standard procedures.[165] Thin sections were visualized on a Philips CM12 electron microscope to determine the degree of loss of cell integrity.

Wet weights of liver and lung samples were measured for all mice at the time of euthanization. Samples were dried for 72 hours at 65^{o}C and dry weights were used to determine wet-to-dry weight ratios.

Terminal Deoxynucleotidyl Transferase dUTP Nick End Labeling (TUNEL)

Half hearts from mice euthanized on day 4 were preserved in a fresh 10% buffered formalin solution. Tissues were then embedded in paraffin as per the standard protocol described above. Six to 10 micron thick sections were subjected to TUNEL assay according to manufactures directions (Trevigen, TumorTACS *In situ* apoptosis detection kit). Briefly, samples were deparaffinized and exposed to Proteinase K as previously described.[166-168] Following a PBS wash, all samples were incubated with TdT Labeling Buffer.[167] Samples were then placed in labeling reaction for 1 hour at 37^{o}C followed by TdT Stop Buffer for 5 min.[167] Each sample was then treated with Strep-HRP and DAB solutions, prior to being counter stained with methyl green.[168] Slides were visualized on a standard light microscope at 40X magnification. [168]

Western Blotting

Frozen half hearts from mice euthanized on day 4 were powdered using liquid nitrogen and homogenized in radioimmunoprecipition assay (RIPA) buffer containing protease and phosphatase inhibitors (Sigma-Aldrich Corporation, St. Louis, MO). Protein lysates underwent centrifugation at 14,000 rpm for 120 minutes at 4^{o}C, at which point the supernatant containing the protein fractions were removed and stored at -80^{o}C. Protein quantification was accomplished using the BioRad protein assay. All protein samples underwent 1-dimensional 8-15% sodium dodecyl sulfate polyacrylamide gel electrophoresis (SDS-PAGE) at 150V for 1.25h in a discontinuous system at room temperature. Each lane was loaded with 5-30ug of protein and was confirmed by Coomassie blue staining. Transfer to a 0.45-mm PVDF membrane was done in either 1.25 hours at 300mA at 4 ^{o}C on ice or over night at 4 ^{o}C on ice at 30mA. Detection of

transfer was accomplished using Ponceau S staining. Membranes were washed in TBS-T until all color was removed. The membranes were blocked in a 5% skim milk TBS-T solution for 1 hour. Membranes were washed 3 times for 15 minutes in TBS-T prior to administration of the primary antibody. Primary polyclonal antibodies for pro-apoptotic proteins Bax, Caspase-3, PARP (Cell Signaling), anti-apoptotic protein Bcl-X_L (Cell Signaling), and NOS3 (BD Transductions) were incubated overnight in a 5% skim milk TBS-T solution. Loading control was accomplished by the use of GAPDH (Cell Signaling). Anti-mouse or anti-rabbit secondary antibody was used to detect the primary antibody and was accomplished with the BM chemiluminescence kit (POD substrate; Roche Diagnostics, Laval, Canada). Protein bands were visualized using the Fluor-S-MutliImager Max system (BioRad Laboratories, Inc) while quantification of band intensity was accomplished using image analysis software (Quantity One; BioRad Laboratories, Inc). All procedures were repeated for significance.

Statistical Analysis

All data are expressed as mean±SD. Statistical significance between echocardiographic measurements was determined using a 2(Genotype) x 2(Time) mixed factorial design with repeated measures on the time factor. For post-hoc analysis, Tukey's multiple comparison test was used to test for significance between independent factors and Duncan's test was used to check for any significant differences within factors over time. In any post-hoc between group analysis, Levene's test was used to check for homogeneity of group variances. P-values for main effects and interactions were also recorded where appropriate. An independent reviewer examined specimens for both light and electron microscopy without prior knowledge of the treatment groups. Non-

parametric comparisons of scores ranging from 0 to 4 were calculated using the Mann-Whitney test. For biochemical analyses, one-way ANOVA and a Student-Newman-Keuls post-hoc test were performed. A p-value less than 0.05 were considered significant. The statistical analysis packages SPSS 15.0 and Graphpad Prism 5 were used to perform the analysis.

Results

Echocardiography

At baseline, there was no significant difference in LV systolic function (LVEF and V_{Endo}) or dimensions (PWT and LVEDD) between WT and $NOS3^{-/-}$ mice in the various treatment groups. Heart rate and PWT were within normal limits and did not change over the course of the study (Table 4A and B).

Left ventricular end diastolic diameter was within normal limits at baseline amongst all treatment groups. WT mice treated with DOX alone demonstrated an increase in LVEDD from 3.2±0.1mm at baseline to 3.9±0.1mm at day 10 ($p<0.05$). In $NOS3^{-/-}$ mice receiving DOX, LVEDD significantly increased from 3.1±0.3mm at baseline to 4.2±0.2mm at day 10 ($p<0.05$; Table 4B). In WT mice treated with DOX+TRZ, there was a significant increase in LVEDD from 3.1±0.2mm at baseline to 4.2±0.2mm at day 10 ($p<0.05$; Table 4A). This effect was potentiated in the $NOS3^{-/-}$ combination treatment group where LVEDD increased from 3.2±0.1mm at baseline to 4.6±0.1mm at day 10 ($p<0.05$). At day 10, $NOS3^{-/-}$ mice demonstrated a significant increase in LV cavity dimensions as compared to WT mice at the same time point ($p<0.05$) (Table 4B).

There was no difference in LVEF at baseline amongst all treatment groups. There was no significant difference in LVEF of saline or TRZ treatment groups in either WT or $NOS3^{-/-}$ mice at day 10. Wild type mice receiving DOX alone demonstrated a significant reduction in LVEF from 74±2% at baseline to 56±3% at day 10 (Figure 11A, Table 4). $NOS3^{-/-}$ mice treated with DOX demonstrated a further reduction in LVEF from 72±3% at baseline to 48±1% at day 10 ($p<0.05$; Figure 11A, Table 5). Co-administration of

DOX+TRZ in WT mice resulted in a significant reduction in LVEF from 75±3% at baseline to 46±2% at day 10 ($p<0.05$). Furthermore, $NOS3^{-/-}$ mice treated with DOX+TRZ, demonstrated a decrease in LVEF from 72±3% at baseline to 35±2% at day 10 ($p<0.05$). More importantly, LVEF of $NOS3^{-/-}$ mice was significantly lower than that of WT at day 10 in those receiving DOX+TRZ therapy ($p<0.05$) (Figure 11B, Table 5).

The tissue velocity index V_{Endo} also demonstrated severe LV systolic dysfunction in those mice treated with DOX and DOX+TRZ. In WT mice receiving DOX alone, V_{Endo} decreased from 3.1±0.2cm/s at baseline to 1.6±0.1cm/s at day 10 ($p<0.05$; Table 4). $NOS3^{-/-}$ mice treated with DOX also demonstrated a reduction in V_{Endo} from 3.2±0.3cm/s at baseline to 1.2±0.1cm/s at day 10. Wild type mice treated with DOX+TRZ demonstrated a further reduction in V_{Endo} to 1.2±0.1cm/s at day 10 ($p<0.05$). $NOS3^{-/-}$ mice co-treated with DOX+TRZ demonstrated the greatest reduction in V_{Endo} at day 10. Endocardial velocity was significantly reduced from 3.2±0.1cm/s at baseline to 0.9±0.1cm/s cm/s at day 10 in this group (Table 5). $NOS3^{-/-}$ mice treated with either DOX or DOX+TRZ did worse at day 10 as compared to WT at the same time point ($p<0.05$; Table 5).

Table 4. Echocardiographic data for WT mice

Echocardiographic Variable	Group	Baseline	Day 10	p-Value
HR (Beats/min)	Saline	694±11	683±7	0.82
	TRZ	675±12	682±9	0.78
	DOX	691±8	698±12	0.83
	DOX+TRZ	678±7	681±10	0.85
PWT (mm)	Saline	0.79±0.01	0.8±0.02	0.89
	TRZ	0.78±002	0.81±0.01	0.56
	DOX	0.79±0.02	0.80±0.03	0.87
	DOX+TRZ	0.77±0.02	0.79±0.02	0.78
LVEDD (mm)	Saline	3.2±0.2	3.3±0.1	0.87
	TRZ	3.1±0.2	3.2±0.2	0.88
	DOX	3.2±0.1	3.9±0.1*	<0.05
	DOX+TRZ	3.1±0.2	4.2±0.2*	<0.05
LVEF (%)	Saline	74±2	73±2	0.82
	TRZ	73±3	72±4	0.77
	DOX	74±2	56±3*	<0.05
	DOX+TRZ	75±3	46±2*	<0.05
V_{Endo} (cm/s)	Saline	3.2±0.2	3.3±0.1	0.89
	TRZ	3.3±0.1	3.2±0.2	0.90
	DOX	3.1±0.2	1.6±0.1*	<0.05
	DOX+TRZ	3.3±0.2	1.2±0.2*	<0.05

Echocardiographic data at baseline and day 10 from WT C57Bl/6 female mice receiving either 0.9% Saline, TRZ, DOX, or DOX+TRZ chemotherapy treatment. *p<0.05 as compared to baseline. HR, Heart Rate; PWT, Posterior Wall Thickness; LVEDD, Left Ventricular End Diastolic Diameter; LVEF, Left Ventricular Ejection Fraction; V_{Endo}, Endocardial Velocity; WT, Wild type; $NOS3^{-/-}$, Nitric Oxide Synthase 3 Knockout; TRZ, Trastuzumab; DOX, Doxorubicin; DOX+TRZ, Doxorubicin+Trastuzumab.

Table 5. Echocardiographic data for NOS3$^{-/-}$ mice

Echocardiographic Variable	Group	Baseline	Day 10	p-Value
HR (Beats/min)	Saline	684±9	691±11	0.67
	TRZ	692±14	698±8	0.81
	DOX	689±11	690±9	0.91
	DOX+TRZ	672±12	682±5	0.77
PWT (mm)	Saline	0.78±0.02	0.81±0.03	0.65
	TRZ	0.79±0.01	0.81±0.02	0.69
	DOX	0.77±0.03	0.79±0.02	0.54
	DOX+TRZ	0.79±0.02	0.80±0.03	0.81
LVEDD (mm)	Saline	3.1±0.3	3.2±0.2	0.76
	TRZ	3.2±0.3	3.3±0.2	0.81
	DOX	3.1±0.2	4.2±0.2*#	<0.05
	DOX+TRZ	3.2±0.1	4.6±0.1*$^{\#}$	<0.05
LVEF (%)	Saline	72±3	74±2	0.76
	TRZ	71±2	73±2	0.66
	DOX	72±3	48±1*$^{\#}$	<0.05
	DOX+TRZ	72±3	35±2*$^{\#}$	<0.05
V_{Endo} (cm/s)	Saline	3.1±0.1	3.0±0.1	0.78
	TRZ	3.1±0.1	3.2±0.2	0.88
	DOX	3.2±0.3	1.2±0.1*$^{\#}$	<0.05
	DOX+TRZ	3.2±0.1	0.9±0.1*$^{\#}$	<0.05

Echocardiographic data at baseline and day 10 from NOS3$^{-/-}$ female mice receiving either 0.9% Saline, TRZ, DOX, or DOX+TRZ chemotherapy treatment. *p<0.05 as compared to baseline. #p<0.05 as compared to WT in Table 4. HR, Heart Rate; PWT, Posterior Wall Thickness; LVEDD, Left Ventricular End Diastolic Diameter; LVEF, Left Ventricular Ejection Fraction; V_{Endo}, Endocardial Velocity; WT, Wild type; NOS3$^{-/-}$, Nitric Oxide Synthase 3 Knockout; TRZ, Trastuzumab; DOX, Doxorubicin; DOX+TRZ, Doxorubicin+Trastuzumab.

A) Left ventricular systolic function in WT and NOS3$^{-/-}$ female mice receiving DOX alone.

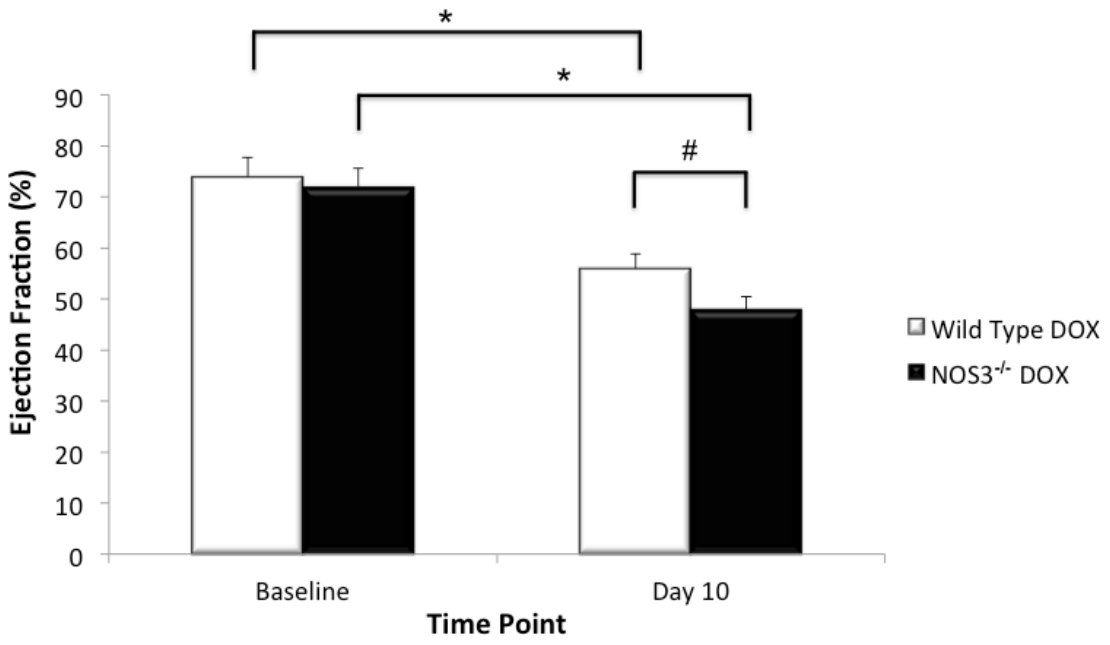

B) Left ventricular systolic function in WT and NOS3$^{-/-}$ female mice receiving DOX+TRZ.

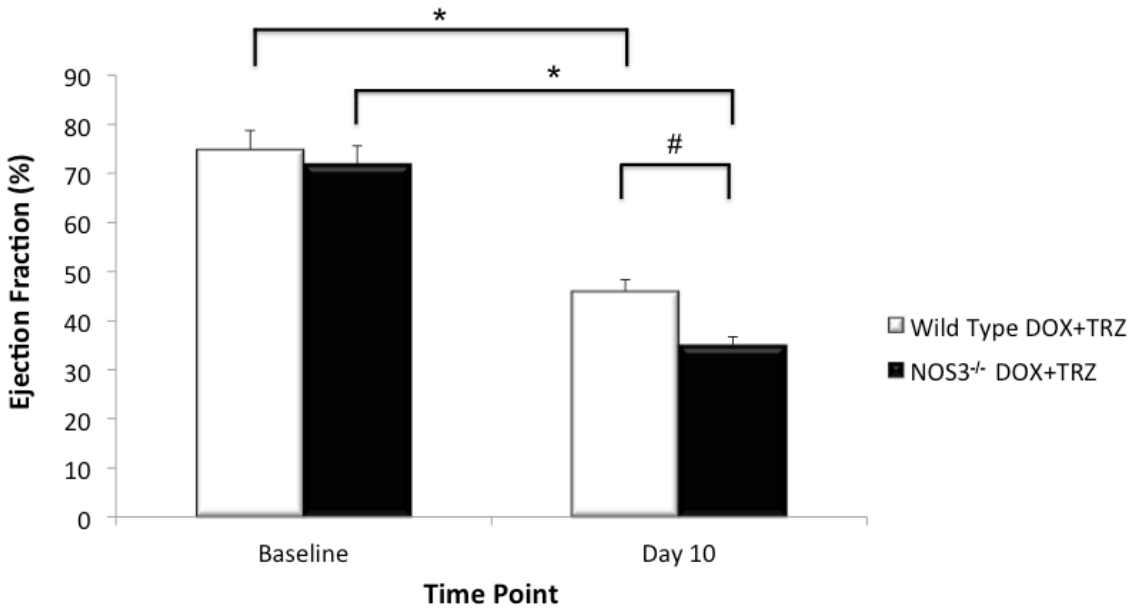

Figure 11. A) Comparison of LVEF between WT and NOS3$^{-/-}$ female mice treated with DOX alone. Although the LVEF significantly decreased in both groups (*p<0.05), the LVEF in the NOS3$^{-/-}$ group was significantly reduced as compared to WT group at day 10 (#p<0.05). **B)** Comparison of LVEF between WT and NOS3$^{-/-}$ female mice treated with DOX+TRZ. Similar to the DOX alone treated group, there was a significant decrease in LVEF at day 10 in both groups (*p<0.05). The LVEF in the NOS3$^{-/-}$ group, however, was significantly reduced as compared to the WT group at day 10 (#p<0.05). Finally, the LVEF was significantly reduced in NOS3$^{-/-}$ female mice receiving DOX+TRZ, as compared to DOX alone. WT Saline n=5; WT DOX n=15; WT TRZ n=15; WT DOX+TRZ n=25; NOS3$^{-/-}$ Saline n=5; NOS3$^{-/-}$ DOX n=15; NOS3$^{-/-}$ TRZ n=15; NOS3$^{-/-}$ DOX+TRZ n=25. LVEF, left ventricular ejection fraction; WT, Wild type; NOS3$^{-/-}$, Nitric Oxide Synthase 3 Knockout; DOX, Doxorubicin; DOX+TRZ, Doxorubicin and Trastuzumab.

Survival

Survival data is shown in Figure 12. Control WT and NOS3$^{-/-}$ female mice demonstrated no mortality over the course of the study. A total of 80% of WT female mice receiving DOX were surviving at day 5, whereas only 33% of NOS3$^{-/-}$ mice were surviving at the same time point. By day 10, WT mice treated with DOX had a survival rate of 46% as compared to NOS3$^{-/-}$ mice who had a survival rate of only 20%. The combination of DOX+TRZ in NOS3$^{-/-}$ mice resulted in a 28% survival rate at day 5 and 8% survival rate at day 10. Conversely, WT mice co-treated with DOX+TRZ displayed a preserved survival rate of 84% at day 5 and 64% at day 10 (Figure 12). Thus, NOS3$^{-/-}$ female mice demonstrated reduced survival than WT mice when treated with either DOX alone or DOX+TRZ.

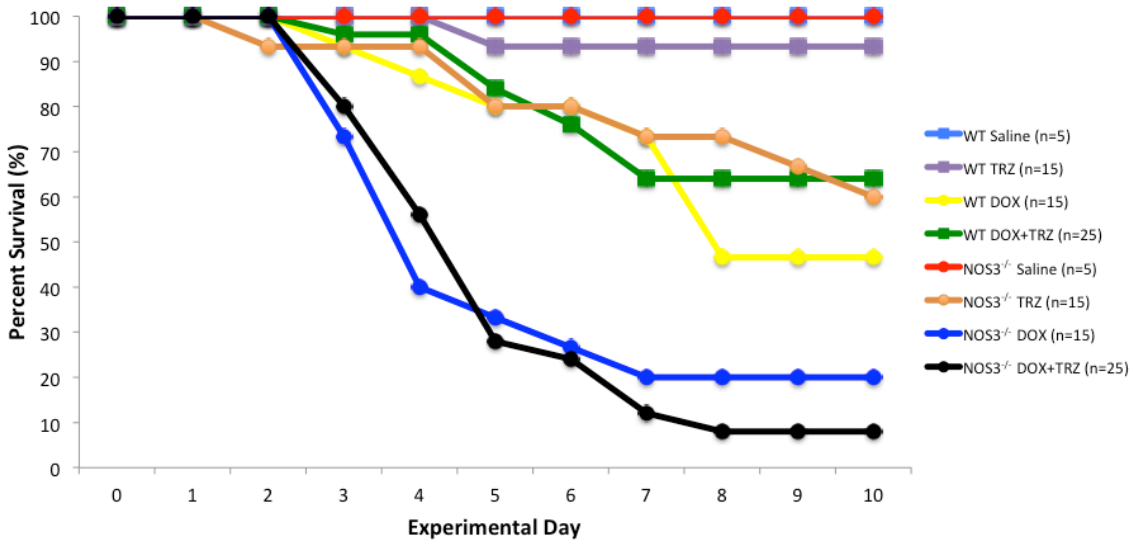

Figure 12. Percent survival of C57Bl/6 and NOS3$^{-/-}$ female mice. Mice treated with DOX demonstrated increased mortality than mice treated with either saline or TRZ. Furthermore, the combination of DOX+TRZ therapy demonstrated increased mortality in both the WT and NOS3$^{-/-}$ groups as compared to DOX alone. NOS3$^{-/-}$ mice treated with DOX+TRZ had a significantly higher mortality rate than WT at day 10. WT Saline n=5; WT DOX n=15; WT TRZ n=15; WT DOX+TRZ n=25; NOS3$^{-/-}$ Saline n=5; NOS3$^{-/-}$ DOX n=15; NOS3$^{-/-}$ TRZ n=15; NOS3$^{-/-}$ DOX+TRZ n=25. WT, Wild type; NOS3$^{-/-}$, Nitric Oxide Synthase 3 Knockout; TRZ, Trastuzumab; DOX, Doxorubicin; DOX+TRZ, Doxorubicin+Trastuzumab.

Tissue Weights

There was no difference in the average wet-to-dry weight ratio of the liver or lungs between the various treatment groups at the time of euthanization (Figure 13).

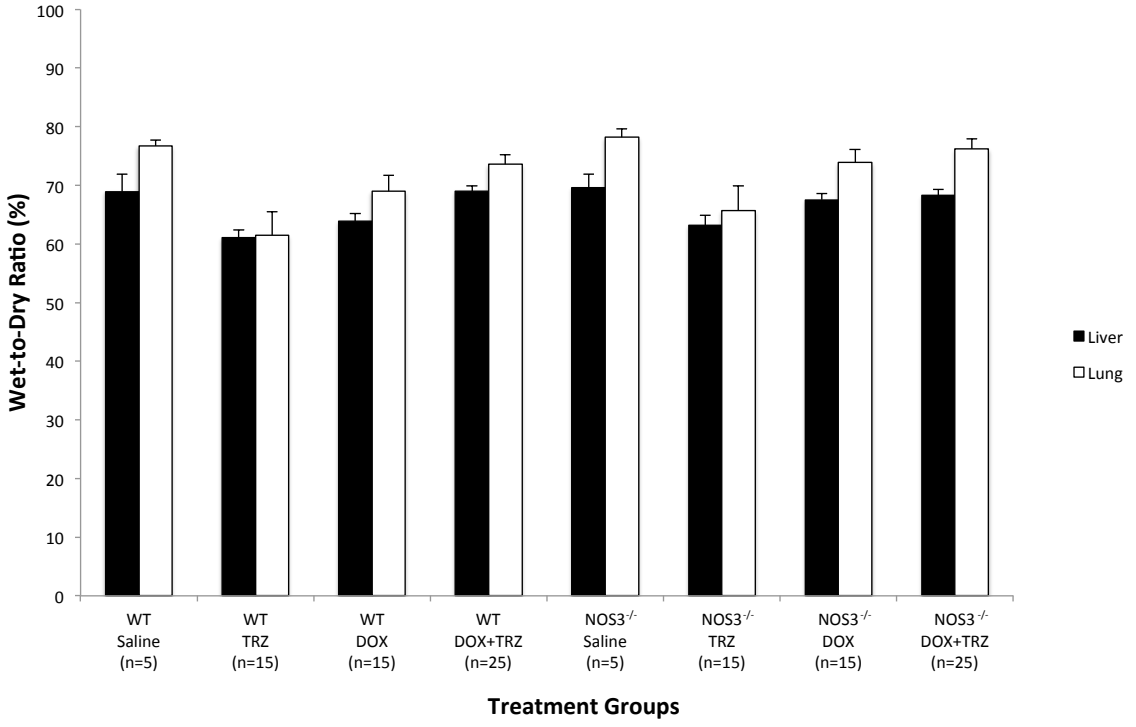

Figure 13. A) Liver and lung wet-to-dry ratios for all treatment groups. No significant difference was found amongst any of the groups. WT Saline n=5; WT DOX n=15; WT TRZ n=15; WT DOX+TRZ n=25; NOS3$^{-/-}$ Saline n=5; NOS3$^{-/-}$ DOX n=15; NOS3$^{-/-}$ TRZ n=15; NOS3$^{-/-}$ DOX+TRZ n=25. WT, Wild type; NOS3$^{-/-}$, Nitric Oxide Synthase 3 Knockout; TRZ, Trastuzumab; DOX, Doxorubicin; DOX+TRZ, Doxorubicin+Trastuzumab.

Histology

Light Microscopy

There was no evidence of myofibril degradation and vacuolization in either the control or TRZ treated groups at day 10 (Figure 14). Evidence of myofibril degradation and vacuolization was apparent in both WT and NOS3$^{-/-}$ mice treated with DOX. This damage was potentiated in both combination treatment groups (Figure 14). There was no difference, however, in histological evidence of cardiac injury between WT and NOS3$^{-/-}$ female mice.

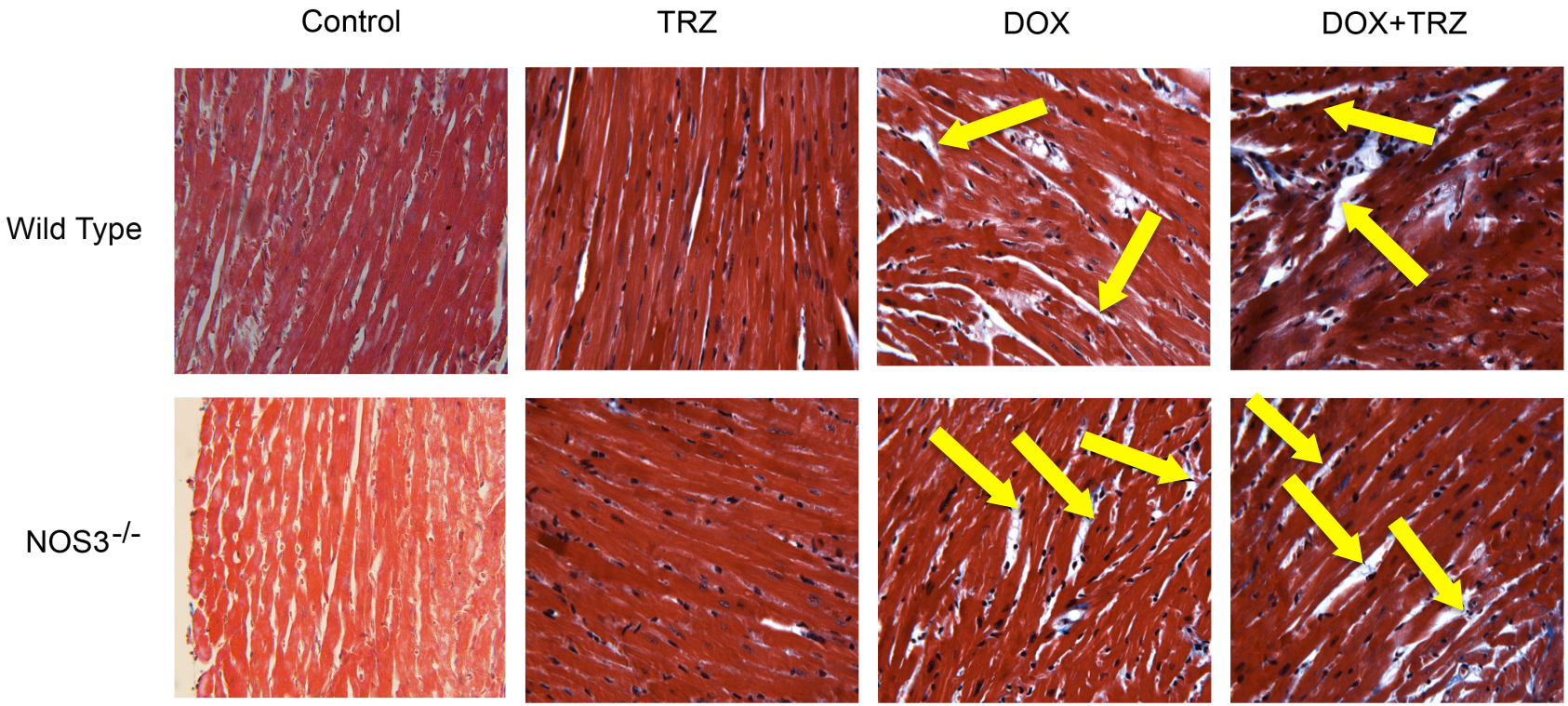

Figure 14. Light microscopy of representative samples from WT and NOS3$^{-/-}$ groups treated with saline, TRZ, DOX, or DOX+TRZ (40x magnification). Myofibrillar degeneration and vacuolization was present in mice receiving DOX and DOX+TRZ. The degree of damage was greatest in the DOX+TRZ treated groups. No difference in the degree of cardiac remodeling was detected when comparing WT to NOS3$^{-/-}$. WT, Wild type; NOS3$^{-/-}$, Nitric Oxide Synthase 3 Knockout; TRZ, Trastuzumab; DOX, Doxorubicin; DOX+TRZ, Doxorubicin+Trastuzumab.

Electron Microscopy

Approximately 16,000 cells were scanned from 3 randomly derived blocks of tissue and evaluated for dilation of the sarcoplasmic reticulum and loss of cell integrity. Significant differences in both sarcoplasmic reticulum structure and the loss of cell integrity were found between WT DOX and DOX+TRZ treated groups when compared to the TRZ treatment group alone. Similar damage was also noted in $NOS3^{-/-}$ DOX and DOX+TRZ groups when compared to $NOS3^{-/-}$ TRZ treated animals ($p<0.001$; Figure 15). There was no significant difference in the degree of cardiac remodeling between the WT and $NOS3^{-/-}$ female mice.

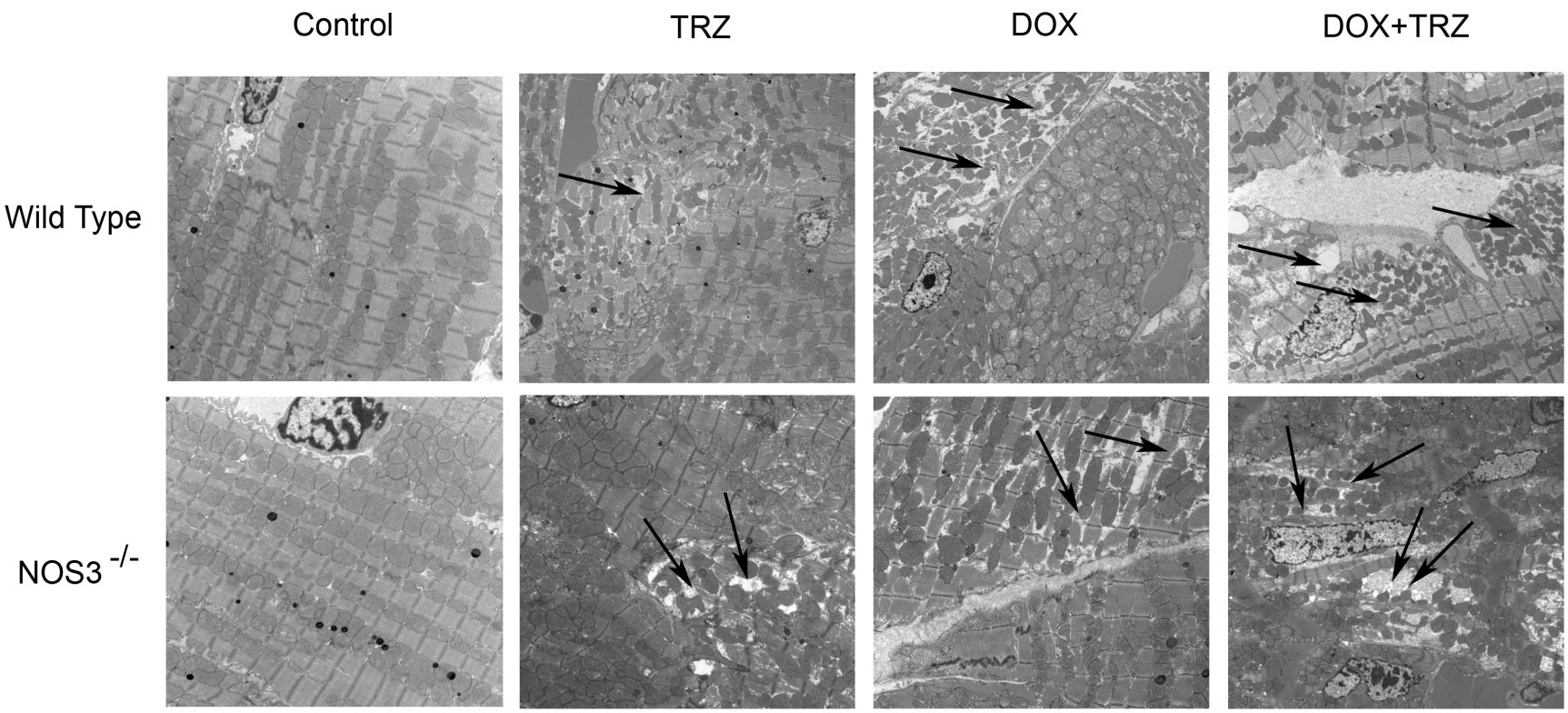

Figure 15. Electron microscopy of representative samples from WT and NOS3$^{-/-}$ groups treated with saline, DOX, TRZ, or DOX+TRZ (4000x magnification). Note the increased amounts of cellular damage in the DOX+TRZ treatment groups compared to the DOX alone group. WT, Wild type; NOS3$^{-/-}$, Nitric Oxide Synthase 3 Knockout; TRZ, Trastuzumab; DOX, Doxorubicin;

TUNEL

There was no evidence of TUNEL positive nuclei amongst the various treatment groups, in either WT or NOS3$^{-/-}$ mice at experimental day 4 (Figure 16).

A)

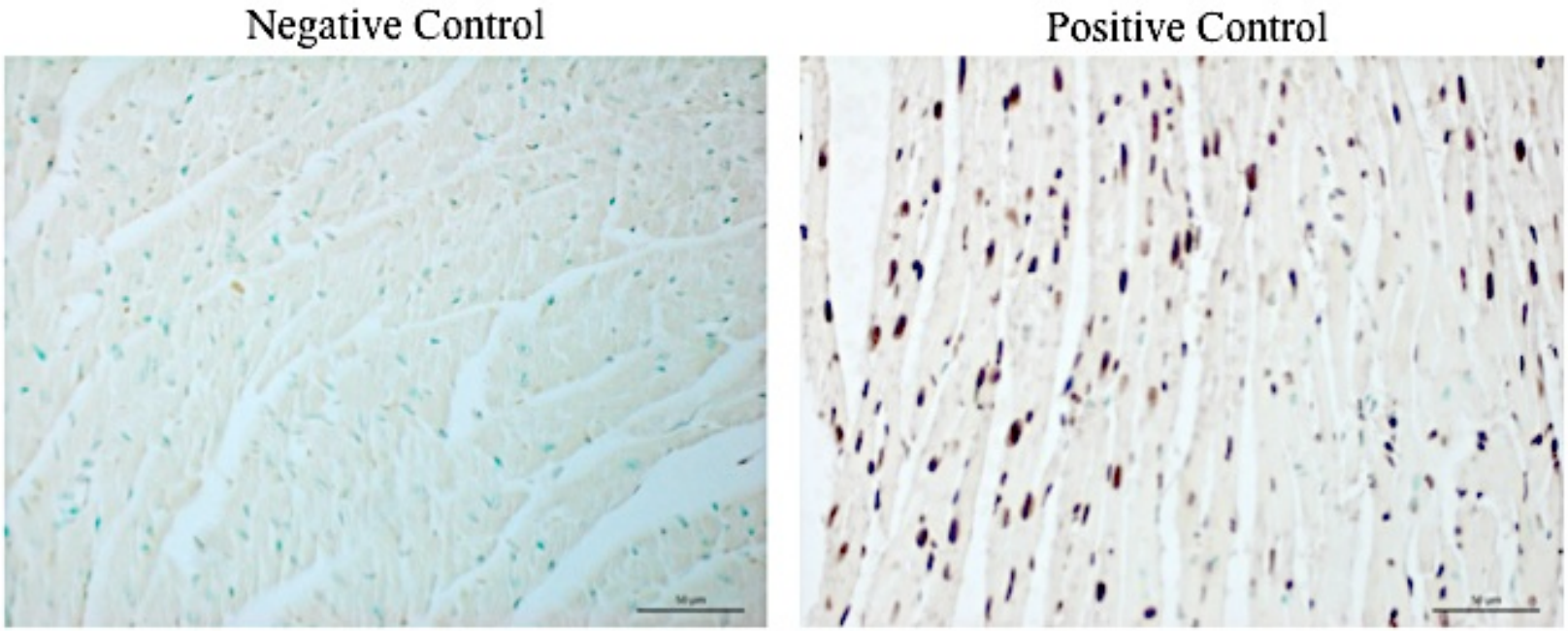

B)

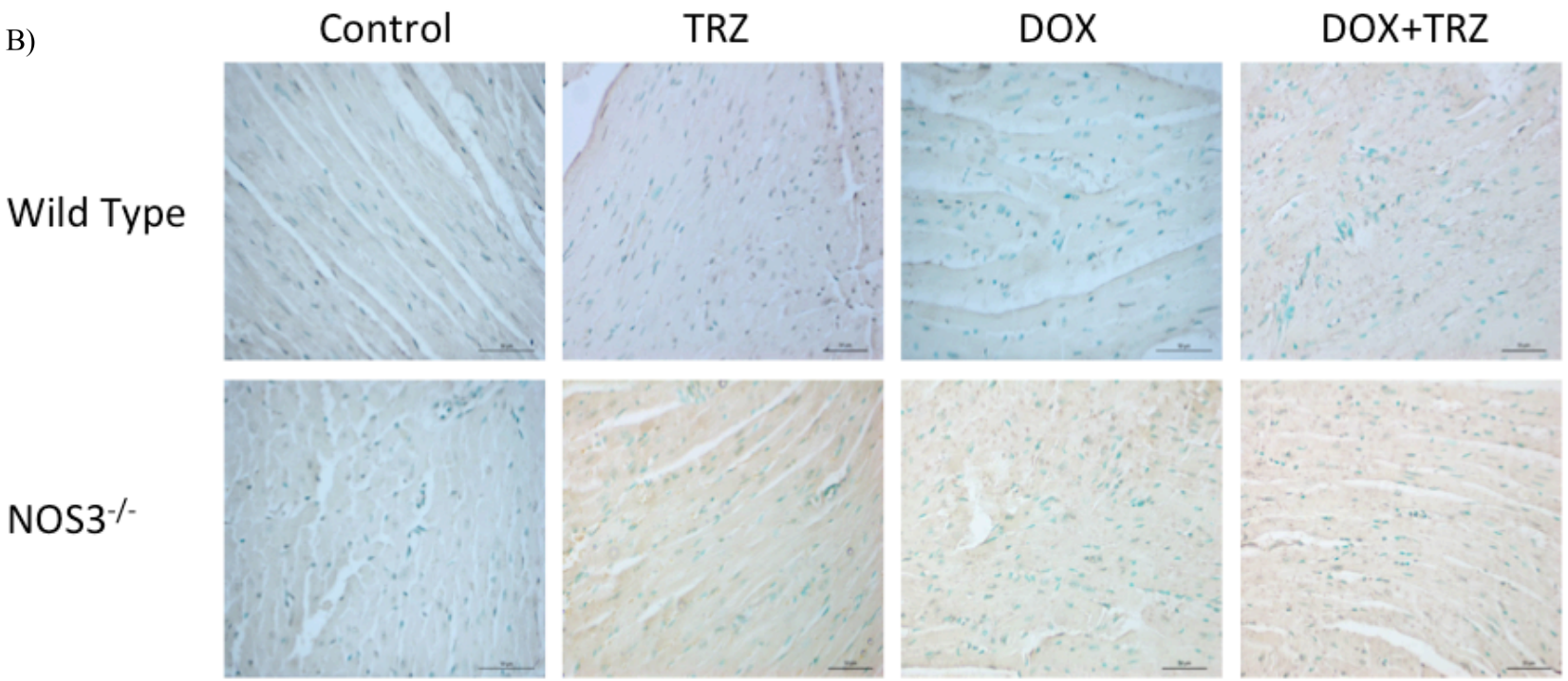

Figure 16. A) Terminal deoxynucleotidyl transferase dUTP nick end labeling (TUNEL) of negative and positive controls from cardiac tissue. Note the dark staining in the positive control as TUNEL positive nuclei. B) Representative samples from WT and NOS3$^{-/-}$ female groups treated with control saline, DOX, TRZ, or DOX+TRZ (40X magnification). There was no evidence of TUNEL positive nuclei amongst any of the treatment groups. WT, Wild type; NOS3$^{-/-}$, Nitric Oxide Synthase 3 Knockout; TRZ, Trastuzumab; DOX, Doxorubicin; DOX+TRZ, Doxorubicin+Trastuzumab.

Western Blot Analysis

Western blot analysis confirmed that there was no evidence of NOS3 protein expression in $NOS3^{-/-}$ female mice (Figure 17). Analysis for cardiac apoptosis is shown in Figures 18. There was no evidence of Caspase 3 cleavage amongst any of the treatment groups (Figure 18). Absence of PARP cleavage (Figure 19) lends further evidence towards lack of Caspase 3 activation (Figure 18) and lack of TUNEL positive nuclei (Figure 16). As compared to saline treated animals, there was no evidence of an increase in the Bax-to-Bcl-X_L ratio in either WT or $NOS3^{-/-}$ mice treated with TRZ alone (Figure 20). While there was an increasing trend in the Bax-to-Bcl-X_L ratio in WT or $NOS3^{-/-}$ mice receiving either DOX alone or the combination of DOX+TRZ, this trend did not reach statistical significance (Figure 20).

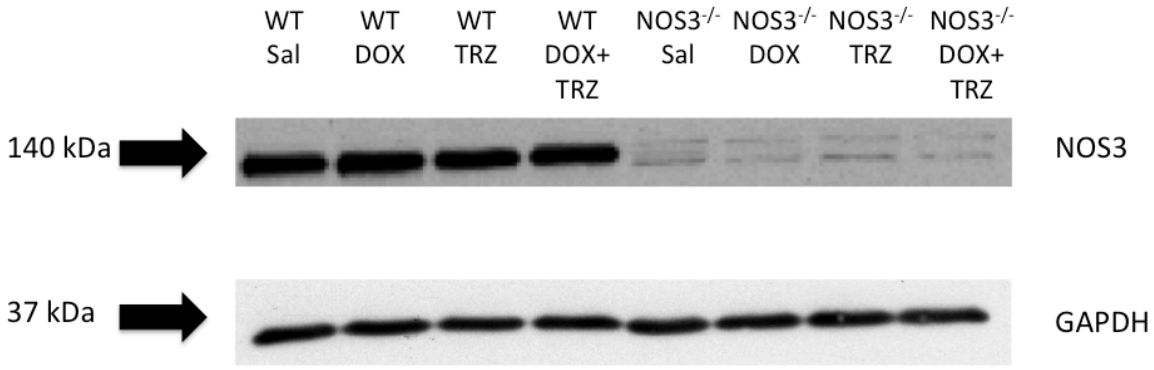

Figure 17. Western blot demonstrating presence of NOS3 protein in WT mice and absence of NOS3 protein in NOS3$^{-/-}$ mice. WT Saline n=4; WT DOX n=6; WT TRZ n=6; WT DOX+TRZ n=6; NOS3$^{-/-}$ Saline n=4; NOS3$^{-/-}$ DOX n=6; NOS3$^{-/-}$ TRZ n=6; NOS3$^{-/-}$ DOX+TRZ n=6. WT, Wild type; NOS3$^{-/-}$, Nitric Oxide Synthase 3 Knockout; TRZ, Trastuzumab; DOX, Doxorubicin; DOX+TRZ, Doxorubicin+Trastuzumab.

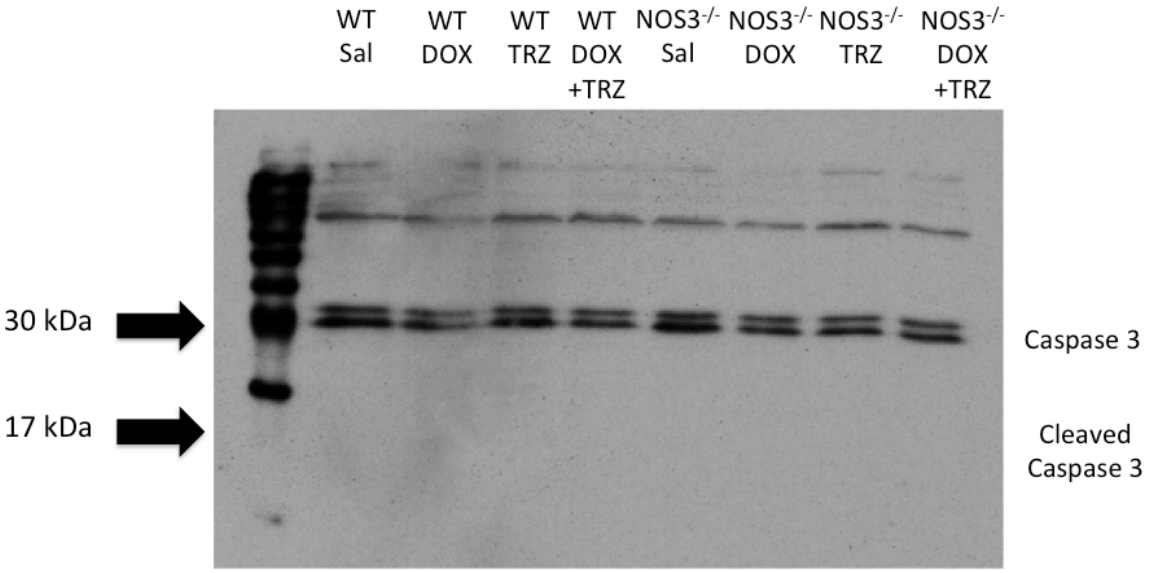

Figure 18. Western blot of Caspase 3 activity. Full length Caspase 3 is indicated by the lower band (30 kDa) of the double band present, as indicated by the arrow. Note there is no evidence of Caspase 3 cleavage amongst any of the treatment groups, indicating a potential for Caspase 3 independent apoptosis. WT Saline n=4; WT DOX n=6; WT TRZ n=6; WT DOX+TRZ n=6; NOS3$^{-/-}$ Saline n=4; NOS3$^{-/-}$ DOX n=6; NOS3$^{-/-}$ TRZ n=6; NOS3$^{-/-}$ DOX+TRZ n=6. WT, Wild type; NOS3$^{-/-}$, Nitric Oxide Synthase 3 Knockout; TRZ, Trastuzumab; DOX, Doxorubicin; DOX+TRZ, Doxorubicin+Trastuzumab.

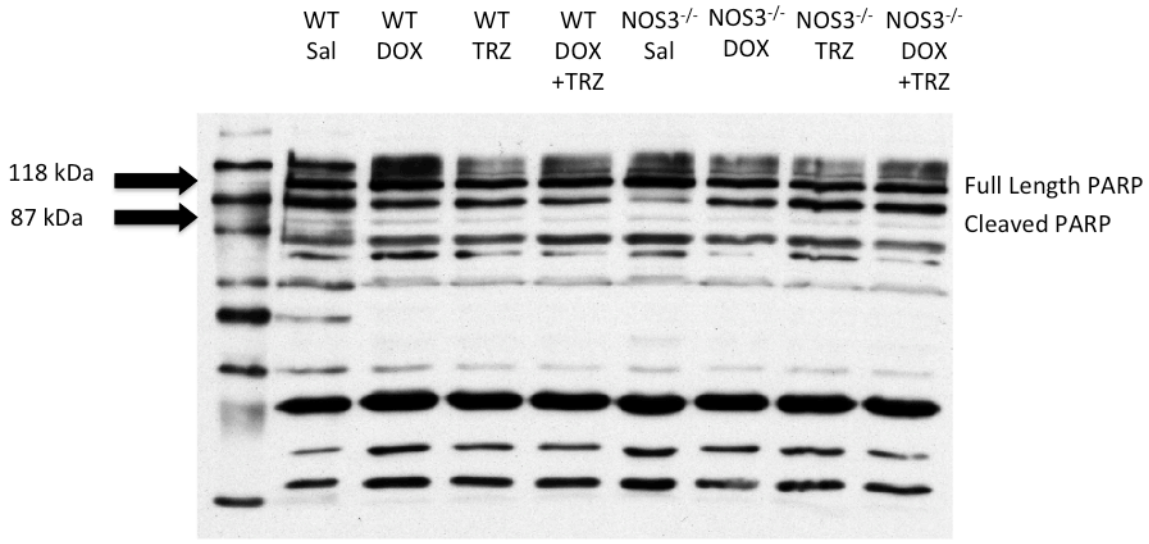

Figure 19. Western blot of PARP activity. Full length PARP is indicated by the 118kDa band as indicated by the arrow. There is no evidence of PARP cleavage amongst any of the treatment groups. WT Saline n=4; WT DOX n=6; WT TRZ n=6; WT DOX+TRZ n=6; $NOS3^{-/-}$ Saline n=4; $NOS3^{-/-}$ DOX n=6; $NOS3^{-/-}$ TRZ n=6; $NOS3^{-/-}$ DOX+TRZ n=6. PARP, Poly (ADP-ribose) polymerase; WT, Wild type; $NOS3^{-/-}$, Nitric Oxide Synthase 3 Knockout; TRZ, Trastuzumab; DOX, Doxorubicin; DOX+TRZ, Doxorubicin+Trastuzumab.

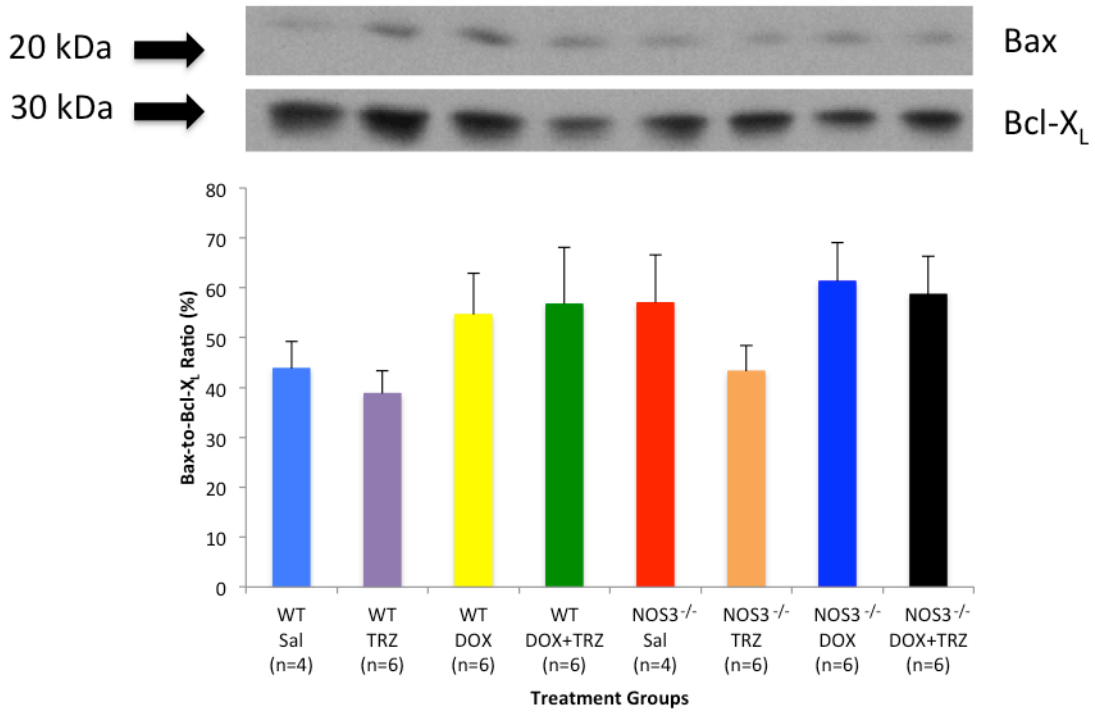

Figure 20. The average percent ratio of Bax-to-Bcl-X_L expression at experimental day 4. As compared to saline, there was no evidence of an increase in the Bax-to-Bcl-X_L ratio in either WT or NOS3$^{-/-}$ mice treated with TRZ alone. While there was an increasing trend in the Bax-to-Bcl-X_L ratio in WT or NOS3$^{-/-}$ mice receiving either DOX alone or the combination of DOX+TRZ, this did not reach statistical significance. WT Saline n=4; WT DOX n=6; WT TRZ n=6; WT DOX+TRZ n=6; NOS3$^{-/-}$ Saline n=4; NOS3$^{-/-}$ DOX n=6; NOS3$^{-/-}$ TRZ n=6; NOS3$^{-/-}$ DOX+TRZ n=6. WT, Wild type; NOS3$^{-/-}$, Nitric Oxide Synthase 3 Knockout; TRZ, Trastuzumab; DOX, Doxorubicin; DOX+TRZ, Doxorubicin+Trastuzumab. Error bars represent SEM.

Discussion

The current study demonstrates that congenital absence of NOS3 is not cardioprotective in a clinically relevant female murine model of DOX+TRZ induced heart failure. As compared to WT, $NOS3^{-/-}$ female mice demonstrated increased mortality following the co-administration of DOX+TRZ. Histological evidence of cardiac damage including loss of cell integrity, vacuolization, myofibrilar degradation, and dilation of the sarcotubular system was observed in both WT and $NOS3^{-/-}$ mice treated with DOX+TRZ. Although there was an increasing trend in the ratio of Bax-to-Bcl-X_L in both WT and $NOS3^{-/-}$ mice treated with DOX+TRZ therapy, this was not statistically significant. This would suggest that in a female murine model of acute chemotherapy-induced heart failure, congenital absence of NOS3 potentiates cardiac dysfunction and increases mortality through apoptotic independent pathways.

Although TRZ is primarily used for the treatment of HER2 positive breast cancer in humans, it contains 5 murine framework residues and two additional murine complementary determining regions, which provides cross-reactivity with the murine HER2 receptor.[3, 129, 169-171] This has allowed for the development of numerous animal models of TRZ mediated cardiotoxicity.[3, 129, 169-171] Recently, Riccio *et al*. 2009 demonstrated binding of TRZ to the HER2 receptor in both mouse and rat cardiomyocytes by immuoprecipitation of the HER2/TRZ complex from cardiac cell extracts.[170] Furthermore, Yousif *et al*. 2011 demonstrated that toll-receptor 4 competent mice exhibited both systolic and diastolic cardiac dysfunction when treated with TRZ (2 mg/kg).[171] Fedele *et al*. 2011 also demonstrated adverse cardiac dysfunction in C57Bl/6 mice treated with TRZ where LV systolic function significantly decreased one-week

following treatment.[172] Furthermore, Jassal *et al*. 2009 evaluated the combined cardiotoxic effects of DOX+TRZ in an acute murine model of chemotherapy-induced heart failure.[3] Co-administration of DOX+TRZ was associated with severe LV systolic dysfunction, increased cardiomyocyte apoptosis, and increased mortality as compared to either agent alone.[3] In a 2011 follow-up study, Walker *et al*. 2011 demonstrated that the prophylactic administration of Probucol, an antioxidant, was partially cardioprotective against DOX+TRZ mediated cardiac dysfunction.[129] Collectively, these 5 studies independently validate the cardiotoxic effects of TRZ in a murine model.[3, 129, 169-171]

Acute animal studies of DOX-induced cardiac dysfunction have been extensively reported.[17, 32, 162, 173] A previous study by Neilan *et al.* 2007 demonstrated that NOS3 may contribute to the pathogenesis of DOX mediated cardiotoxicity through a ROS dependent mechanism in male mice.[162] As early as 24 hours following DOX treatment, there was an increase in lucigen-enhanced chemiluminescence and DHE staining in WT, but not $NOS3^{-/-}$ male mice. This increase in ROS production was directly correlated to the development of adverse LV systolic dysfunction in WT mice. Although FS decreased from 57±2% to 47±1% in the WT group, FS was relatively well preserved in $NOS3^{-/-}$ male mice.[162] Similarly in WT mice, LVEF decreased from 78±2% at baseline to 66±3% at day 5, whereas $NOS3^{-/-}$ male mice experienced a decrease from 78±2% at baseline to 74±2% at day 5 ($p<0.05$). Alternatively, overexpression of NOS3 ($NOS3^{TG}$) was associated with decreased cardiac performance and increased mortality. Thus, this previous study concluded that congenital absence of NOS3 ($NOS3^{-/-}$) was cardioprotective in a male murine model of DOX-induced cardiac dysfunction.[162] Although their study confirmed an important role for NOS3 as a key mediator in ROS

production in a predominantly male model of DOX-induced cardiotoxicity, little is known regarding the role of NOS3 and ROS in a clinically relevant female model.

In contrast to the study by Neilan *et al*. 2007, the current study suggests that congenital absence of NOS3 ($NOS3^{-/-}$) potentiates the cardiotoxic effects of DOX in a female murine model of chemotherapy-induced cardiac dysfunction.[162] As compared to WT, $NOS3^{-/-}$ female mice treated with DOX demonstrated a significant reduction in LVEF, which was potentiated by the addition of TRZ ($p<0.05$). Furthermore, LV cavity dimensions were significantly increased in all mice treated with DOX alone at day 10. This affect was potentiated by the co-administration of DOX+TRZ and greatest in $NOS3^{-/-}$ female mice ($p<0.05$). Overall, these findings suggest a sexual dichotomy for the role of NOS3 in cardioprotection during chemotherapy.

Early detection of cardiac dysfunction is important in mitigating the hazardous effects of DOX+TRZ mediated cardiac dysfunction. Tissue velocity imaging measures the maximal V_{Endo} within the LV myocardium and can detect early, subtle changes in LV systolic function. When compared to conventional echocardiographic measurements such as LVEF, TVI-derived parameters are less influenced by loading conditions, which commonly occur with chemotherapy treatment. Recently, several animal based models have demonstrated the utility of TVI in the early detection of DOX and DOX+TRZ mediated cardiac dysfunction.[3, 129, 162] In 2009, Jassal *et al.* demonstrated that V_{Endo} was abnormal as early as 24 hours following acute high dose chemotherapy treatment (DOX 20mg/kg or DOX 20mg/kg+TRZ 10mg/kg); 3 days earlier than an observable change in LVEF. In a 2011 follow-up study, Walker *et al.* confirmed that TVI is a sensitive marker of DOX+TRZ induced cardiac dysfunction.[129] Although LVEF did

not decrease until day 4, V_{Endo} and SR were able to detect early subtle changes in the myocardium within 24 hours, indicative of ensuing cardiac dysfunction. In a 2007 chronic study of DOX mediated cardiotoxicity, Neilan *et al.* demonstrated that although LVEF did not decrease until week 12 in WT mice, V_{Endo} was significantly reduced by week 6, whereas $NOS3^{-/-}$ mice did not display any evidence of early injury.[162] Similarly, our current study confirms that TVI is a sensitive, reproducible measure of early cardiac dysfunction following chemotherapy treatment in a female model of DOX+TRZ mediated cardiotoxicity. Thus, TVI may be a more feasible non-invasive imaging modality for the early detection of subclinical LV systolic dysfunction.

Translating these basic science findings to the clinical arena, Fallah-Rad *et al*. recently evaluated the role of TVI and strain in the early detection of DOX+TRZ mediated cardiac dysfunction in women with breast cancer.[116] Out of 42 women (mean age 47±9 years) prospectively followed between 2007-2009, 10 women (25%) developed TRZ mediated cardiomyopathy. Within 3 months of adjuvant therapy with TRZ, there was a significant decrease in the lateral S' between those women who did not display evidence of cardiac injury and those patients who developed LV systolic dysfunction (9.1±1.6 cm/s and 6.4±0.9 cm/s, respectively, $p<0.05$). Similarly, the peak global longitudinal and radial strain decreased as early as 3 months in the TRZ mediated cardiotoxicity group. Left ventricular ejection fraction was decreased at 6 months of follow-up in all 10 patients, necessitating discontinuation of TRZ. Both TVI and strain imaging were able to detect preclinical changes in LV systolic function, prior to conventional changes in LVEF, in patients receiving TRZ in the adjuvant setting.[116]

Several other clinical studies have confirmed these findings.[112-115] Di Lisi *et al*. 2011 conducted a prospective study of 72 women who received either FEC or FEC+TRZ treatment in the adjuvant breast cancer setting. They demonstrated that there was a significant reduction in TVI indices but not LVEF during 3 and 6-month follow-up. Furthermore, there was significant reduction in isovolumic relaxation time, total ejection isovolumic index and myocardial systolic velocity at each time point (3 and 6 months respectively), demonstrating an early reduction in cardiac systolic and diastolic function following chemotherapy treatment. More importantly, they did not find a reduction in LVEF in any women treated for breast cancer over the course of the study. Similarly, Hare *et al.* 2009 demonstrated an early, sub-clinical reduction in TVI indices for both strain and SR as early as 3 months following chemotherapy plus TRZ treatment.[112] In another study, Sawaya *et al*. 2011 prospectively evaluated 43 women undergoing chemotherapy for breast cancer.[115] As early as 3 months following treatment, there was a significant decrease in both longitudinal and circumferential strain. Conventional echocardiographic measures, particularly LVEF, did not change, however, until month 6 in this patient population.[115] Collectively, these clinical studies confirm the utility of TVI and strain for the early detection of LV systolic dysfunction in women receiving antineoplastic agents, thereby potentially preventing irreversible cardiac damage from occurring. Whether TVI and strain will become a standard of care in the noninvasive monitoring of LV systolic function in this select patient population will require further study.

In addition to an increased incidence of cardiac dysfunction, chemotherapeutic agents including DOX and TRZ lead to increased mortality in murine models. Previous

studies by Neilan *et al*. 2007, Jassal *et al.* 2009 and Walker *et al*. 2011 have demonstrated that there is a significant mortality rate in male mice treated with DOX (20mg/kg) as early as day 5, which continued to increase until day 10.[3, 162] Additionally, Jassal *et al.* 2009 and Walker *et al.* 2011 have demonstrated that the addition of TRZ to DOX potentiates the mortality rate that is observed with DOX treatment alone.[3, 129] Our current study supports these findings in that WT female treated with DOX demonstrate a reduced survival rate which was potentiated with the co-administration of DOX+TRZ.

Similar to LV functional parameters, there was a notable disparity in survival rates detected between our current study and that previously conducted by Neilan *et al.* 2007. Neilan *et al*. 2007 demonstrated that as compared to WT, $NOS3^{-/-}$ male mice had a preserved survival rate at day 8.[162] On the contrary, our study demonstrates that $NOS3^{-/-}$ female mice treated with DOX have a significant reduction in survival rate at day 10 as compared to WT. Whether or not hormonal differences between the sexes can account for the divergent echocardiographic and survival data observed between the two studies merits further evaluation.

We are not the first to demonstrate that male and female $NOS3^{-/-}$ mice display different phenotypic characteristics. A study by Miller *et al*. 2005 evaluated differences in systemic and pulmonary hypertension between male and female $NOS3^{-/-}$ mice.[174] They demonstrated that there was greater early postnatal reduction of muscularity in the pulmonary vessels of females than in males. Furthermore, by day 14, the extent of pulmonary arterial muscularization had normalized in females, but remained excessive in male $NOS3^{-/-}$ mice and was associated with pulmonary hypertension. Increased RV pressure associated with pulmonary hypertension continued into adulthood and was

significantly greater in the NOS3$^{-/-}$ males than the females. Additionally, male NOS3$^{-/-}$ mice demonstrated significantly higher systemic hypertension than in either WT males or NOS3$^{-/-}$ females. In another study by Moore *et al*. 2010, male NOS3$^{-/-}$ mice demonstrated prolonged bleeding times as compared to their female counterparts.[175] These studies along with our current study lend evidence to a sexual dichotomy for NOS3 in regulating various physiological conditions.

Several animal models have demonstrated microscopic changes in the myocardium as a direct result of DOX therapy. Under the electron microscope, Siveski-Iliskovic *et al*. 1994 demonstrated severe mitochondrial swelling, vacuolization of the cytoplasm, formation of lysosomal bodies, and dilation of the sarcotubular system.[42] They also noted significant disarrangement and disruption of the cristae within the mitochondria. Using light microscopy, Jassal et al. 2009 and Walker *et al*. 2011 recently demonstrated that mice treated with DOX displayed extensive myofibrillar degradation and cellular vacuolization.[3, 129] Additionally, mice that received combination therapy with DOX+TRZ demonstrated significantly more myocardial damage as compared to those mice treated with DOX alone. [3, 129] Similarly, in our study, we demonstrated that DOX and DOX+TRZ therapy is associated with significant cardiac remodeling in a female murine model of acute chemotherapy-induced cardiac dysfunction. In both WT and NOS3$^{-/-}$ female mice treated with DOX, there was evidence of myofibrillar degradation, vacuolization, loss of cell integrity and dilation of the sarcoplasmic reticulum, which was potentiated by the addition of TRZ.

Direct evidence of cardiac remodeling due to DOX therapy is best accomplished through invasive myocardial biopsies. Invasive assessment of cardiac structure provides

the best sensitivity and specificity for diagnosing DOX-mediated cardiac remodeling. Clinical biopsies of the right ventricle (RV) have demonstrated that DOX treatment is most commonly associated with loss of myofibrils, distension of the sarcoplasmic reticulum, and vacuolization of the cytoplasm. Bristow *et al*. 1978 correlated the amount of myocardial damage with the degree of severity due to DOX therapy.[176] They determined that a biopsy score of 2.5 or greater may be indicative of DOX-induced cardiac remodeling and discontinuation of therapy should be considered.[176] Clinical investigations of TRZ-mediated cardiac remodeling has also been evaluated. Ewer *et al.* 2005 obtained RV biopsies from 9 women who received TRZ therapy alone and evaluated them for the presence of myocyte remodeling.[96] Interestingly, of the 9 women tested, none displayed any evidence of ultrastructural remodeling typical to that what is seen with anthracycline therapy.[96]

Programmed cell death, or apoptosis, has been reported in a variety of experimental and clinical models of cardiac dysfunction.[177-179] Several of these studies have suggested that cardiac remodeling associated with chemotherapy treatment is a direct result of DOX mediated apoptosis.[131, 162, 180, 181] Rat cardiomyocytes exposed to DOX demonstrated a significant increase in the number of cells undergoing apoptosis within 24 hours of DOX treatment and was confirmed by Hoechst 33258 staining, TUNEL, and DNA laddering.[180-183] In a chronic *in vivo* study, rats exposed to high dose DOX treatment over 2 weeks demonstrated a significantly higher event rate of apoptosis by TUNEL as early as day 4 and progressed until day 21 ($p<0.05$).[131] Immunohistochemical staining revealed an increase in Bax expression in the DOX treated group as compared to saline controls.[131, 181] Maximal staining for Caspase 3

occurred at day 4 following treatment and progressively declined until day 21.[131, 181] Bax and Bcl-2 ratio demonstrated a biphasic response to DOX within the heart. A higher Bax-to-Bcl-2 ratio is indicative of apoptosis.[131] Mouse models have demonstrated that both WT and $NOS3^{-/-}$ male mice treated with a single high dose concentration of DOX lead to an increase in TUNEL-positive cardiac nuclei as early as 24 hours following treatment.[162] $NOS3^{-/-}$ mice, however, demonstrated preserved cardiac function and were correlated with a reduction of TUNEL positive nuclei.[162] These studies provide strong evidence for the increased occurrence of apoptosis in cardiac myocytes in male animals treated with DOX.

Trastuzumab therapy has also been correlated with an increase in cellular apoptosis. Recently, Grazette *et al*. 2004 demonstrated that TRZ binding to the HER2 receptor in an in vitro model resulted in a significant increase in the ratio between Bcl-X_S and Bcl-X_L.[93] Trastuzumab therapy resulted in the down-regulation of the anti-apoptotic protein Bcl-X_L, and up-regulation of the pro-apoptotic Bcl-X_S and Bax, resulting in mitochondrial dysfunction.[93] The ratio of anti- to pro-apoptotic proteins from the Bcl protein family is key, as they are important mediators of mitochondrial function and cellular apoptosis. Additionally, there was a modest increase in TUNEL staining and flow cytometry for propidium iodide labeled neonatal rat ventricular cardiomyocytes despite the observed increase in the mitochondria death pathway.[93] Furthermore, there was no observable increase in DNA laddering, likely due to low levels of apoptosis that could not be detected with this technique. Therefore, while an increase in pro-apoptotic proteins is beneficial in cancer treatment, it is correlated with mitochondrial dysfunction, leading to myocyte death.[93, 95]

In 2009 Jassal *et al.* characterized the degree of apoptosis in the heart associated with the combination of DOX+TRZ therapy.[3] Co-administration of DOX+TRZ in WT male mice induced the greatest degree of apoptosis at day 10 compared to either agent alone. An increase in PARP cleavage, activation of Caspase 3, and alteration in the Bax/Bcl-X_L ratio within the heart of those mice undergoing chemotherapy treatment was indicative of apoptosis. This suggests that co-adminsitration with DOX+TRZ results in a greater pro-apoptotic signaling event than either agent alone. In a 2011 study, Walker *et al.* treated male mice with DOX (20mg/kg), TRZ (10mg/kg) or a combination of both and evaluated them for the degree of cardiac dysfunction.[129] The degree of cardiac dysfunction was greatest in those co-treated with DOX+TRZ than with either agent alone, and was directly correlated to an increased apoptotic response. This apoptotic response was characterized primarily by a significant increase in the Bax-to-Bcl-X_L ratio at day 10. However, prophylactic administration of Probucol attenuated this response and was characterized by improved survival, preserved cardiac systolic function, reduced apoptosis and cardiac remodeling.[129]

A review of the survival data from the current study demonstrates that the greatest morality in female mice receiving either DOX or the combination of DOX+TRZ occurred on day 4. As such, we chose day 4 for detecting the presence of cardiac apoptosis via TUNEL and Western analyses. There was no evidence of Caspase 3, PARP, nor TUNEL positive nuclei at day 4 in any of the treatment groups. However, there was an increasing trend in the Bax-to-Bcl-X_L ratio in WT or $NOS3^{-/-}$ mice receiving either DOX alone or the combination of DOX+TRZ. This contrasts to previous studies that illustrated the presence of cardiac apoptosis in male mice and rats 10 and 21 days following DOX

treatment. [3, 129, 131] Neilan *et al*. 2007 demonstrated the presence of cardiac apoptosis via TUNEL positive nuclei 24 hours following DOX treatment in male mice.[162] Additionally, Jassal *et al* 2009 and Walker *et al*. 2011 demonstrated an increase in PARP and Caspase cleavage at day 10.[3, 129] As we demonstrated no evidence of apoptosis at day 4, this suggests that other non-apopototic pathways may be involved in the echocardiographic and survival findings in our study.

We did, however, detect an increasing trend in Bax-to-Bcl-X_L ratio amongst the various treatment groups in both WT and $NOS3^{-/-}$ female mice. Although there was an increasing trend in Bax-to-Bcl-X_L ratio in both WT and $NOS3^{-/-}$ DOX+TRZ female mice as compared to TRZ at day 4, it was not statistically significant. A biphasic response to DOX and DOX+TRZ therapy may account for the lack of positive apoptotic markers in our treatment groups. Previously, Kumar *et al*. 2001 demonstrated that male rats treated with DOX had a significant increase in the degree of cardiac apoptosis at day 4 following DOX treatment, that had declined by day 10. By day 21, however, there was again a significant increase in the degree of cardiac apoptosis detected in DOX treated male rats.[131] Increased apoptosis at days 4 and 21 was indicated by an increase in Bax expression and a decrease in Bcl-2 expression. At day 10, the inverse was true, in that Bcl-2 was up regulated whereas Bax expression was depressed.[131] Although we did not detect any TUNEL positive nuclei or Caspase 3 cleavage at day 4 in female mice, we did demonstrate an increasing trend in Bax-to-Bcl-X_L ratio, corroborating previous reports.[3, 129, 131, 162] To determine the exact timing of the apoptotic waves associated with DOX+TRZ therapy, an in-depth time course study in mice is warranted. Based on the current study, however, this would suggest that in a female murine model of acute

chemotherapy-induced heart failure, congenital absence of NOS3 potentiates cardiac dysfunction and increased mortality possibly through an apoptotic independent pathway.

Autophagy and necrosis are apoptotic independent pathways that may account for the development of cardiac dysfunction in our murine model. Autophagy has been described to have a dual effect within the heart as it removes protein aggregates and damaged organelles in the heart and acts as a pro-survival pathway to maintain homeostasis[184] On the other hand, significant induction of autophagy can lead to cardiomyocyte death. Several previous studies have indicated that microtubule-associated light chain 3 (LC3) is a specific marker for autophagy.[184, 185] During autophagy, LC3-I is converted to LC3-II through lipodation by an ubiquitin-like system.[186-189] A higher ratio of LC3-II to LC3-I is indicative of autophagy induction. Induction of autophagy in mice treated with DOX has been previously described to play a critical role in the development of cardiac dysfunction.[186, 190] In a study by Kobayashi *et al.* 2010, cardiomyocytes exposed to DOX had a significant increase in LC3-II protein levels.[186] Additionally, Kobayashi *et al.* 2010 demonstrated that DOX decreases GATA4 activity and is associated with DOX-induced cardiotoxicity.[186] Using an adenovirus, they overexpressed GATA4 expression and treated cardiomyocytes with DOX. They found that overexpression of GATA4 protected cardiomyocytes from DOX-induced cardiotoxicity by inhibiting autophagy induction.[186] In another study, Zhang *et al.* 2011 demonstrated *in vivo,* that mice treated with DOX had significantly higher levels of LC3-II to LC3-I as early as 24 hours following DOX treatment.[190] Additionally, electron microscopy demonstrated accumulation of vacuoles in cardiomyocytes following DOX treatment. Most of these vacuoles were described as electron dense lysosomes.[190] Together, these

studies validate a potential role for autophagy in the development of DOX mediated heart failure. Whether autophagy plays a significant role in DOX+TRZ mediated cardiotoxicity requires further study.

Necrosis may be another process by which DOX induces its cardiotoxic side effects. Necrosis is characterized by early rupture of the plasma membrane and swelling of cytoplasmic organelles.[184] Several previous studies have indicted the mouse hearts treated with DOX demonstrate increased cardiac expression of pro-inflammatory cytokines, inflammatory cell infiltration and necrosis.[191-193] In 2004 Lim *et al.* subjected adult rat cardiomyocytes to DOX therapy. They found that although there was an increase in Caspase 3 activity, there was no change in TUNEL staining 48 hours after DOX treatment. There was however increased cell loss, as well as an increase in trypan blue uptake and CK release, which suggests loss of cell membrane integrity, a key feature of necrosis.[194] These results were directly correlated with increased calpain expression, and inhibition of calpains completely prevented trypan blue uptake.[194] While necrosis due to DOX therapy has been indicated by mitochondrial dysregulationtion and dysfunction, an inflammatory response and loss of cell membrane integrity have been described, a clear understanding into the role that necrosis truly plays in DOX-mediated cardiac dysfunction remains incompletely known. It is likely that DOX and TRZ mediated heart failure stems from a combination of apoptosis, autophagy, and necrosis and an in depth analysis to compare the activation of each is warranted.

Future Directions

Although we have demonstrated a sexual dichotomy between male and female $NOS3^{-/-}$ mice in an acute model chemotherapy-induced cardiac dysfunction, the underlying mechanism remains unknown. Future studies will determine whether ROS, autophagy and necrosis play a significant role in cardiac remodeling and dysfunction in this model. Additionally, investigations into whether pharmacological inhibition of NOS3 can reproduce the current studies findings are warranted. If so, increased NOS3 expression by genetic modification or pharmacological drugs in female mice may provide protection against DOX+TRZ mediated cardiotoxicity. Finally, hormonal variance between male and female mice may play an important role in the development of chemotherapy-induced cardiac dysfunction.

Limitations

There are several limitations to our study. First, we only characterized chemotherapy-induced cardiac dysfunction in an acute female murine model of DOX+TRZ mediated heart failure. When pre-clinical animal models are considered, many acute *in vivo* studies involve the use of higher than normal concentrations of DOX+TRZ, which complicates the translation of basic science findings into the clinical setting. Therefore, a chronic model of DOX+TRZ mediated cardiac dysfunction that more closely mimics the clinical setting in a female model is warranted. Second, we focused only on female mice during the course of the study. It would be useful to compare equal populations of both male and female mice at the same time in order to make direct comparisons. Finally, although we focus primarily on apoptosis, little is known regarding the MAPK, cytoarchitecture signaling, and the RAS pathways in chemotherapy mediated cardiac dysfunction that requires further exploration.

Clinical Implications

To the best of our knowledge, we are the first to describe a sexual dichotomy for the development of chemotherapy-induced cardiac dysfunction in NOS3$^{-/-}$ mice. Generally, women who develop breast cancer and have lower levels of NOS3 activity, tend to respond less often to treatment and experience poor outcomes.[195] Our study is novel in that it suggests a key role of NOS3 in the pathophysiology of chemotherapy-induced cardiac dysfunction in females. Thus, by exploring the role of NOS3 overexpression in DOX+TRZ induced cardiac dysfunction, we may shine light onto novel cardioprotective treatment options, such as nitrites and phosphodiesterase inhibitors, for women with breast cancer who develop CHF symptoms. Although using drugs to increase NOS3 activity may prove to be useful within the breast cancer setting, further investigation is required.

Conclusion

For the first time, our novel study demonstrates that congenital absence of NOS3 potentiates the cardiotoxic effects of DOX+TRZ in an acute female murine model of chemotherapy-induced cardiomyopathy. Further research is required to determine whether overexpression or over activation of NOS3 through pharmacological measures is cardioprotective in a more clinically relevant female murine model of DOX+TRZ mediated cardiac dysfunction.

References

1. Canadian Cancer Society's Steering Committee on Cancer Statistics. Canadian cancer statistics 2011. 2011
2. Canadian Cancer Society's Steering Committee on Cancer Statistics. Canadian cancer statistics 2010. 2010
3. Jassal DS, Han SY, Hans C, Sharma A, Fang T, Ahmadie R, Lytwyn M, Walker JR, Bhalla RS, Czarnecki A, Moussa T, Singal PK. Utility of tissue doppler and strain rate imaging in the early detection of trastuzumab and anthracycline mediated cardiomyopathy. *J Am Soc Echocardiogr*. 2009;22:418-424
4. Canadian Cancer Society's Steering Committee on Cancer Statistics. Canadian cancer statistics 2007. 2007
5. Armstrong K, Eisen A, Weber B. Assessing the risk of breast cancer. *N Engl J Med*. 2000;342:564-571
6. Warner E, Hill K, Causer P, Plewes D, Jong R, Yaffe M, Foulkes WD, Ghadirian P, Lynch H, Couch F, Wong J, Wright F, Sun P, Narod SA. Prospective study of breast cancer incidence in women with a brca1 or brca2 mutation under surveillance with and without magnetic resonance imaging. *J Clin Oncol*. 2011;29:1664-1669
7. Warner E, Plewes DB, Hill KA, Causer PA, Zubovits JT, Jong RA, Cutrara MR, DeBoer G, Yaffe MJ, Messner SJ, Meschino WS, Piron CA, Narod SA. Surveillance of brca1 and brca2 mutation carriers with magnetic resonance imaging, ultrasound, mammography, and clinical breast examination. *JAMA*. 2004;292:1317-1325

8. Berman CG. Recent advances in breast-specific imaging. *Cancer Control*. 2007;14:338-349

9. Kolb TM, Lichy J, Newhouse JH. Comparison of the performance of screening mammography, physical examination, and breast us and evaluation of factors that influence them: An analysis of 27,825 patient evaluations. *Radiology*. 2002;225:165-175

10. Capala J, Bouchelouche K. Molecular imaging of her2-positive breast cancer: A step toward an individualized 'image and treat' strategy. *Curr Opin Oncol*. 2010;22:559-566

11. Hazard HW, Gorla SR, Scholtens D, Kiel K, Gradishar WJ, Khan SA. Surgical resection of the primary tumor, chest wall control, and survival in women with metastatic breast cancer. *Cancer*. 2008;113:2011-2019

12. Ragaz J, Olivotto IA, Spinelli JJ, Phillips N, Jackson SM, Wilson KS, Knowling MA, Coppin CM, Weir L, Gelmon K, Le N, Durand R, Coldman AJ, Manji M. Locoregional radiation therapy in patients with high-risk breast cancer receiving adjuvant chemotherapy: 20-year results of the british columbia randomized trial. *J Natl Cancer Inst*. 2005;97:116-126

13. Taghian AG, Powell SN. The role of radiation therapy for primary breast cancer. *Surg Clin North Am*. 1999;79:1091-1115

14. Network NCC. Practice guideline in oncology – v.1.2009: Breast cancer. 2009

15. Rabbani A, Finn RM, Ausio J. The anthracycline antibiotics: Antitumor drugs that alter chromatin structure. *Bioessays*. 2005;27:50-56

16. Weiss RB, Sarosy G, Clagett-Carr K, Russo M, Leyland-Jones B. Anthracycline analogs: The past, present, and future. *Cancer Chemother Pharmacol*. 1986;18:185-197

17. Singal PK, Li T, Kumar D, Danelisen I, Iliskovic N. Adriamycin-induced heart failure: Mechanism and modulation. *Mol Cell Biochem*. 2000;207:77-86

18. Minotti G, Menna P, Salvatorelli E, Cairo G, Gianni L. Anthracyclines: Molecular advances and pharmacologic developments in antitumor activity and cardiotoxicity. *Pharmacol Rev*. 2004;56:185-229

19. Takemura G, Fujiwara H. Doxorubicin-induced cardiomyopathy from the cardiotoxic mechanisms to management. *Prog Cardiovasc Dis*. 2007;49:330-352

20. Muggia FM, Green MD. New anthracycline antitumor antibiotics. *Crit Rev Oncol Hematol*. 1991;11:43-64

21. Gewirtz DA. A critical evaluation of the mechanisms of action proposed for the antitumor effects of the anthracycline antibiotics adriamycin and daunorubicin. *Biochem Pharmacol*. 1999;57:727-741

22. Wishart DS, Knox C, Guo AC, Cheng D, Shrivastava S, Tzur D, Gautam B, Hassanali M. Drugbank: A knowledgebase for drugs, drug actions and drug targets. *Nucleic Acids Res*. 2008;36:D901-906

23. Peng X, Chen B, Lim CC, Sawyer DB. The cardiotoxicology of anthracycline chemotherapeutics: Translating molecular mechanism into preventative medicine. *Mol Interv*. 2005;5:163-171

24. Chen GL, Yang L, Rowe TC, Halligan BD, Tewey KM, Liu LF. Nonintercalative antitumor drugs interfere with the breakage-reunion reaction of mammalian DNA topoisomerase ii. *J Biol Chem*. 1984;259:13560-13566

25. Sawyer DB, Peng X, Chen B, Pentassuglia L, Lim CC. Mechanisms of anthracycline cardiac injury: Can we identify strategies for cardioprotection? *Prog Cardiovasc Dis*. 2010;53:105-113

26. Singal PK, Iliskovic N, Li T, Kumar D. Adriamycin cardiomyopathy: Pathophysiology and prevention. *FASEB J*. 1997;11:931-936

27. Guano F, Pourquier P, Tinelli S, Binaschi M, Bigioni M, Animati F, Manzini S, Zunino F, Kohlhagen G, Pommier Y, Capranico G. Topoisomerase poisoning activity of novel disaccharide anthracyclines. *Mol Pharmacol*. 1999;56:77-84

28. Binaschi M, Capranico G, Dal Bo L, Zunino F. Relationship between lethal effects and topoisomerase ii-mediated double-stranded DNA breaks produced by anthracyclines with different sequence specificity. *Mol Pharmacol*. 1997;51:1053-1059

29. Fisher LM, Austin CA, Hopewell R, Margerrison EE, Oram M, Patel S, Plummer K, Sng JH, Sreedharan S. DNA supercoiling and relaxation by atp-dependent DNA topoisomerases. *Philos Trans R Soc Lond B Biol Sci*. 1992;336:83-91

30. Zunino F, Pratesi G, Perego P. Role of the sugar moiety in the pharmacological activity of anthracyclines: Development of a novel series of disaccharide analogs. *Biochem Pharmacol*. 2001;61:933-938

31. Ludke AR, Al-Shudiefat AA, Dhingra S, Jassal DS, Singal PK. A concise description of cardioprotective strategies in doxorubicin-induced cardiotoxicity. *Can J Physiol Pharmacol*. 2009;87:756-763

32. Singal PK, Iliskovic N. Doxorubicin-induced cardiomyopathy. *N Engl J Med*. 1998;339:900-905

33. Singal PK, Siveski-Iliskovic N, Kaul N, Sahai M. Significance of adaptation mechanisms in adriamycin induced congestive heart failure. *Basic Res Cardiol*. 1992;87:512-518

34. Chen B, Peng X, Pentassuglia L, Lim CC, Sawyer DB. Molecular and cellular mechanisms of anthracycline cardiotoxicity. *Cardiovasc Toxicol*. 2007;7:114-121

35. Lefrak EA, Pitha J, Rosenheim S, Gottlieb JA. A clinicopathologic analysis of adriamycin cardiotoxicity. *Cancer*. 1973;32:302-314

36. Praga C, Beretta G, Vigo PL, Lenaz GR, Pollini C, Bonadonna G, Canetta R, Castellani R, Villa E, Gallagher CG, von Melchner H, Hayat M, Ribaud P, De Wasch G, Mattsson W, Heinz R, Waldner R, Kolaric K, Buehner R, Ten Bokkel-Huyninck W, Perevodchikova NI, Manziuk LA, Senn HJ, Mayr AC. Adriamycin cardiotoxicity: A survey of 1273 patients. *Cancer Treat Rep*. 1979;63:827-834

37. Gilladoga AC, Manuel C, Tan CT, Wollner N, Sternberg SS, Murphy ML. The cardiotoxicity of adriamycin and daunomycin in children. *Cancer*. 1976;37:1070-1078

38. Bonadonna G, Monfardini S, De Lena M, Fossati-Bellani F, Beretta G. Phase i and preliminary phase ii evaluation of adriamycin (nsc 123127). *Cancer Res*. 1970;30:2572-2582

39. Cvetkovic RS, Scott LJ. Dexrazoxane : A review of its use for cardioprotection during anthracycline chemotherapy. *Drugs*. 2005;65:1005-1024

40. Wiseman LR, Spencer CM. Dexrazoxane. A review of its use as a cardioprotective agent in patients receiving anthracycline-based chemotherapy. *Drugs*. 1998;56:385-403

41. Schuchter LM, Hensley ML, Meropol NJ, Winer EP, American Society of Clinical Oncology C, Radiotherapy Expert P. 2002 update of recommendations for the use of chemotherapy and radiotherapy protectants: Clinical practice guidelines of the american society of clinical oncology. *J Clin Oncol*. 2002;20:2895-2903

42. Siveski-Iliskovic N, Kaul N, Singal PK. Probucol promotes endogenous antioxidants and provides protection against adriamycin-induced cardiomyopathy in rats. *Circulation*. 1994;89:2829-2835

43. Injac R, Strukelj B. Recent advances in protection against doxorubicin-induced toxicity. *Technol Cancer Res Treat*. 2008;7:497-516

44. Quiles JL, Huertas JR, Battino M, Mataix J, Ramirez-Tortosa MC. Antioxidant nutrients and adriamycin toxicity. *Toxicology*. 2002;180:79-95

45. Silber JH, Cnaan A, Clark BJ, Paridon SM, Chin AJ, Rychik J, Hogarty AN, Cohen MI, Barber G, Rutkowsky M, Kimball TR, Delaat C, Steinherz LJ, Zhao H, Tartaglione MR. Design and baseline characteristics for the ace inhibitor after anthracycline (aaa) study of cardiac dysfunction in long-term pediatric cancer survivors. *Am Heart J*. 2001;142:577-585

46. Shaddy RE, Olsen SL, Bristow MR, Taylor DO, Bullock EA, Tani LY, Renlund DG. Efficacy and safety of metoprolol in the treatment of doxorubicin-induced cardiomyopathy in pediatric patients. *Am Heart J*. 1995;129:197-199

47. Hackel PO, Zwick E, Prenzel N, Ullrich A. Epidermal growth factor receptors: Critical mediators of multiple receptor pathways. *Curr Opin Cell Biol*. 1999;11:184-189

48. Moghal N, Sternberg PW. Multiple positive and negative regulators of signaling by the egf-receptor. *Curr Opin Cell Biol*. 1999;11:190-196

49. Yarden Y, Sliwkowski MX. Untangling the erbb signalling network. *Nat Rev Mol Cell Biol*. 2001;2:127-137

50. Jiang Z, Zhou M. Neuregulin signaling and heart failure. *Curr Heart Fail Rep*. 2010;7:42-47

51. Worthylake R, Wiley HS. Structural aspects of the epidermal growth factor receptor required for transmodulation of erbb-2/neu. *J Biol Chem*. 1997;272:8594-8601

52. Landgraf R. Her2 therapy. Her2 (erbb2): Functional diversity from structurally conserved building blocks. *Breast Cancer Res*. 2007;9:202

53. Cho HS, Mason K, Ramyar KX, Stanley AM, Gabelli SB, Denney DW, Jr., Leahy DJ. Structure of the extracellular region of her2 alone and in complex with the herceptin fab. *Nature*. 2003;421:756-760

54. Negro A, Brar BK, Lee KF. Essential roles of her2/erbb2 in cardiac development and function. *Recent Prog Horm Res*. 2004;59:1-12

55. Graus-Porta D, Beerli RR, Daly JM, Hynes NE. Erbb-2, the preferred heterodimerization partner of all erbb receptors, is a mediator of lateral signaling. *EMBO J*. 1997;16:1647-1655

56. Pentassuglia L, Sawyer DB. The role of neuregulin-1beta/erbb signaling in the heart. *Exp Cell Res*. 2009;315:627-637

57. Ozcelik C, Erdmann B, Pilz B, Wettschureck N, Britsch S, Hubner N, Chien KR, Birchmeier C, Garratt AN. Conditional mutation of the erbb2 (her2) receptor in cardiomyocytes leads to dilated cardiomyopathy. *Proc Natl Acad Sci U S A*. 2002;99:8880-8885

58. Slichenmyer WJ, Fry DW. Anticancer therapy targeting the erbb family of receptor tyrosine kinases. *Semin Oncol*. 2001;28:67-79

59. Kuramochi Y, Guo X, Sawyer DB. Neuregulin activates erbb2-dependent src/fak signaling and cytoskeletal remodeling in isolated adult rat cardiac myocytes. *J Mol Cell Cardiol*. 2006;41:228-235

60. Slamon DJ, Clark GM, Wong SG, Levin WJ, Ullrich A, McGuire WL. Human breast cancer: Correlation of relapse and survival with amplification of the her-2/neu oncogene. *Science*. 1987;235:177-182

61. Baselga J, Albanell J, Molina MA, Arribas J. Mechanism of action of trastuzumab and scientific update. *Semin Oncol*. 2001;28:4-11

62. Yu D, Hung MC. Overexpression of erbb2 in cancer and erbb2-targeting strategies. *Oncogene*. 2000;19:6115-6121

63. Piccart-Gebhart MJ, Procter M, Leyland-Jones B, Goldhirsch A, Untch M, Smith I, Gianni L, Baselga J, Bell R, Jackisch C, Cameron D, Dowsett M, Barrios CH,

Steger G, Huang CS, Andersson M, Inbar M, Lichinitser M, Lang I, Nitz U, Iwata H, Thomssen C, Lohrisch C, Suter TM, Ruschoff J, Suto T, Greatorex V, Ward C, Straehle C, McFadden E, Dolci MS, Gelber RD, Herceptin Adjuvant Trial Study T. Trastuzumab after adjuvant chemotherapy in her2-positive breast cancer. *N Engl J Med*. 2005;353:1659-1672

64. Xing WR, Gilchrist KW, Harris CP, Samson W, Meisner LF. Fish detection of her-2/neu oncogene amplification in early onset breast cancer. *Breast Cancer Res Treat*. 1996;39:203-212

65. Press MF, Slamon DJ, Flom KJ, Park J, Zhou JY, Bernstein L. Evaluation of her-2/neu gene amplification and overexpression: Comparison of frequently used assay methods in a molecularly characterized cohort of breast cancer specimens. *J Clin Oncol*. 2002;20:3095-3105

66. Hicks DG, Tubbs RR. Assessment of the her2 status in breast cancer by fluorescence in situ hybridization: A technical review with interpretive guidelines. *Hum Pathol*. 2005;36:250-261

67. Dendukuri N, Khetani K, McIsaac M, Brophy J. Testing for her2-positive breast cancer: A systematic review and cost-effectiveness analysis. *CMAJ*. 2007;176:1429-1434

68. Yaziji H, Gown AM. Accuracy and precision in her2/neu testing in breast cancer: Are we there yet? *Hum Pathol*. 2004;35:143-146

69. Bilous M, Ades C, Armes J, Bishop J, Brown R, Cooke B, Cummings M, Farshid G, Field A, Morey A, McKenzie P, Raymond W, Robbins P, Tan L. Predicting the her2 status of breast cancer from basic histopathology data: An analysis of

1500 breast cancers as part of the her2000 international study. *Breast*. 2003;12:92-98

70. Perez EA, Suman VJ, Davidson NE, Sledge GW, Kaufman PA, Hudis CA, Martino S, Gralow JR, Dakhil SR, Ingle JN, Winer EP, Gelmon KA, Gersh BJ, Jaffe AS, Rodeheffer RJ. Cardiac safety analysis of doxorubicin and cyclophosphamide followed by paclitaxel with or without trastuzumab in the north central cancer treatment group n9831 adjuvant breast cancer trial. *J Clin Oncol*. 2008;26:1231-1238

71. Ewer MS, Ewer SM. Cardiotoxicity of anticancer treatments: What the cardiologist needs to know. *Nat Rev Cardiol*. 2010;7:564-575

72. Guglin M, Hartlage G, Reynolds C, Chen R, Patel V. Trastuzumab-induced cardiomyopathy: Not as benign as it looks? A retrospective study. *J Card Fail*. 2009;15:651-657

73. Tsang RY, Finn RS. Beyond trastuzumab: Novel therapeutic strategies in her2-positive metastatic breast cancer. *Br J Cancer*. 2012;106:6-13

74. Crone SA, Zhao YY, Fan L, Gu Y, Minamisawa S, Liu Y, Peterson KL, Chen J, Kahn R, Condorelli G, Ross J, Jr., Chien KR, Lee KF. Erbb2 is essential in the prevention of dilated cardiomyopathy. *Nat Med*. 2002;8:459-465

75. Sawyer DB, Zuppinger C, Miller TA, Eppenberger HM, Suter TM. Modulation of anthracycline-induced myofibrillar disarray in rat ventricular myocytes by neuregulin-1beta and anti-erbb2: Potential mechanism for trastuzumab-induced cardiotoxicity. *Circulation*. 2002;105:1551-1554

76. Sliwkowski MX, Lofgren JA, Lewis GD, Hotaling TE, Fendly BM, Fox JA. Nonclinical studies addressing the mechanism of action of trastuzumab (herceptin). *Semin Oncol*. 1999;26:60-70

77. Vogel CL, Cobleigh MA, Tripathy D, Gutheil JC, Harris LN, Fehrenbacher L, Slamon DJ, Murphy M, Novotny WF, Burchmore M, Shak S, Stewart SJ. First-line herceptin monotherapy in metastatic breast cancer. *Oncology*. 2001;61 Suppl 2:37-42

78. Slamon DJ, Leyland-Jones B, Shak S, Fuchs H, Paton V, Bajamonde A, Fleming T, Eiermann W, Wolter J, Pegram M, Baselga J, Norton L. Use of chemotherapy plus a monoclonal antibody against her2 for metastatic breast cancer that overexpresses her2. *N Engl J Med*. 2001;344:783-792

79. Romond EH, Perez EA, Bryant J, Suman VJ, Geyer CE, Jr., Davidson NE, Tan-Chiu E, Martino S, Paik S, Kaufman PA, Swain SM, Pisansky TM, Fehrenbacher L, Kutteh LA, Vogel VG, Visscher DW, Yothers G, Jenkins RB, Brown AM, Dakhil SR, Mamounas EP, Lingle WL, Klein PM, Ingle JN, Wolmark N. Trastuzumab plus adjuvant chemotherapy for operable her2-positive breast cancer. *N Engl J Med*. 2005;353:1673-1684

80. Plosker GL, Keam SJ. Trastuzumab: A review of its use in the management of her2-positive metastatic and early-stage breast cancer. *Drugs*. 2006;66:449-475

81. Tokuda Y, Suzuki Y, Saito Y, Umemura S. The role of trastuzumab in the management of her2-positive metastatic breast cancer: An updated review. *Breast Cancer*. 2009;16:295-300

82. Gianni L, Dafni U, Gelber RD, Azambuja E, Muehlbauer S, Goldhirsch A, Untch M, Smith I, Baselga J, Jackisch C, Cameron D, Mano M, Pedrini JL, Veronesi A, Mendiola C, Pluzanska A, Semiglazov V, Vrdoljak E, Eckart MJ, Shen Z, Skiadopoulos G, Procter M, Pritchard KI, Piccart-Gebhart MJ, Bell R, Herceptin Adjuvant Trial Study T. Treatment with trastuzumab for 1 year after adjuvant chemotherapy in patients with her2-positive early breast cancer: A 4-year follow-up of a randomised controlled trial. *Lancet Oncol*. 2011;12:236-244

83. Yin W, Jiang Y, Shen Z, Shao Z, Lu J. Trastuzumab in the adjuvant treatment of her2-positive early breast cancer patients: A meta-analysis of published randomized controlled trials. *PLoS One*. 2011;6:e21030

84. Baselga J, Carbonell X, Castaneda-Soto NJ, Clemens M, Green M, Harvey V, Morales S, Barton C, Ghahramani P. Phase ii study of efficacy, safety, and pharmacokinetics of trastuzumab monotherapy administered on a 3-weekly schedule. *J Clin Oncol*. 2005;23:2162-2171

85. Baselga J, Norton L, Albanell J, Kim YM, Mendelsohn J. Recombinant humanized anti-her2 antibody (herceptin) enhances the antitumor activity of paclitaxel and doxorubicin against her2/neu overexpressing human breast cancer xenografts. *Cancer Res*. 1998;58:2825-2831

86. Nakagami H, Takemoto M, Liao JK. Nadph oxidase-derived superoxide anion mediates angiotensin ii-induced cardiac hypertrophy. *J Mol Cell Cardiol*. 2003;35:851-859

87. Baselga J, Perez EA, Pienkowski T, Bell R. Adjuvant trastuzumab: A milestone in the treatment of her-2-positive early breast cancer. *Oncologist*. 2006;11 Suppl 1:4-12

88. NewYorkHeartAssociation. Nomenclature and criteria for diagnosis of diseases of the heart and great vessels. 1994:253-256

89. Seidman A, Hudis C, Pierri MK, Shak S, Paton V, Ashby M, Murphy M, Stewart SJ, Keefe D. Cardiac dysfunction in the trastuzumab clinical trials experience. *J Clin Oncol*. 2002;20:1215-1221

90. Wadhwa D, Fallah-Rad N, Grenier D, Krahn M, Fang T, Ahmadie R, Walker JR, Lister D, Arora RC, Barac I, Morris A, Jassal DS. Trastuzumab mediated cardiotoxicity in the setting of adjuvant chemotherapy for breast cancer: A retrospective study. *Breast Cancer Res Treat*. 2009;117:357-364

91. Zeglinski M, Ludke A, Jassal DS, Singal PK. Trastuzumab-induced cardiac dysfunction: A 'dual-hit'. *Exp Clin Cardiol*. 2011;16:70-74

92. Walker J, Bhullar N, Fallah-Rad N, Lytwyn M, Golian M, Fang T, Summers AR, Singal PK, Barac I, Kirkpatrick ID, Jassal DS. Role of three-dimensional echocardiography in breast cancer: Comparison with two-dimensional echocardiography, multiple-gated acquisition scans, and cardiac magnetic resonance imaging. *J Clin Oncol*. 2010;28:3429-3436

93. Grazette LP, Boecker W, Matsui T, Semigran M, Force TL, Hajjar RJ, Rosenzweig A. Inhibition of erbb2 causes mitochondrial dysfunction in cardiomyocytes: Implications for herceptin-induced cardiomyopathy. *J Am Coll Cardiol*. 2004;44:2231-2238

94. Cardinale D, Colombo A, Sandri MT, Lamantia G, Colombo N, Civelli M, Martinelli G, Veglia F, Fiorentini C, Cipolla CM. Prevention of high-dose chemotherapy-induced cardiotoxicity in high-risk patients by angiotensin-converting enzyme inhibition. *Circulation*. 2006;114:2474-2481

95. Gordon LI, Burke MA, Singh AT, Prachand S, Lieberman ED, Sun L, Naik TJ, Prasad SV, Ardehali H. Blockade of the erbb2 receptor induces cardiomyocyte death through mitochondrial and reactive oxygen species-dependent pathways. *J Biol Chem*. 2009;284:2080-2087

96. Ewer MS, Vooletich MT, Durand JB, Woods ML, Davis JR, Valero V, Lenihan DJ. Reversibility of trastuzumab-related cardiotoxicity: New insights based on clinical course and response to medical treatment. *J Clin Oncol*. 2005;23:7820-7826

97. Guarneri V, Lenihan DJ, Valero V, Durand JB, Broglio K, Hess KR, Michaud LB, Gonzalez-Angulo AM, Hortobagyi GN, Esteva FJ. Long-term cardiac tolerability of trastuzumab in metastatic breast cancer: The m.D. Anderson cancer center experience. *J Clin Oncol*. 2006;24:4107-4115

98. Suter TM, Procter M, van Veldhuisen DJ, Muscholl M, Bergh J, Carlomagno C, Perren T, Passalacqua R, Bighin C, Klijn JG, Ageev FT, Hitre E, Groetz J, Iwata H, Knap M, Gnant M, Muehlbauer S, Spence A, Gelber RD, Piccart-Gebhart MJ. Trastuzumab-associated cardiac adverse effects in the herceptin adjuvant trial. *J Clin Oncol*. 2007;25:3859-3865

99. Guglin M, Cutro R, Mishkin JD. Trastuzumab-induced cardiomyopathy. *J Card Fail*. 2008;14:437-444

100. Russell SD, Blackwell KL, Lawrence J, Pippen JE, Jr., Roe MT, Wood F, Paton V, Holmgren E, Mahaffey KW. Independent adjudication of symptomatic heart failure with the use of doxorubicin and cyclophosphamide followed by trastuzumab adjuvant therapy: A combined review of cardiac data from the national surgical adjuvant breast and bowel project b-31 and the north central cancer treatment group n9831 clinical trials. *J Clin Oncol*. 2010;28:3416-3421

101. Ewer MS, Tan-Chiu E. Reversibility of trastuzumab cardiotoxicity: Is the concept alive and well? *J Clin Oncol*. 2007;25:5532-5533; author reply 5533-5534

102. Tham YL, Verani MS, Chang J. Reversible and irreversible cardiac dysfunction associated with trastuzumab in breast cancer. *Breast Cancer Res Treat*. 2002;74:131-134

103. Villani F, Meazza R, Materazzo C. Non-invasive monitoring of cardiac hemodynamic parameters in doxorubicin-treated patients: Comparison with echocardiography. *Anticancer Res*. 2006;26:797-801

104. Ganz WI, Sridhar KS, Ganz SS, Gonzalez R, Chakko S, Serafini A. Review of tests for monitoring doxorubicin-induced cardiomyopathy. *Oncology*. 1996;53:461-470

105. Meinardi MT, van der Graaf WT, van Veldhuisen DJ, Gietema JA, de Vries EG, Sleijfer DT. Detection of anthracycline-induced cardiotoxicity. *Cancer Treat Rev*. 1999;25:237-247

106. Yu CM, Sanderson JE, Marwick TH, Oh JK. Tissue doppler imaging a new prognosticator for cardiovascular diseases. *J Am Coll Cardiol*. 2007;49:1903-1914

107. Shan Y, Villarraga HR, Pislaru C, Shah AA, Cha SS, Pellikka PA. Quantitative assessment of strain and strain rate by velocity vector imaging during dobutamine stress echocardiography to predict outcome in patients with left bundle branch block. *J Am Soc Echocardiogr*. 2009;22:1212-1219

108. Saleh HK, Villarraga HR, Kane GC, Pereira NL, Raichlin E, Yu Y, Koshino Y, Kushwaha SS, Miller FA, Jr., Oh JK, Pellikka PA. Normal left ventricular mechanical function and synchrony values by speckle-tracking echocardiography in the transplanted heart with normal ejection fraction. *J Heart Lung Transplant*. 2011;30:652-658

109. Neilan TG, Jassal DS, Perez-Sanz TM, Raher MJ, Pradhan AD, Buys ES, Ichinose F, Bayne DB, Halpern EF, Weyman AE, Derumeaux G, Bloch KD, Picard MH, Scherrer-Crosbie M. Tissue doppler imaging predicts left ventricular dysfunction and mortality in a murine model of cardiac injury. *Eur Heart J*. 2006;27:1868-1875

110. Rajappan K, Bellenger NG, Anderson L, Pennell DJ. The role of cardiovascular magnetic resonance in heart failure. *Eur J Heart Fail*. 2000;2:241-252

111. Walker JR, Singal PK, Jassal DS. The art of healing broken hearts in breast cancer patients: Trastuzumab and heart failure. *Exp Clin Cardiol*. 2009;14:e62-67

112. Hare JL, Brown JK, Leano R, Jenkins C, Woodward N, Marwick TH. Use of myocardial deformation imaging to detect preclinical myocardial dysfunction before conventional measures in patients undergoing breast cancer treatment with trastuzumab. *Am Heart J*. 2009;158:294-301

113. Ho E, Brown A, Barrett P, Morgan RB, King G, Kennedy MJ, Murphy RT. Subclinical anthracycline- and trastuzumab-induced cardiotoxicity in the long-term follow-up of asymptomatic breast cancer survivors: A speckle tracking echocardiographic study. *Heart*. 2010;96:701-707

114. Di Lisi D, Bonura F, Macaione F, Peritore A, Meschisi M, Cuttitta F, Novo G, D'Alessandro N, Novo S. Chemotherapy-induced cardiotoxicity: Role of the tissue doppler in the early diagnosis of left ventricular dysfunction. *Anticancer Drugs*. 2011;22:468-472

115. Sawaya H, Sebag IA, Plana JC, Januzzi JL, Ky B, Cohen V, Gosavi S, Carver JR, Wiegers SE, Martin RP, Picard MH, Gerszten RE, Halpern EF, Passeri J, Kuter I, Scherrer-Crosbie M. Early detection and prediction of cardiotoxicity in chemotherapy-treated patients. *Am J Cardiol*. 2011;107:1375-1380

116. Fallah-Rad N, Walker JR, Wassef A, Lytwyn M, Bohonis S, Fang T, Tian G, Kirkpatrick ID, Singal PK, Krahn M, Grenier D, Jassal DS. The utility of cardiac biomarkers, tissue velocity and strain imaging, and cardiac magnetic resonance imaging in predicting early left ventricular dysfunction in patients with human epidermal growth factor receptor ii-positive breast cancer treated with adjuvant trastuzumab therapy. *J Am Coll Cardiol*. 2011;57:2263-2270

117. Cardinale D, Sandri MT, Martinoni A, Tricca A, Civelli M, Lamantia G, Cinieri S, Martinelli G, Cipolla CM, Fiorentini C. Left ventricular dysfunction predicted by early troponin i release after high-dose chemotherapy. *J Am Coll Cardiol*. 2000;36:517-522

118. Cardinale D, Sandri MT, Colombo A, Colombo N, Boeri M, Lamantia G, Civelli M, Peccatori F, Martinelli G, Fiorentini C, Cipolla CM. Prognostic value of troponin i in cardiac risk stratification of cancer patients undergoing high-dose chemotherapy. *Circulation*. 2004;109:2749-2754

119. Cardinale D, Colombo A, Torrisi R, Sandri MT, Civelli M, Salvatici M, Lamantia G, Colombo N, Cortinovis S, Dessanai MA, Nole F, Veglia F, Cipolla CM. Trastuzumab-induced cardiotoxicity: Clinical and prognostic implications of troponin i evaluation. *J Clin Oncol*. 2010;28:3910-3916

120. Hasinoff BB, Schnabl KL, Marusak RA, Patel D, Huebner E. Dexrazoxane (icrf-187) protects cardiac myocytes against doxorubicin by preventing damage to mitochondria. *Cardiovasc Toxicol*. 2003;3:89-99

121. Swain SM, Whaley FS, Gerber MC, Ewer MS, Bianchine JR, Gams RA. Delayed administration of dexrazoxane provides cardioprotection for patients with advanced breast cancer treated with doxorubicin-containing therapy. *J Clin Oncol*. 1997;15:1333-1340

122. Marty M, Espie M, Llombart A, Monnier A, Rapoport BL, Stahalova V, Dexrazoxane Study G. Multicenter randomized phase iii study of the cardioprotective effect of dexrazoxane (cardioxane) in advanced/metastatic breast cancer patients treated with anthracycline-based chemotherapy. *Ann Oncol*. 2006;17:614-622

123. Speyer JL, Green MD, Zeleniuch-Jacquotte A, Wernz JC, Rey M, Sanger J, Kramer E, Ferrans V, Hochster H, Meyers M, et al. Icrf-187 permits longer

treatment with doxorubicin in women with breast cancer. *J Clin Oncol*. 1992;10:117-127

124. Singal PK, Siveski-Iliskovic N, Hill M, Thomas TP, Li T. Combination therapy with probucol prevents adriamycin-induced cardiomyopathy. *J Mol Cell Cardiol*. 1995;27:1055-1063

125. Zimetbaum P, Eder H, Frishman W. Probucol: Pharmacology and clinical application. *J Clin Pharmacol*. 1990;30:3-9

126. Li T, Danelisen I, Bello-Klein A, Singal PK. Effects of probucol on changes of antioxidant enzymes in adriamycin-induced cardiomyopathy in rats. *Cardiovasc Res*. 2000;46:523-530

127. Siveski-Iliskovic N, Hill M, Chow DA, Singal PK. Probucol protects against adriamycin cardiomyopathy without interfering with its antitumor effect. *Circulation*. 1995;91:10-15

128. Iliskovic N, Hasinoff BB, Malisza KL, Li T, Danelisen I, Singal PK. Mechanisms of beneficial effects of probucol in adriamycin cardiomyopathy. *Mol Cell Biochem*. 1999;196:43-49

129. Walker JR, Sharma A, Lytwyn M, Bohonis S, Thliveris J, Singal PK, Jassal DS. The cardioprotective role of probucol against anthracycline and trastuzumab-mediated cardiotoxicity. *J Am Soc Echocardiogr*. 2011;24:699-705

130. Li T, Singal PK. Adriamycin-induced early changes in myocardial antioxidant enzymes and their modulation by probucol. *Circulation*. 2000;102:2105-2110

131. Kumar D, Kirshenbaum LA, Li T, Danelisen I, Singal PK. Apoptosis in adriamycin cardiomyopathy and its modulation by probucol. *Antioxid Redox Signal*. 2001;3:135-145

132. Ray PD, Huang BW, Tsuji Y. Reactive oxygen species (ros) homeostasis and redox regulation in cellular signaling. *Cell Signal*. 2012;24:981-990

133. Forman HJ, Fukuto JM, Torres M. Redox signaling: Thiol chemistry defines which reactive oxygen and nitrogen species can act as second messengers. *Am J Physiol Cell Physiol*. 2004;287:C246-256

134. Li J, Stouffs M, Serrander L, Banfi B, Bettiol E, Charnay Y, Steger K, Krause KH, Jaconi ME. The nadph oxidase nox4 drives cardiac differentiation: Role in regulating cardiac transcription factors and map kinase activation. *Mol Biol Cell*. 2006;17:3978-3988

135. Sauer H, Rahimi G, Hescheler J, Wartenberg M. Role of reactive oxygen species and phosphatidylinositol 3-kinase in cardiomyocyte differentiation of embryonic stem cells. *FEBS Lett*. 2000;476:218-223

136. Moncada S, Higgs A. The l-arginine-nitric oxide pathway. *N Engl J Med*. 1993;329:2002-2012

137. Higashi Y, Noma K, Yoshizumi M, Kihara Y. Endothelial function and oxidative stress in cardiovascular diseases. *Circ J*. 2009;73:411-418

138. Fleming I, Busse R. Molecular mechanisms involved in the regulation of the endothelial nitric oxide synthase. *Am J Physiol Regul Integr Comp Physiol*. 2003;284:R1-12

139. Palmer RM, Ashton DS, Moncada S. Vascular endothelial cells synthesize nitric oxide from l-arginine. *Nature*. 1988;333:664-666

140. Moncada S, Palmer RM, Higgs EA. Biosynthesis of nitric oxide from l-arginine. A pathway for the regulation of cell function and communication. *Biochem Pharmacol*. 1989;38:1709-1715

141. Ignarro LJ. Biosynthesis and metabolism of endothelium-derived nitric oxide. *Annu Rev Pharmacol Toxicol*. 1990;30:535-560

142. Marletta MA. Nitric oxide: Biosynthesis and biological significance. *Trends Biochem Sci*. 1989;14:488-492

143. Xia Y, Tsai AL, Berka V, Zweier JL. Superoxide generation from endothelial nitric-oxide synthase. A ca2+/calmodulin-dependent and tetrahydrobiopterin regulatory process. *J Biol Chem*. 1998;273:25804-25808

144. Snyder SH, Bredt DS. Biological roles of nitric oxide. *Sci Am*. 1992;266:68-71, 74-67

145. Moncada S. The 1991 ulf von euler lecture. The l-arginine: Nitric oxide pathway. *Acta Physiol Scand*. 1992;145:201-227

146. Forstermann U, Boissel JP, Kleinert H. Expressional control of the 'constitutive' isoforms of nitric oxide synthase (nos i and nos iii). *FASEB J*. 1998;12:773-790

147. Fleming I, Busse R. Signal transduction of enos activation. *Cardiovasc Res*. 1999;43:532-541

148. Chen PF, Tsai AL, Berka V, Wu KK. Mutation of glu-361 in human endothelial nitric-oxide synthase selectively abolishes l-arginine binding without perturbing the behavior of heme and other redox centers. *J Biol Chem*. 1997;272:6114-6118

149. Sessa WC, Harrison JK, Barber CM, Zeng D, Durieux ME, D'Angelo DD, Lynch KR, Peach MJ. Molecular cloning and expression of a cdna encoding endothelial cell nitric oxide synthase. *J Biol Chem*. 1992;267:15274-15276

150. Garcia-Cardena G, Fan R, Shah V, Sorrentino R, Cirino G, Papapetropoulos A, Sessa WC. Dynamic activation of endothelial nitric oxide synthase by hsp90. *Nature*. 1998;392:821-824

151. Presta A, Liu J, Sessa WC, Stuehr DJ. Substrate binding and calmodulin binding to endothelial nitric oxide synthase coregulate its enzymatic activity. *Nitric Oxide*. 1997;1:74-87

152. Abu-Soud HM, Stuehr DJ. Nitric oxide synthases reveal a role for calmodulin in controlling electron transfer. *Proc Natl Acad Sci U S A*. 1993;90:10769-10772

153. Scherrer-Crosbie M, Ullrich R, Bloch KD, Nakajima H, Nasseri B, Aretz HT, Lindsey ML, Vancon AC, Huang PL, Lee RT, Zapol WM, Picard MH. Endothelial nitric oxide synthase limits left ventricular remodeling after myocardial infarction in mice. *Circulation*. 2001;104:1286-1291

154. Janssens S, Pokreisz P, Schoonjans L, Pellens M, Vermeersch P, Tjwa M, Jans P, Scherrer-Crosbie M, Picard MH, Szelid Z, Gillijns H, Van de Werf F, Collen D, Bloch KD. Cardiomyocyte-specific overexpression of nitric oxide synthase 3 improves left ventricular performance and reduces compensatory hypertrophy after myocardial infarction. *Circ Res*. 2004;94:1256-1262

155. Ichinose F, Bloch KD, Wu JC, Hataishi R, Aretz HT, Picard MH, Scherrer-Crosbie M. Pressure overload-induced lv hypertrophy and dysfunction in mice are

exacerbated by congenital nos3 deficiency. *Am J Physiol Heart Circ Physiol*. 2004;286:H1070-1075

156. Ichinose F, Buys ES, Neilan TG, Furutani EM, Morgan JG, Jassal DS, Graveline AR, Searles RJ, Lim CC, Kaneki M, Picard MH, Scherrer-Crosbie M, Janssens S, Liao R, Bloch KD. Cardiomyocyte-specific overexpression of nitric oxide synthase 3 prevents myocardial dysfunction in murine models of septic shock. *Circ Res*. 2007;100:130-139

157. Ahmadie R, Santiago JJ, Walker J, Fang T, Le K, Zhao Z, Azordegan N, Bage S, Lytwyn M, Rattan S, Dixon IM, Kardami E, Moghadasian MH, Jassal DS. A high-lipid diet potentiates left ventricular dysfunction in nitric oxide synthase 3-deficient mice after chronic pressure overload. *J Nutr*. 2010;140:1438-1444

158. Vasquez-Vivar J, Martasek P, Hogg N, Masters BS, Pritchard KA, Jr., Kalyanaraman B. Endothelial nitric oxide synthase-dependent superoxide generation from adriamycin. *Biochemistry*. 1997;36:11293-11297

159. Garner AP, Paine MJ, Rodriguez-Crespo I, Chinje EC, Ortiz De Montellano P, Stratford IJ, Tew DG, Wolf CR. Nitric oxide synthases catalyze the activation of redox cycling and bioreductive anticancer agents. *Cancer Res*. 1999;59:1929-1934

160. Weinstein DM, Mihm MJ, Bauer JA. Cardiac peroxynitrite formation and left ventricular dysfunction following doxorubicin treatment in mice. *J Pharmacol Exp Ther*. 2000;294:396-401

161. Griffith OW, Stuehr DJ. Nitric oxide synthases: Properties and catalytic mechanism. *Annu Rev Physiol*. 1995;57:707-736

162. Neilan TG, Blake SL, Ichinose F, Raher MJ, Buys ES, Jassal DS, Furutani E, Perez-Sanz TM, Graveline A, Janssens SP, Picard MH, Scherrer-Crosbie M, Bloch KD. Disruption of nitric oxide synthase 3 protects against the cardiac injury, dysfunction, and mortality induced by doxorubicin. *Circulation*. 2007;116:506-514

163. Sebag IA, Handschumacher MD, Ichinose F, Morgan JG, Hataishi R, Rodrigues AC, Guerrero JL, Steudel W, Raher MJ, Halpern EF, Derumeaux G, Bloch KD, Picard MH, Scherrer-Crosbie M. Quantitative assessment of regional myocardial function in mice by tissue doppler imaging: Comparison with hemodynamics and sonomicrometry. *Circulation*. 2005;111:2611-2616

164. Nagy AC, Cserep Z, Tolnay E, Nagykalnai T, Forster T. Early diagnosis of chemotherapy-induced cardiomyopathy: A prospective tissue doppler imaging study. *Pathol Oncol Res*. 2008;14:69-77

165. Luft JH. Improvements in epoxy resin embedding methods. *J Biophys Biochem Cytol*. 1961;9:409-414

166. Gavrieli Y, Sherman Y, Ben-Sasson SA. Identification of programmed cell death in situ via specific labeling of nuclear DNA fragmentation. *J Cell Biol*. 1992;119:493-501

167. Csizmadia E, Csizmadia V. Detection of apoptosis in tissue sections. *Methods Mol Biol*. 2009;559:49-63

168. Adinolfi E, Raffaghello L, Giuliani AL, Cavazzini L, Capece M, Chiozzi P, Bianchi G, Kroemer G, Pistoia V, Di Virgilio F. Expression of p2x7 receptor increases in vivo tumor growth. *Cancer Res*. 2012

169. Carter P, Presta L, Gorman CM, Ridgway JB, Henner D, Wong WL, Rowland AM, Kotts C, Carver ME, Shepard HM. Humanization of an anti-p185her2 antibody for human cancer therapy. *Proc Natl Acad Sci U S A*. 1992;89:4285-4289

170. Riccio G, Esposito G, Leoncini E, Contu R, Condorelli G, Chiariello M, Laccetti P, Hrelia S, D'Alessio G, De Lorenzo C. Cardiotoxic effects, or lack thereof, of anti-erbb2 immunoagents. *FASEB J*. 2009;23:3171-3178

171. Yousif NG, Al-Amran FG. Novel toll-like receptor-4 deficiency attenuates trastuzumab (herceptin) induced cardiac injury in mice. *BMC Cardiovasc Disord*. 2011;11:62

172. Fedele C, Riccio G, Coppola C, Barbieri A, Monti MG, Arra C, Tocchetti CG, D'Alessio G, Maurea N, De Lorenzo C. Comparison of preclinical cardiotoxic effects of different erbb2 inhibitors. *Breast Cancer Res Treat*. 2011

173. Singal PK, Tong JG. Vitamin e deficiency accentuates adriamycin-induced cardiomyopathy and cell surface changes. *Mol Cell Biochem*. 1988;84:163-171

174. Miller AA, Hislop AA, Vallance PJ, Haworth SG. Deletion of the enos gene has a greater impact on the pulmonary circulation of male than female mice. *Am J Physiol Lung Cell Mol Physiol*. 2005;289:L299-306

175. Moore C, Sanz-Rosa D, Emerson M. Distinct role and location of the endothelial isoform of nitric oxide synthase in regulating platelet aggregation in males and females in vivo. *Eur J Pharmacol*. 2011;651:152-158

176. Bristow MR, Mason JW, Billingham ME, Daniels JR. Doxorubicin cardiomyopathy: Evaluation by phonocardiography, endomyocardial biopsy, and cardiac catheterization. *Ann Intern Med*. 1978;88:168-175

177. Sharov VG, Sabbah HN, Shimoyama H, Goussev AV, Lesch M, Goldstein S. Evidence of cardiocyte apoptosis in myocardium of dogs with chronic heart failure. *Am J Pathol*. 1996;148:141-149

178. Saraste A, Pulkki K, Kallajoki M, Henriksen K, Parvinen M, Voipio-Pulkki LM. Apoptosis in human acute myocardial infarction. *Circulation*. 1997;95:320-323

179. Narula J, Haider N, Virmani R, DiSalvo TG, Kolodgie FD, Hajjar RJ, Schmidt U, Semigran MJ, Dec GW, Khaw BA. Apoptosis in myocytes in end-stage heart failure. *N Engl J Med*. 1996;335:1182-1189

180. Kumar D, Kirshenbaum L, Li T, Danelisen I, Singal P. Apoptosis in isolated adult cardiomyocytes exposed to adriamycin. *Ann N Y Acad Sci*. 1999;874:156-168

181. Wu S, Ko YS, Teng MS, Ko YL, Hsu LA, Hsueh C, Chou YY, Liew CC, Lee YS. Adriamycin-induced cardiomyocyte and endothelial cell apoptosis: In vitro and in vivo studies. *J Mol Cell Cardiol*. 2002;34:1595-1607

182. Zhang J, Clark JR, Jr., Herman EH, Ferrans VJ. Doxorubicin-induced apoptosis in spontaneously hypertensive rats: Differential effects in heart, kidney and intestine, and inhibition by icrf-187. *J Mol Cell Cardiol*. 1996;28:1931-1943

183. Arola OJ, Saraste A, Pulkki K, Kallajoki M, Parvinen M, Voipio-Pulkki LM. Acute doxorubicin cardiotoxicity involves cardiomyocyte apoptosis. *Cancer Res*. 2000;60:1789-1792

184. Zhang YW, Shi J, Li YJ, Wei L. Cardiomyocyte death in doxorubicin-induced cardiotoxicity. *Arch Immunol Ther Exp (Warsz)*. 2009;57:435-445

185. Kobayashi S, Volden P, Timm D, Mao K, Xu X, Liang Q. Transcription factor gata4 inhibits doxorubicin-induced autophagy and cardiomyocyte death. *J Biol Chem*. 2010;285:793-804

186. Kabeya Y, Mizushima N, Ueno T, Yamamoto A, Kirisako T, Noda T, Kominami E, Ohsumi Y, Yoshimori T. Lc3, a mammalian homologue of yeast apg8p, is localized in autophagosome membranes after processing. *EMBO J*. 2000;19:5720-5728

187. He H, Dang Y, Dai F, Guo Z, Wu J, She X, Pei Y, Chen Y, Ling W, Wu C, Zhao S, Liu JO, Yu L. Post-translational modifications of three members of the human map1lc3 family and detection of a novel type of modification for map1lc3b. *J Biol Chem*. 2003;278:29278-29287

188. Tanida I, Ueno T, Kominami E. Human light chain 3/map1lc3b is cleaved at its carboxyl-terminal met121 to expose gly120 for lipidation and targeting to autophagosomal membranes. *J Biol Chem*. 2004;279:47704-47710

189. Wu J, Dang Y, Su W, Liu C, Ma H, Shan Y, Pei Y, Wan B, Guo J, Yu L. Molecular cloning and characterization of rat lc3a and lc3b--two novel markers of autophagosome. *Biochem Biophys Res Commun*. 2006;339:437-442

190. Zhang Y, Kang YM, Tian C, Zeng Y, Jia LX, Ma X, Du J, Li HH. Overexpression of nrdp1 in the heart exacerbates doxorubicin-induced cardiac dysfunction in mice. *PLoS One*. 2011;6:e21104

191. Li K, Sung RY, Huang WZ, Yang M, Pong NH, Lee SM, Chan WY, Zhao H, To MY, Fok TF, Li CK, Wong YO, Ng PC. Thrombopoietin protects against in vitro and in vivo cardiotoxicity induced by doxorubicin. *Circulation*. 2006;113:2211-2220

192. Riad A, Bien S, Westermann D, Becher PM, Loya K, Landmesser U, Kroemer HK, Schultheiss HP, Tschope C. Pretreatment with statin attenuates the cardiotoxicity of doxorubicin in mice. *Cancer Res*. 2009;69:695-699

193. Ikegami E, Fukazawa R, Kanbe M, Watanabe M, Abe M, Kamisago M, Hajikano M, Katsube Y, Ogawa S. Edaravone, a potent free radical scavenger, prevents anthracycline-induced myocardial cell death. *Circ J*. 2007;71:1815-1820

194. Lim CC, Zuppinger C, Guo X, Kuster GM, Helmes M, Eppenberger HM, Suter TM, Liao R, Sawyer DB. Anthracyclines induce calpain-dependent titin proteolysis and necrosis in cardiomyocytes. *J Biol Chem*. 2004;279:8290-8299

195. Choi JY, Barlow WE, Albain KS, Hong CC, Blanco JG, Livingston RB, Davis W, Rae JM, Yeh IT, Hutchins LF, Ravdin PM, Martino S, Lyss AP, Osborne CK, Abeloff MD, Hayes DF, Ambrosone CB. Nitric oxide synthase variants and disease-free survival among treated and untreated breast cancer patients in a southwest oncology group clinical trial. *Clin Cancer Res*. 2009;15:5258-5266